Università Politecnica delle Marche
Scuola di Dottorato di Ricerca in Scienze dell'Ingegneria
Curriculum in Ingegneria Industriale - Meccanica

Study and Development of a Novel Radio Frequency Electromedical Device for the Treatment of Peri-Implantitis: Experimental Performance Analysis, Modelling of the Electromagnetic Interaction with Tissues and In Vitro and In Vivo Evaluation

Ph.D. Dissertation of:

Gloria Cosoli

Advisor:

Prof. Enrico Primo Tomasini

XV edition - new series

Università Politecnica delle Marche
Scuola di Dottorato di Ricerca in Scienze dell'Ingegneria
Curriculum in Ingegneria Industriale - Meccanica

Study and Development of a Novel Radio Frequency Electromedical Device for the Treatment of Peri-Implantitis: Experimental Performance Analysis, Modelling of the Electromagnetic Interaction with Tissues and In Vitro and In Vivo Evaluation

Ph.D. Dissertation of:

Gloria Cosoli

Advisor:

Prof. Enrico Primo Tomasini

XV edition - new series

Università Politecnica delle Marche
Dipartimento di Ingegneria Industriale e Scienze Matematiche
Via Brecce Bianche — 60131 - Ancona, Italy

Ringraziamenti

Alla fine di questa tesi, che posso considerare il mattoncino conclusivo del mio percorso di dottorato, posso senza dubbio affermare che nella vita nessun traguardo si raggiunge da soli, perché ci sarà sempre qualcuno che, in un modo o nell'altro, ci darà una mano, un consiglio o semplicemente ci dirà le parole giuste, quando da soli ci sentivamo persi.
La prima persona che voglio ringraziare per esserci sempre è Simone, da qualche mese mio marito… fa ancora strano chiamarti così! Credo non ci sia cosa più bella nella vita che avere qualcuno al proprio fianco ogni giorno, con cui condividere tutto e con cui costruire un passo dopo l'altro la propria famiglia. A te va un grazie enorme, perché non mi hai lasciato sola neppure un giorno... spero tanto di riuscire a ricambiare quello che fai per me!
Per seconda voglio ringraziare Mery, l'amica di una vita, la mia piccola grande donna! Negli ultimi mesi la nostra amicizia è diventata ancora più forte e non smetterò mai di dirti quanto sono orgogliosa di te e che per te ci sarò sempre e per qualsiasi cosa, anche quando non dovessimo essere vicine. Sei come una sorella per me e sì, per te sarei disposta a fare quello che non farei neanche per me!
Un grazie va anche ai miei altri amici... a quelli che mi conoscono da quando ero solo una bambina, a quelli conosciuti nei periodi del liceo e dell'università, alle persone incontrate per caso che hanno subito conquistato un posto nel mio cuore! Voglio ringraziare in particolare Alessia e Lucia, che negli ultimi anni sono ormai diventate una parte fondamentale della mia vita. Grazie perché ci siete sempre e siete davvero delle persone speciali, che io ho la fortuna di avere come amiche. Con le vostre parole sapete sempre come prendermi e incoraggiarmi anche nei momenti più difficili… vi voglio tanto bene!
A seguire (ma non per importanza!) voglio ringraziare la mia famiglia e i miei nonni. Mi avete visto crescere e so che per voi sono sempre stata motivo di orgoglio, me l'avete sempre ripetuto (a volte facendomi anche sentire in imbarazzo!) e avete sempre creduto in me. Grazie perché mi avete supportata e mi avete fatto crescere e diventare la donna che sono oggi.
Un grazie va quindi ai miei colleghi, in particolare Sara, Luigi, Filippo e Rachele: volenti o nolenti, siete dovuti stare al mio fianco ogni giorno di questi 3 anni! Ma non siete semplici colleghi, per me siete diventati dei veri amici! E lo stesso vale per gli ex-colleghi, che vedo ormai poco ma che hanno un posticino nel mio cuore… tra di loro un grazie particolare va ad Ilaria ed Annalisa, che mi piacerebbe avere ogni giorno al mio fianco!
Grazie a Lorenzo Scalise (non ti chiamo Prof perché sennò ti arrabbi!), perché è riuscito ad ascoltare ogni giorno le mie preoccupazioni e mi ha aiutato a chiarire i miei dubbi. Grazie perché hai creduto in me e hai dimostrato di fidarti delle mie capacità (più di quanto io stessa mi fidi!).
Grazie al Professor Graziano Cerri, che ha saputo sempre ascoltarmi con infinita disponibilità e gentilezza e darmi i suoi preziosi consigli ogni volta che ne avevo bisogno.

Grazie anche a Gerardo Tricarico, che ha avuto l'idea iniziale ed ha contribuito alla realizzazione di questo progetto di ricerca.
Per ultimo, non per importanza, un sentito ed enorme grazie va al Professor Enrico Primo Tomasini, mio tutor in questo Dottorato, che mi ha accolta nel suo gruppo di ricerca come quasi fossi una figlia. Grazie Prof perché crede in me e si fida delle cose che faccio. Sono felice che continueremo a lavorare insieme nei prossimi mesi e spero che sarò ancora motivo di orgoglio per lei.

Gloria

"La felicità è reale solo quand'è condivisa."

Acknowledgements

At the end of this PhD thesis, which I can consider as the last brick of my doctoral project, I can state without any doubt that in life you never reach a goal on your own. In fact, there will be always someone who gives some help, some advice or simply finds the right words, when we all alone get lost.
The first I wish to thank for being always present is Simone, who is my husband since some months… still feels weird to call you that! I think there is nothing more beautiful in life than having someone beside you, with whom sharing everything and building together your family, step by step. I would like to thank you immensely because you've never let me alone, not even a single day… I really hope that somehow I am able to pay back everything you do for me!
Then, I would like to thank Mery, my lifelong friend, my little big woman! In latest months our friendship has become stronger and stronger. I will never stop to tell you how much I'm proud of you! I'll always be there for you, for anything, also when we are not close to each other. You are like a sister to me and yes, for you I would be willing to do what I wouldn't do even for me!
I would like to thank also all my other friends… those who know me since I was only a child, those met during high school and university, those met by chance who have immediately conquered a room in my heart! I wish to thank particularly Alessia and Lucia, who in recent years have become fundamental in my life. Thank you because you are always present. You are very special people and I am so lucky to have you in my life. You always know how to handle me and to support me even in the most difficult situations… I love you so much!
To follow, I would like to thank my family and my grandparents. You have seen me grow up and I know you have always been proud of me. You have always told it to me (sometimes making me feel embarassed!) and you have always believed in me. Thank you because you have supported me and made me grow and become who I am today.
Thank you to my colleagues, in particular to Sara, Luigi, Filippo and Rachele: willing or not, you had to be at my side everyday in last 3 years! But you are not simple colleagues, you have become real friends for me! And this is true also for my ex-colleagues, who I rarely meet but I have a room in my heart for you. I would like to especially thank Ilaria and Annalisa, whom I wish to have by my side everyday!
I would like to thank Lorenzo Scalise (I don't call you Prof or you get angry!), because he has been able to listen to my worries everyday and has satisfied my doubts. Thanks because you have believed in me and you have proved to be confident in my capabilities (more than I myself am confident in them!).
Thanks to Professor Graziano Cerri, who has always listened to me with endless willingness and kindness. You have given me advices every time I needed them.

I would like to thank also Gerardo Tricarico, who has got the original idea and contributed to the realization of this research project.
Last but not least, I wish to immensely thank Professor Enrico Primo Tomasini, who is my tutor in this research project. You have greeted me in your research group almost as a daughter. Thank you Prof because you are confident in what I do. I am happy I will continue working with you over the next months and I hope you will be proud of me again.

Gloria

"Happiness real only when shared."

Motivations and aims of the work

Peri-implantitis is a serious disease and, to this day, it represents the main cause of implant failure. It affects soft and hard tissues surrounding a dental implant; more precisely, it is characterized by inflammation, bacterial growth and bone level reduction. It can be caused by different factors, like poor oral hygiene and periodontitis. The prevalence is estimated at 9.6% of annually placed dental implants (over a million only in Italy).

Huge amounts of money (some billion dollars) are at stake, so there is a great interest in finding new therapies for such pathology. In fact, different therapies exist (e.g. non-surgical treatments, antibiotics, antiseptics and laser therapy), but none has proved to be satisfactorily effective (the state of the art is reported in Chapter 1). So, at present, prevention is the only way to contrast peri-implantitis.

But in recent years an electric therapy based on the application of a radio frequency alternating electric current was administered by Dr. Tricarico in his dental laboratory (the detailed description of this therapy is in Chapter 2). Such a treatment was first employed in 2002, when the positive effects on peri-implantitis characteristics were observed by chance during endodontic root canal treatment. However, the underlying mechanisms were not known, even if the outcomes were very interesting. Follow-up data concerning the treated patients are available up to 2015; they represent the clinical evidence of the effectiveness of such an innovative electric therapy.

This PhD study aims to investigate the working principle of the aforementioned treatment, in order to better understand the underlying mechanisms and to connect them with the therapeutic benefits (e.g. Which physical factor causes inflammation reduction? Which one promotes the bone healing?).

So, starting from the clinical evidence provided by the above cited clinical trial (Paragraph 2.1), the author wants to characterize the therapeutic device in terms of equivalent model and electrical parameters (e.g. power delivered during a therapeutic session) (Paragraph 2.2). Then, the model will be used in numerical simulations made on a 3D geometry (Paragraph 2.3), in order to observe what happens during the therapy delivering. In this way, it will be possible to try to understand the causes of the observed positive effects on the pathology symptoms.

Moreover, it is desirable to improve the therapy, for example by localizing the inflamed portion of the tissue, so limiting the involvement of the surrounding healthy area. The therapy could also be personalized according to the severity of the pathology. This information could be gathered by means of bioimpedance measurements, since the physio-pathological condition of a biological tissue determines its electrical properties (in particular, electrical conductivity and relative permittivity). Also in this part of the study, numerical simulations were run in order to investigate the feasibility of such an approach (Paragraph 3.1). Then, experimental measurements were made on three patients with dental implants (healthy, inflamed and peri-implantitis cases); in addition, bioimpedance measurements were performed on natural tooth roots of healthy subjects, in order to evaluate the repeatability of such measures (Paragraph 3.2).

Hence, the electrical safety of the treatment was evaluated by means of in vitro trials and of the numerical simulation of possible thermal effects of the therapy (Chapter 4).

Discussion and conclusions are reported in Chapter 5.

As the concluding part of the project, a prototype of a specific device dedicated to peri-implantitis therapy is being developed (Appendix). The certification process is still underway and the relative documentation is being drawn up.

A flow chart related to this thesis organization is reported below.

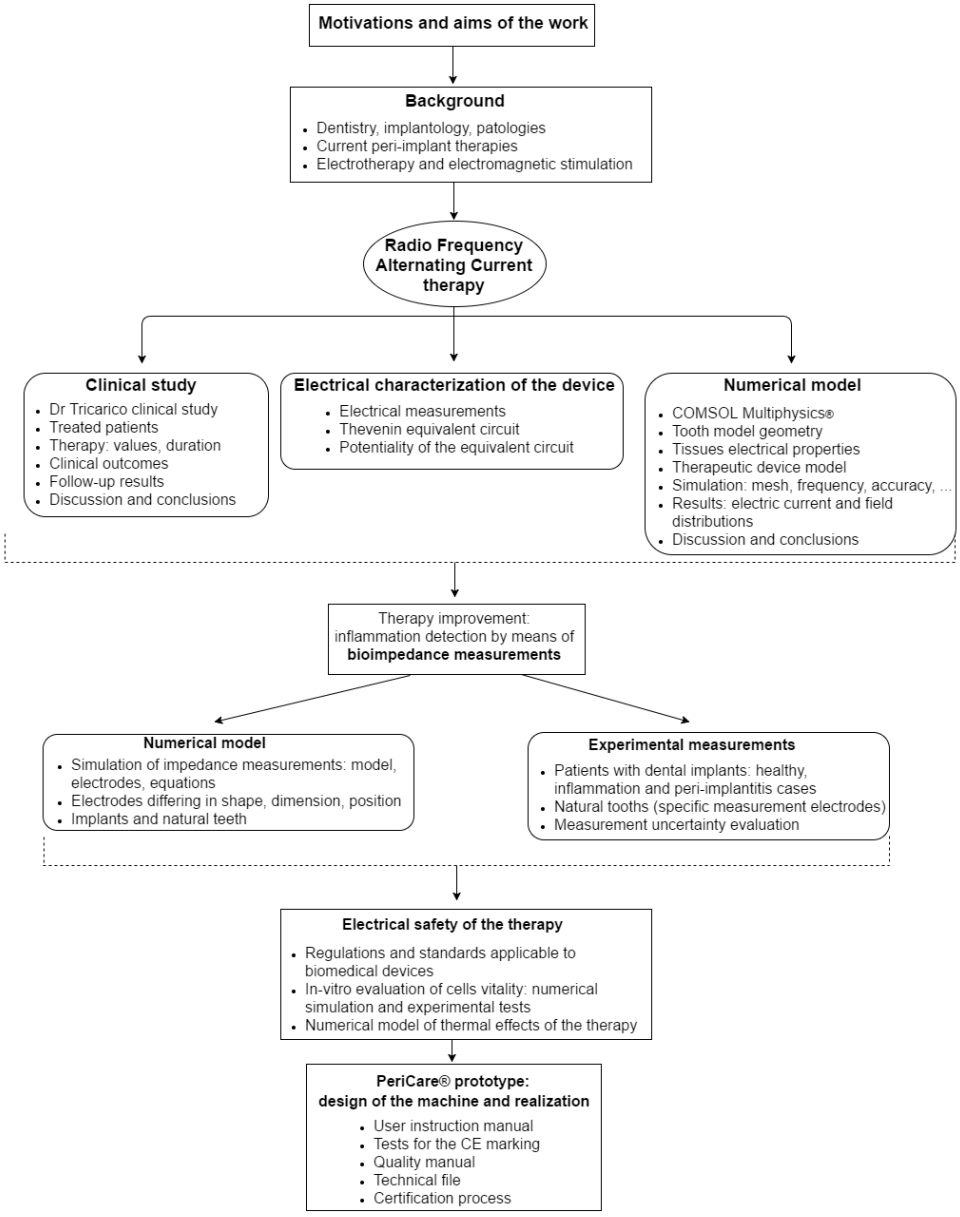

Abstract

Peri-implantitis is a severe disease affecting both the hard and the soft tissues around a dental implant. This pathology presents three main characteristics: soft tissues inflammation, bacterial growth at the implant-tissue interface and bone loss around the implant itself. There is a great interest on peri-implant disease, since its prevalence is estimated at 9.6% of the annually placed dental implants (i.e. millions of implants), for a global market of some billion dollars.
Nowadays, there are different therapies, such as mechanical treatment, antibiotics, antiseptics and also laser therapy. However, none of these are satisfactorily efficient, so that at present prevention is the only means to contrast peri-implantitis.
In recent years, an innovative therapy based on the administration of radio frequency electric current has been experimented in a clinical trial, reporting a success rate equal to 81% of the treated implants. These outcomes were significant, so that the used device (originally designed for endodontic treatment) has been electrically characterized, also providing an equivalent circuit.
In order to better understand the underlying mechanisms of the therapy, the treatment has been numerically simulated in COMSOL Multiphysics® environment. In particular, the therapeutic device has been modelled by means of its equivalent circuit and a simplified geometry of the implant screwed in the jawbone and the surrounding tissues has been realized. In this way, it has been possible to analyse the electric current and field distributions in peri-implant tissues when the therapeutic signal is applied. From the results, it is possible to infer that the anti-inflammatory effect is probably associated to the electric current, which is focused on soft tissues and particularly on their inflamed portion (because of the higher electrical conductivity with respect to the surrounding tissues), while perhaps the bone regeneration effect is linked to the electric field, whose lines cross both hard and soft tissues surrounding the implant.
Since healthy and inflamed tissues have different electrical properties, the authors have investigated the use of bioimpedance measurements to localize and quantify inflammations. The feasibility of this approach has been studied by means of numerical simulations of the measure. From the numerical results, it is possible to observe changes in the measured impedance modulus equal to 4-20%, depending on different parameters (e.g. electrodes size and shape or inflammation severity and dimension). In experimental measurements, the observed variations are also more evident: 35% in case of mere inflammation and 56% in case of peri-implantitis (which includes also bone loss, causing a further impedance decrease). This is partly due to the fact that in reality the inflamed tissue is swollen and so the impedance is lower, but, for the sake of simplicity, in the realized model geometry this has not been represented. Anyway, bioimpedance measurements seem to be suitable to discriminate between healthy and inflamed tissues, even if it is necessary to carry out a measurement campaign including a wider population, in order to build a database allowing the classification of individual measurements (in fact, at present only comparison between healthy and impaired tissues is possible). The inclusion of bioimpedance measurement in the proposed treatment would make possible to personalize the therapy according to the severity of the disease and to focus the therapeutic current on the impaired area.

In order to study the repeatability of bioimpedance method in oral environment, experimental measures have been made on natural tooth roots; the results have been compared to the numerical ones obtained from the simulation of bioimpedance measurements on different teeth (i.e. incisor, canine and premolar). The order of magnitude is the same (i.e. some kΩ), even if there are differences probably attributable to a different electrodes positioning and to the actual contact surface between electrodes and gingiva. With regard to the repeatability, an intra-subject variability equal to 10% has been reported in the same day, but the value goes up to 26% in different days. Inter-subject variability has been assessed at higher values (e.g. ≈ 20% for the premolar tooth root).
Furthermore, the electrical safety of the device has been accurately taken into account, also towards the certification process. First of all, the applicable directives have been individuated: IEC 60601-1 (dealing with the safety of medical electrical systems and the necessary requirements to protect the patient, the operator and the surroundings), the collateral standard IEC 60601-1-2 (defining the tests to assess the performance of a medical electrical device in presence of electromagnetic disturbances/emissions) and the particular standard IEC 60601-2-2 (providing requirements for basic safety and essential performance of high frequency surgical equipment, such as surgical knife, which is similar to the considered therapeutic device in terms of working frequency and signal amplitude).
Preliminar in vitro tests have been carried out in order to evaluate the effect of the therapy on cell vitality. The setup configuration has been chosen according to the results of numerical simulations, to avoid interferences between different cell cultures and to define the optimal test arrangement. The results show the electric current and field distributions and also confirm that the chosen plastic container for the cell cultures (i.e. Petri dishes) are suitable, since no interferences between adjacent dishes have been observed. The experimental results have shown that the therapy does not cause a significant increase in necrosis (the assessed vitality was of ≈ 85% for the tests versus 94% of the controls); the main negative effect is apoptosis, which is a kind of programmed cell death, granting advantages during the life cycle of an organism.
One last point concerning the safety of the device has been the numerical simulation of possible thermal effects produced by the therapy, potentially caused by the Joule effect. The results have shown that the temperature distribution is not significantly influenced by the treatment (the global temperature increase in the implant surroundings is < 1°C, except for those elements close to sharp edges, which cannot be considered reliable because of numerical errors due to field singularities). This let us state that the proposed therapy for peri-implantitis does not produce dangerous heating effects on the surrounding tissues.
Finally, a new device, named PeriCare®, has been designed specifically for the treatment of peri-implantitis disease. It includes both a diagnostic part and a therapeutic one, aimed at bioimpedance measurement and therapeutic signal administration, respectively. Proper electrodes are being designed for such purposes and the prototype is being realized. A sort of block diagram has been drawn and the device instruction manual is available. The technical file is being compiled and the conformity verification tests are being planned in order to start the certification process to obtain the CE marking. Hopefully, the medical device will be placed into the market during this year.

Contents

List of Figures

List of Tables

List of Quantities and Units

Quantity		Unit	
Name	**Symbol**	**Name**	**Symbol**
Electric current	i	Ampere	A
Electric current density	$\bar{J}$	Ampere per square meter	A/m^2
Electric field	$\bar{E}$	Volt per meter	V/m
Electric impedance	Z	Ohm	Ω
Electrical conductivity	σ	Siemens per meter	S/m
Relative dielectric permittivity	ε_r	dimensionless	-
Relative magnetic permeability	μ_r	dimensionless	-
Density	ρ	kilogram per cubic meter	kg/m^3
Temperature	T	Kelvin	K
Thermal capacity	Q	Joule per kilogram Kelvin	J/(kg*K)
Thermal conductivity	k	Watt per meter Kelvin	W/(m*K)

Chapter 1.

Introduction

1.1. Dentistry and oral pathologies: dental implants and peri-implant diseases

Tooth loss is a very common problem, resulting from diseases and traumas [1]. Dental implants are the gold standard choice to replace missing teeth (or, more precisely, their roots), in order to restore the patient to normal functionality, since the 1960s [2]. In fact, contrary to traditional removable prostheses, a dental implant allows normal function, contour, comfort and speech, restoring the oral health near to normal limits [3]. Implant therapy has extremely expanded because of several causes: the much better acceptance by patients and clinicians, the availability of more and more detailed indications for the therapy, its simplification and especially the technological advancement in bone augmentation procedures (enabling implant placement also in patients with local bone deficiencies) [4].
A dental implant is a surgical component inserted into a residual bony ridge and is similar to a root of a natural tooth [5] (we speak about "root form implants" [6]). The implant body (i.e. the implant fixture) is placed into the bone, then the implant abutment is attached and it will hold the dental prosthetic (Fig. 1).

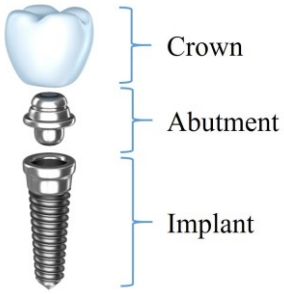

Figure 1. Dental implant components: implant, abutment and crown

The osseous and the tissue responses to the implant are influenced by surface properties, such as morphology and roughness (which can be increased by means of different techniques, like machining, plasma spraying, acid-etching, anodisation and laser treatment) [1]. Osseointegration (from the Greek *osteon*, bone, and the Latin *integrare*, to make whole) is a fundamental biologic process, consisting in the integration of the implant

material with the natural bone; failures are often associated with poor bone quality and/or quantity, which provokes poor anchorage and stability of the implant itself [7]–[9]. To reach an optimal result, the kind of material is crucial; the characteristics of an ideal material are biocompatibility, adequate toughness, strength, corrosion, wear and fracture resistance [10]. Despite the introduction of new materials (e.g. zirconia), titanium (approved for the use in dental implants in 1982 by the FDA, Food and Drug Administration) remains the gold standard material for the fabrication of oral implants [11]–[13]. Also titanium alloys (mainly Ti6A14V) are used, since they are stronger and more fatigue resistant than pure titanium [14].

Nowadays implants positioning is more and more frequent: the numbers have increased more than tenfold from 1983 to 2002, fivefold from 2000 to 2005 and keep growing [5]; more frequent dental caries, the increasing incidences of tooth loss and the rising aging population (besides the rising general population) are the major factors making the dental implants market grow [15]. According to the European Federation of Periodontology, it is expected that there will be an increase in implant-related diseases up to 2025, despite the improvement in surgical techniques [16].

Only in Italy, over a million implants are placed every year [17]; since dentistry is mainly private, the economic aspects are essential.

Due to such great numbers of positioned implants, high amounts of money are involved. The global dental implantology market has a volume of some billion dollars [15], [18] and at present Europe is the largest market (followed by North America and Asia-Pacific [15]). There are both fixed and variable costs; the former are linked, for example, to radiation protection, sterilisation, insurance policies and utilities [17]. To not add further costs linked to trivial errors, inaccuracies or to non-sterile conditions during surgery procedures, it is important to pay attention to all these aspects. In fact, some problems and complications following the implant placement are consequent to non-correct procedures related both to surgery and sterilisation. So, it is fundamental not to save money in aspects interfering with the final quality of the outcome.

So, in spite of all the developments in dental implantology techniques, peri-implant diseases are frequent, resulting from an imbalance between bacterial load and host defence [19], [20]. In a follow-up of implant treatments on 999 implants [21], it is reported that peri-implant lesions are common in titanium implants after 10 years from their placement without systematic supportive treatment. These pathologies can be classified into two main categories: peri-implant mucositis and peri-implantitis [19], [22] which can be defined according to the consensus report from the 1st European Workshop on Periodontology [23]. The former (Fig 2, left) is an inflammatory lesion of the mucosa (i.e. soft tissue) surrounding the dental implant (but it can be a precursor of peri-implantitis); it is also called gingivitis, since it refers to a gingival inflammation, characterized by redness and swelling [20]. The latter (Fig. 2, right) includes not only gingivitis, but also the loss of the supporting bone around an implant [23], [24], often associated with suppuration and deepened pockets [20].

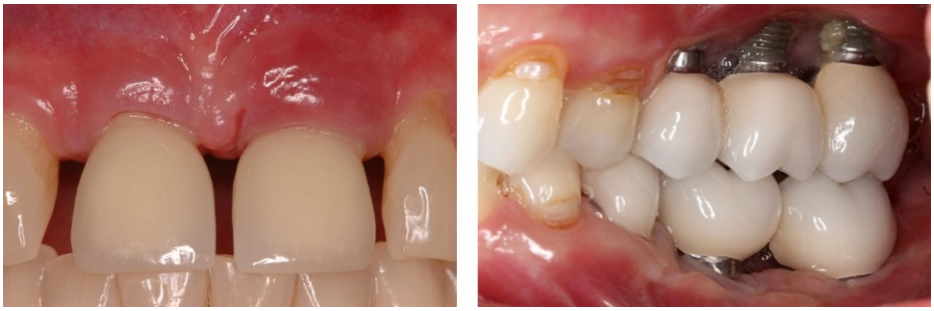

Figure 2. Peri-implant mucositis (left) and peri-implantitis (right)

Data about prevalence (i.e. the number of people in a population who have a disease at a given time [25]) on implant-treated subjects are rare [20], but quite recent reviews (2008) report the results from two main studies [20], [24]. In particular, it results that mucositis occurs in about 80% of the subjects and in 50% of the implants, while peri-implantitis in 28-56% of the subjects and in 12-43% of implant sites. In a more recent review (2013) it is stated that the frequency of peri-implant mucositis is 63.4% of participants and 30.7% of implants, while that of peri-implantitis is estimated at 18.8% of subjects and at 9.6% of annually placed dental implants [26]. Anyway, important numbers are involved.

The risk indicators for peri-implant diseases are different and opinions are sometimes conflicting [19], [20], [27]; anyway, the most acknowledged are: poor oral hygiene, poor quality of alveolar bone, bad positioning of the implant, diabetes, smoking, alcohol consumption, presence of keratinized mucosa, untreated periodontitis or dental caries near the implant itself and also genetic traits.

The diagnosis of such pathologies is made by means of different techniques; in particular, the standard peri-implantitis diagnosis is made by observing the colour of the gingiva, bleeding, the probing depth of peri-implant pockets, suppuration and also by means of x-rays (to measure the bone height around the implant) [28].

Periodontal probing (Fig. 3) is used to detect inflammation in the peri-implant mucosa thanks to the identification of bleeding and/or suppuration [24]; if the probing depth increases over time, it means that there is bone loss [29], [30]. Moreover, bleeding on probing is a useful parameter for the diagnosis of mucosal inflammation, since it increases in case of mucositis (67%) and peri-implantitis (91%) [29], while its absence indicates stable peri-implant conditions (i.e. it has a high negative predictive value) [31]. Suppuration is the presence of pus and indicates infection and inflammatory lesion [19]; in two studies pus is considered explanatory for peri-implantitis causing a bone level inferior to 3 implant threads [21], [32].

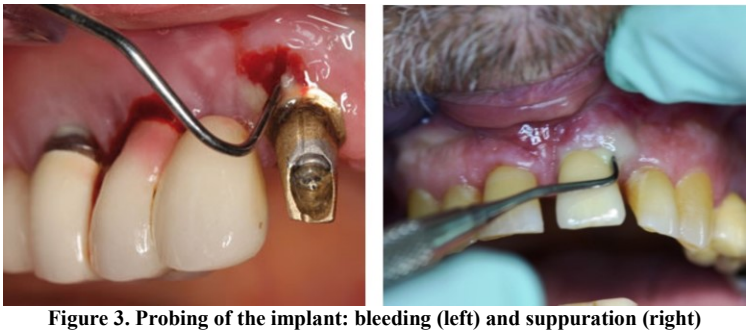

Figure 3. Probing of the implant: bleeding (left) and suppuration (right)

Radiographic evaluation (e.g. panoramic tomography and intra-oral radiography, Fig. 4) is widely employed to monitor marginal bone levels and to detect the marginal bone loss characterizing peri-implantitis [24], [33]; nowadays it is also possible to represent osseous structures in three planes without distortion thanks to multi-slice computer tomography and cone beam volume imaging [19].

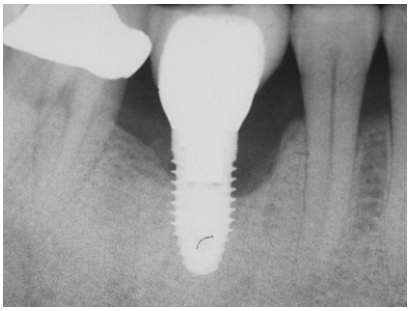

Figure 4. Radiographic image of a peri-implantitis case

The success of an implant can be assessed by means of the bone resorption quantification: not more than 1.5 mm in the first year after the placement, not more that 0.2 mm a year in the following period [34].

1.2. Current peri-implantitis treatments

Peri-implantitis main characteristics are bone loss, inflammation of soft tissue (i.e. gingiva and connective tissue in general) and bacterial infection (which determines bacteria adhesion to the implant surface and abutment, with consequent immune reaction) [22], [35]. It can lead to the complete loss of osseointegration (in fact, the rate of bone loss increases over time [36]) and so to the implant failure [37], [38]. This pathology is still the main cause of late implant failure (while the early implant failure is associated with the unsuccessful osseointegration of the implant with the bone [37], more frequent in smokers, in case of systemic diseases and in presence of periodontitis [4], [39]), since no completely effective therapies are acknowledged so far [19], [35].

There is a general agreement that the treatment of peri-implant disease must include anti-infective measures [20], since it is associated with biofilms [40], [41] of oral microorganisms (particularly Gram-negative bacilli [35]); these layers are characterized by the rapid growth of bacterial communities [42], [43], playing a major role in the aetiology of peri-implant mucositis and peri-implantitis.

The reduction of bacterial load to a level allowing healing is difficult to obtain by means of mechanical treatments used alone [44]. These non-surgical therapies can be effective in the treatment of peri-implant mucositis, but not in peri-implantitis cases [45]. So, during the years, other techniques have been proposed, like antibiotics and antiseptics; but, for example, the adjunctive chlorhexidine application together with mechanical treatment has only limited effects [44]. Administration of antibiotics reduces bleeding on probing and probing depths, but is not able to cure the disease [46], [47].

Laser therapy has shown minor beneficial effects, but further evaluations on this approach are needed [48]–[50]. Therefore, it seems that the outcome of non-surgical treatments is unpredictable [20].

Surgical treatment of peri-implantitis consists in open debridement (i.e. removal of infected tissue) and decontamination, in order to cure the inflammatory lesion. This technique has been experimented on animals and humans, but the available evidence is extremely limited [51] and the success rate is not satisfactory (only one study [52] addresses disease resolution, obtained in 58% of the lesions with the adjunctive use of antibiotics). Neither regenerative procedures are able to fix the problem, in fact they limit themselves to fill the osseous defect [20] and there is no evidence of additional beneficial effects.

Hence, the success rate of current peri-implantitis therapies is not satisfying, so that at present prevention is the only means to contrast peri-implantitis [35].

1.3. New perspectives in electrotherapy and electromagnetic stimulation

Electricity has a well-accepted important role in contemporary medicine, both in diagnostic (e.g. electrocardiography and impedance tests) and in therapeutic applications (e.g. transcutaneous electric nerve stimulation and transcranial electric stimulation) [53]. After all, the nature of human body is mainly electric [54]. Nowadays therapies based on the application of electric currents and/or electromagnetic (EM) fields are used more and more; electricity has been a powerful diagnostic and therapeutic tool in medicine for hundreds of years, in the so-called electrotherapy, whose safety has been established through its extensive clinical use [55].

One of the newest and the most topical subjects in bioelectromagnetics is how to induce an adaptive response with electromagnetic stimulation [56]. In fact, it is evident that electric field-based therapies arouse molecular patterns triggering an adaptive immune response against inflammatory processes; moreover, the immune system adapts itself to the exposure to radiation [57].

Inflammation presents different characteristics: vasodilatation, clotting in the interstitial spaces, swelling, pain, redness, hyperthermia; it can be provoked by bacteria, viruses, external injuries or chemicals [58]. Steroids block the inflammatory process, but have also not-negligible side effects (e.g. hyperglycaemia and hypertension) [55].

Anti-inflammatory effect of radiation can be associated with the content of lipid messengers in phospholipids of immunocompetent cells membranes [59]; the exposition to low-intensity high-frequency radiation increases the content of such substance, actively involved in inflammatory and immune reactions. In addition, there are different cellular mechanisms supporting the anti-inflammatory effect of electronic signals, such as pH normalization, cell membrane repair and stabilization, enhancement of filtration/diffusion processes, increased tissue metabolism, immune system support and benefits on increases in blood flow and oedema reduction [55], [60]. EM radiation (particularly in radio frequency range) may also influence enzymatic activity, synaptic transmission, bioelectric activity, DNA molecule integrity and other biological processes, all involved in anti-inflammatory response [61].

High-frequency electromagnetic radiation is widely used in different clinical fields, for prevention, diagnosis and therapy of different pathologies [62]–[64], even if the underlying mechanisms are not completely clear and their usage is mostly empirical [59], [63]. It was demonstrated that it produces a high anti-inflammatory effect, through a decrease in the exudative oedema and hyperthermia (due to histamine release [60], [65]), comparable to those obtained by means of the administration of therapeutic doses of anti-inflammatory drugs [66], [67], which in the long term can be dangerous [55]. Since inflammation is present in the pathogenesis of several diseases, electromagnetic exposition can improve the wellbeing of many different patients; the effect is strongly dependent on frequency, power and duration of the treatment, so they must be chosen accurately [61], [63], [66].

The effect of electric/electromagnetic therapies is not only anti-inflammatory. In fact, EM irradiation has also an anti-bacterial effect and promotes bone formation (meanwhile reducing the bone resorption); moreover, EM irradiation also reinforces the effect of some

antibiotics and anti-inflammatory drugs by changing metabolic pathways and membranes [35], [68], [69].
More precisely, there is the evidence that high frequency and low intensity electromagnetic irradiation presents antibacterial effects on *Escherichia coli* and other bacteria [68], [70]; this phenomenon was recently exploited to inactivate *Escherichia coli* bacteria in water samples [71], by applying an alternating magnetic field at radio frequency. There is also a patent on the use of electric field to selectively kill microbes in root canals [72].
With regard to the bone remodelling effect, there is a great interest in the application of electromagnetism to heal bone fractures since 1953, when Yasuda et al. talked about the piezoelectric forces in bones [73]. It is possible to state that electrical stimulation can promote bone healing and accelerate bone formation [74], provided that intensity, duration per day and length of the treatment are properly chosen [75]. The underlying mechanisms are not clear, but it is likely that pulsed EM irradiation increases DNA synthesis, alters the cellular calcium content in osteoblasts and can also improve the differentiation of mesenchymal stem cells, which enhance the synthesis of extracellular matrix and the mineralisation in osteoblast-like cells [35], [76]. In addition, osteoclastogenesis is inhibited [77]. In fact, electromagnetic stimulation has an acknowledged role in the management of established non-union of long bone fractures, which cause significant morbidity to the patient [78].
In conclusion, the main effects of electromagnetic irradiation are to inhibit bacteria, to increase bone formation, to positively remodel bone (i.e. not only to increase bone formation, but also to decrease bone resorption) and to reduce the inflammation. Therefore, it can be observed that EM signal acts just on the principal hallmarks of peri-implantitis: soft tissues inflammation, peri-implant bone loss and bacterial growth. Hence, EM signal could be a possible therapy for peri-implantitis disease; in literature, there is a clinical study (started in 2002) exploring this possibility [79] and the same hypothesis is reported in [35].

Chapter 2.

Radio Frequency Alternating Current (RFAC) therapy

This chapter is intended to examine in depth the therapy employed in the clinical study conducted by Dr. Tricarico in his dental office (situated in Chiaravalle, Ancona, Italy) since 2002. The idea of the aforementioned therapy was born consequently to an Eureka moment: Dr. Tricarico, after having done the endodontic treatment by means of Endox® Endodontic System [80] (using radio frequency electric current and electromagnetic field), has observed some side effects on the tissues surrounding the treated tooth roots. There were biological effects more positive than those expected for the mere endodontic treatment and neither cellular necrosis nor tissue injuries were present. On the contrary, there were positive effects on the healing of acute or chronic inflammatory lesions, on infections and on cellular reparations. These phenomena have suggested the use of this kind of treatment also in the event of extra-radicular lesions.

This innovative therapy is based on the application of electric current at Radio Frequency (more precisely, at 312.5 kHz in the Medium Frequency, MF, band) in the tissues surrounding the dental implant affected by peri-implantitis disease. The characteristics of the therapeutic signal will be discussed more in detail in Paragraph 2.1, where the whole clinical study is described: patients' characteristics, therapy modalities, clinical outcomes and also follow-up results.

Starting from the goodness of the results of this medical trial, in 2013 a doctoral research project started with the main objective of exploring the underlying mechanisms and of electrically characterizing the therapeutic device, in order to optimize the therapy. In Paragraph 2.2, it is reported the electrical characterization of the therapeutic device by means of the equivalent circuit obtained according to Thevenin's theorem. This modelling procedure has permitted to numerically simulate the therapy, in order to be able to analyse the electric field/current lines paths in biological tissues.

Paragraph 2.3 is related to such numerical model, realized in COMSOL Multiphysics® environment; the model will be described in its geometrical and electrical properties. In the Results section it will be discussed the distribution of the electric field and of the electric current in relation to the inflamed tissue.

2.1. Clinical trial

A clinical study is an instrument of clinical research involving participants with the main goal of adding medical knowledge [81]. There are two different kinds of clinical studies: the medical trial and the observational study; the former consists in specific interventions on the subject, while the latter aims to assess the health outcomes of people without assigning specific treatments.
In this thesis, the one of interest is the clinical trial; in fact, the study carried out by Dr. Tricarico consisted in the administration of an innovative therapy for peri-implantitis, comparing its outcome with the (unsatisfying) ones of standard approaches (which were described in Paragraph 1.2).
A first documentation of such clinical trial dates back to 2012 [82]; then, the study has been expanded and more recent reports were written in 2015 and 2016 [79], [83].
So far, a single medical centre (i.e. Tricarico s.r.l. dental centre in Chiaravalle, Ancona, Italy) has been involved in the clinical trial. No ethic review committees were formally involved in this research; anyway, the trial was performed following the principles outlined in the WMA Declaration of Helsinki - Ethical Principles for Medical Research Involving Human Subjects [84].
The treatment was administered by means of a proper electro-medical device, originally born for the endodontic therapy (also known as root canal therapy) [80], [85]. This device had been already proved to be effective in the treatment of acute pulpitis, showing also the advantages of avoiding the pain typical of the conventional treatment and of shortening the treatment duration [86].
Patients' and therapy characteristics will be described in Paragraph 2.1.1; the goodness of the results related to the clinical outcome, reported in Paragraph 2.1.2, represented the starting point of this PhD research project.

2.1.1. Materials and methods

55 patients (27 males and 28 females, aged 55±8), for a total of 81 dental implants, were treated with such innovative therapy; all the implants showed signs of acute peri-implantitis with bone loss, mobility, inflammation and bacterial infection.
The therapy consists in the application of a radio frequency (precisely 312.5 kHz) alternating electric current burst, with a time duration of 140 ms (very short, in order to avoid dangerous effects to the tissues, since the signal intensity is very high).
The therapeutic signal is delivered between two electrodes (realized in metallic biocompatible material): an active electrode, screwed to the implant fixture (in order to make a good electrical connection), and an electrode of return (also called neutral or passive electrode), put in contact with the gingiva, as illustrated in Fig. 5 C).
A single treatment entails five electric current bursts; in this way, the whole duration of the treatment (included the pauses between two delivered bursts) is of about 2 minutes.

The treatment is given under local anaesthesia and sometimes antibiotics and/or anti-inflammatory drugs are administered to the patient in order to enhance the therapeutic effect [35], [68].

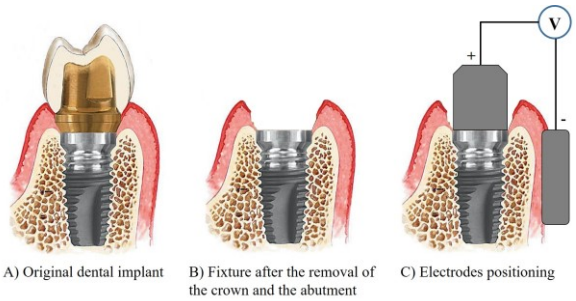

Figure 5. Electrodes positioning: after having removed the crown and the abutment (B), the active electrode is screwed into the fixture, while the neutral one is put in contact with gingiva (C)

In case of particularly severe pathology, the treatment was repeated, up to a maximum of three times.

The implants included in the therapeutic treatment were placed in different positions (i.e. to replace molar, premolar, canine or incisor teeth), as reported in Fig. 6. The number of treated implants per year is reported in Fig. 7.

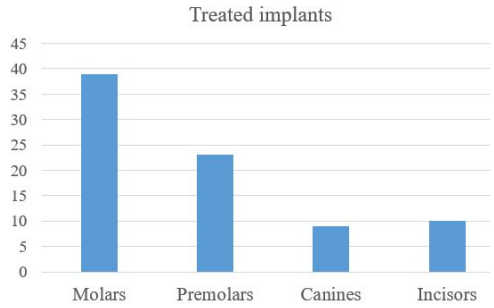

Figure 6. Distribution of the positions of the treated implants

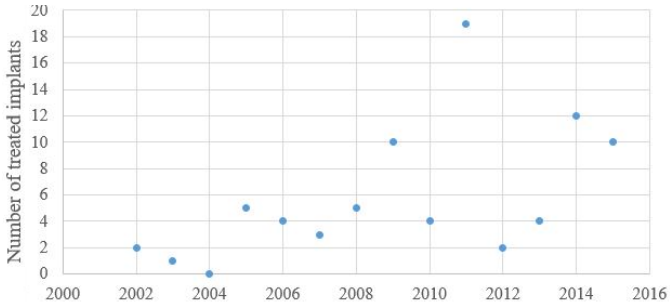

Figure 7. Number of implants treated per year

The success of the therapy was evaluated by observing the colour of the gingiva, by evaluating bleeding and suppuration, by measuring the probing depth of peri-implant pockets and by means of x-rays imaging, in order to measure the bone height around the implant. Such diagnostic instruments are those of a typical peri-implantitis diagnosis [28].

2.1.2. Results

81% of the implants (i.e. 66), corresponding to 84% of the patients, were successfully treated by Dr. Tricarico in his dental office. Follow-up data considered in this research are related to 2002-2015 years.
In the follow-up checks, neither bleeding nor suppuration from the peri-implant soft tissues were observed. In addition, the gingiva showed neither oedema nor redness. So, it is possible to state that none of the inflammation symptoms were present. In Fig. 8 there is an example of images showing the gingiva conditions before and after the treatment.

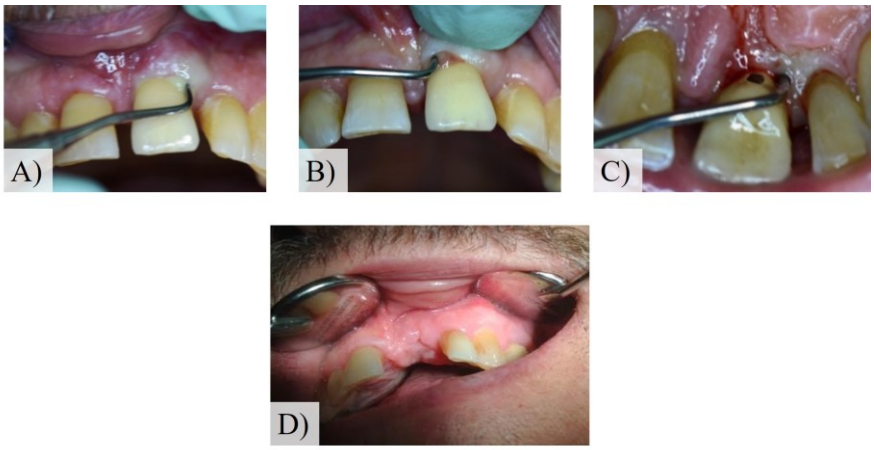

Figure 8. Example of gingiva conditions before the therapy: A) with suppuration, B) with deep gingival pockets and C) with bleeding on probing; and after the therapy: D) healthy gingiva (no inflammation)

As regards the hard tissues, in order to prove the success of such therapeutic methodology, x-ray images were examined. They show that the peri-implant bone healed after the therapy and the bone resorption was arrested (not more than 0.2 mm per year, which can be considered not pathologic [21]); in some cases, it was possible to note also a phenomenon of peri-implant bone regeneration. In this regard, an example of x-ray images before and after the therapy is reported in Fig. 9; it is possible to observe that the bone has completely regenerated after the therapy, allowing the dental implant to recover its stability.

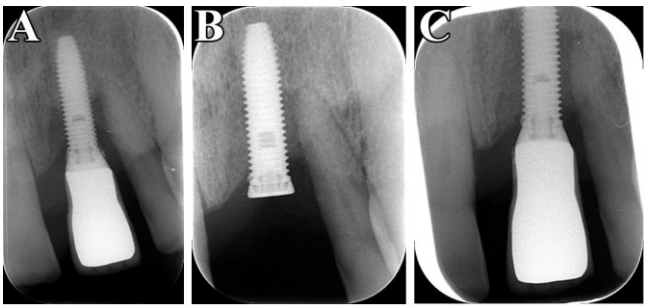

Figure 9: Example of x-ray image of an implant in three different moments: A) before the therapy, B) 1 month after the treatment and C) 8 months after the treatment

The unsuccessful cases (i.e. 19% of the implants, corresponding to 16% of the patients) were linked to very particular conditions or concurrent diseases: chemotherapy, serious aenemia or significant horizontal/vertical bone reduction, hematologic diseases and metabolic disorders. The critical aspects just mentioned will be considered as exclusion criteria for the therapy in the future, so that the success rate will probably be higher.

2.1.3. Discussion and conclusions

The proposed radio frequency current-based therapy for peri-implantitis can be considered among electric treatments and electromagnetic stimulation (whose beneficial effects are described in Paragraph 1.3).
Such trial permitted to obtain information about the safety and the efficacy of the adopted treatment. No complications occurred: the treatment sessions were fast, painless and the benefit for the treated patients was immediate, allowing to functionally recover dental implants otherwise fated to be removed.
As stated in Paragraph 1.3, the main effects of electromagnetic radiation are to inhibit bacteria, to increase bone formation, to positively remodel bone and to reduce inflammation. All these were verified in this clinical trial and allowed to successfully treat peri-implantitis cases, eliminating suppuration, stabilizing the bone level and promoting its regeneration, besides healing the inflamed soft tissues.
So, the adopted approach showed promising results, even more if we consider the unsatisfying outcomes achievable by means of standard therapies [35], [44].
It is now of interest to broaden the present clinical trial, by getting dragged not only Italian but also foreign dentistry and implantology experts, so as to obtain a larger sample to be evaluated.
As it will be described in the Appendix, a prototype of a specific device for peri-implantitis treatment (named PeriCare®) is being developed (the present therapy for peri-implantitis has already been patented) and it will be used for a wider multicenter clinical trial. This would permit to optimize the treatment parameters, both in terms of therapeutic doses and of used instrumentation (e.g. the electrodes shape). In addition, it could be possible to obtain further indications also on the methodologies applied to quantify the pathology

severity; in fact, during the present PhD research project, bioimpedance measures have been evaluated as a means to detect inflamed tissues and they can be useful also to assess the bone level (bioimpedance measurements will be described in detail in Chapter 3).

2.2. Electrical characterization of the therapeutic device

Endox® Endodontic System is a device used in endodontic therapy since the late 90s [80]. According to the standards of IEC 60601 published by the International Electrotechnical Commission, it is a Class I device (in fact it is a hand-held surgical instrument) of type BF (since there is a conductive contact with the patient) [87]. According to the European directive 93/42/CEE (imposing the obligation of CE marking for products sold within the European Economic Area [88]), this device is of class IIb, which means that a notified body had to do determined inspections during the realization phase [89, p. 42].

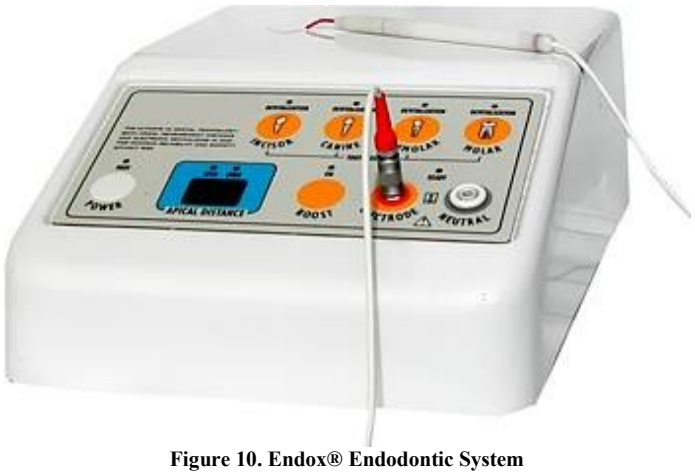

Figure 10. Endox® Endodontic System

It is in compliance with the regulations EN 60601-1 (Medical electrical equipment – Part 1: General requirements for basic safety and essential performance), EN 60601-1-2 (Medical electrical equipment - Part 1-2: General requirements for basic safety and essential performance - Collateral Standard: Electromagnetic disturbances - Requirements and tests) and EN 60601-2-2 (Medical electrical equipment - Part 2-2: Particular requirements for the basic safety and essential performance of high frequency surgical equipment and high frequency surgical accessories).
This electromedical device has a rating power of 110 W on a resistive load of 1000 **Ω**, for a duration of 140 ms. Its working frequency is equal to 312.5 kHz.
Endox® has two stages application: the former is the root canal length measurement to localise the radicular apex (done in Direct Current - DC - with a 9 V battery, sometimes causing an itching sensation due to the direct current passage), while the latter is the root canal treatment (also known as “devitalisation”), consisting in pulp removal, canal cleaning, disinfection and sealing. The power of the treatment can be regulated depending on the tooth type; different levels are available: incisor, canine, premolar, molar and molar plus boost (that is, ever higher than molar option).
Such a system is more powerful than the traditional methods for the root canal treatment [90], since it allows to efficiently reduce bacteria, to remove pulp residues not only in the

main canal but also in lateral canals and dental tubules (barely reachable mechanically), to avoid excessive pain and to save time. The effectiveness of the treatment was proved by means of Reflection Electron Microscope (REM) and histological analysis; neither thermal effects nor other damages to the surrounding tissues were observed [91]. However, proper cleanliness and optimal efficacy are reached only after the conventional canal preparation [92]. Finally, literature results about the antibacterial effectiveness (compared with conventional irrigation protocols, e.g. with sodium hypochlorite) in the endodontic treatment are controversial [93].
Endox® scheme is not known, so it is possible to consider it as a black box (Fig. 11) with two different functions, that is, the measurement of the canal length (by means of a DC electric apex locator, which is actually been largely overtaken [94]) and devitalisation (by means of a Radio Frequency - RF - current).

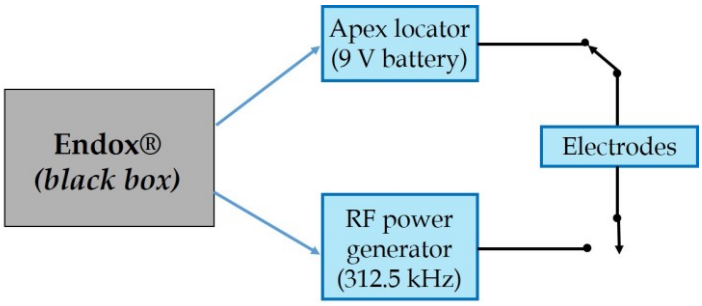

Figure 11. Endox® scheme: black box with two different functions, that is the measurement of root canal length (i.e. apex locator) and treatment (i.e. Radio Frequency - RF - power generator)

Both the measurement and the therapeutic signals are supplied between an active electrode (which is a fine surgical stainless steel needle, acting as the electrode, inserted in the open root canal) and a passive one, cylindrical, held in the patient's hand, suggesting an unbalanced scheme for the circuit representation.
As said in the introduction of this chapter, positive side effects of such signals have been noticed in tissues surrounding the treated tooth root, beyond the expected ones of the mere endodontic treatment, so that a research project to better understand the underlying mechanisms has been started.
The first aim was to electrically characterize this medical device, in order to obtain an equivalent circuit (according to Thevenin's theorem [95]), which can be used to numerically simulate the therapy and consequently to study the effects on biological tissues.

2.2.1. Materials and methods

In order to better understand the working principle of Endox® device, it is necessary to electrically characterize it. The simplest way to do it consists in the computation of the equivalent circuit obtained by means of the application of Thevenin's theorem [95].

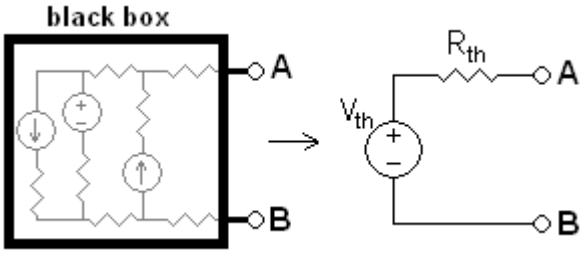

Figure 12. Thevenin's theorem principle scheme: any black box containing current/voltage sources and resistors can be replaced by a series connection between an equivalent voltage source (V_{th}) and an equivalent resistance (R_{th})

The equivalent voltage source is the open-circuit voltage at the network terminals, while the equivalent resistance is that observable at the network terminals A-B when all the ideal voltage sources were replaced by short circuits and the ideal current source by open circuits (i.e. when all the independent sources are deactivated).
This theorem also applies to Alternating Current (AC) circuits, consisting of reactive and resistive impedances. The main assumption is that the electric network is linear, but actually many circuits are linear only over a certain range of values and this is a limit of such a technique. Performed tests allow us to assume circuit linearity during the RF burst generation in the present work.
To obtain the Thevenin equivalent circuit of the device, the scheme reported in Fig. 13 can be used.

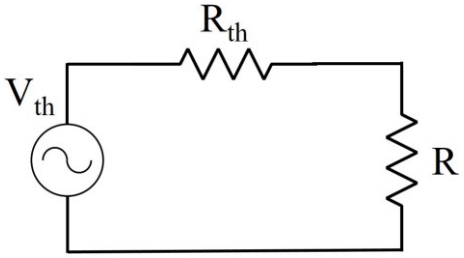

Figure 13. Thevenin electrical circuit and measurement resistor (R)

The computation of the characteristic parameters V_{th} and R_{th} is based on the Root Mean Square (RMS) values of the voltage V, measured on the load R for different values of the measurement resistor R. Resistors were used because at this frequency the prevailing conduction mechanism is the conductive one (this was verified by comparing σ with ωε and, so, by evaluating conduction and displacement current).
The circuit can be considered as a voltage divider and so described by the Eq. 1:

$$V = V_{th}\frac{R}{R + R_{th}} \tag{1}$$

By doing the inverse of Eq. 1, Eq. 2 is obtained:

$$\frac{1}{V} = \frac{1}{V_{th}} \frac{R + R_{th}}{R} = \frac{1}{V_{th}} + \frac{R_{th}}{V_{th}} \frac{1}{R} \tag{2}$$

The measurements were done on three resistors of different values: 750 Ω, 3 kΩ and 6 kΩ (nominal values). Then, the plot of 1/V versus 1/R was considered and the fitting straight line was computed according to the method of linear least squares. This line is characterised by two parameters: slope (m) and y-intercept (q); they can be computed according to Eq. 3 and Eq. 4, respectively.

$$m = \frac{R_{th}}{V_{th}} \tag{3}$$

$$q = \frac{1}{V_{th}} \tag{4}$$

So, Thevenin circuit parameters can be computed as indicated in Eq. 5 and Eq. 6, for V_{th} and R_{th}, respectively.

$$V_{th} = \frac{1}{q} \tag{5}$$

$$R_{th} = m * V_{th} \tag{6}$$

Once the Thevenin circuit was obtained, it was verified by means of two different resistive loads: 1 kΩ and 4.5 kΩ.
All the resistors used was suitable for the delivered power values (power-resistors were used), as well as for the used measurement frequency (i.e. 312.5 kHz).
Finally, the power level was computed to evaluate the agreement with the nominal one (i.e. 110 W on a resistive load of 1000 Ω, as previously said). The obtained values were then compared with the shape of the power curve, which is described by Eq. 7:

$$P = \frac{V^2}{R} = \frac{R}{(R + R_{th})^2} * {V_{th}}^2 \tag{7}$$

This procedure was repeated for each power option of the device: incisor, canine, premolar, molar and molar plus boost (as described in Paragraph 2.2).

2.2.2. Results

Thevenin equivalent circuits were computed for each power option available (i.e. incisor, canine, premolar, molar and molar plus boost).

Results are reported in terms of plots concerning the relationship between 1/V and 1/R (where V is the measured RMS value on the resistance R) and of the Thevenin equivalent circuit parameters. Fitting lines are reported in Fig. 14-18 for incisor, canine, premolar, molar and molar plus boost levels, respectively; Tab. 1 shows V_{th} and R_{th} parameters for all the levels.

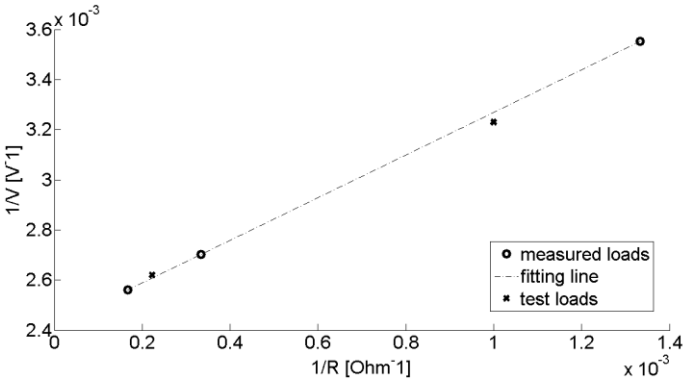

Figure 14. Fitting line between 1/V and 1/R obtained on three measured loads and verified on two test loads - incisor power level

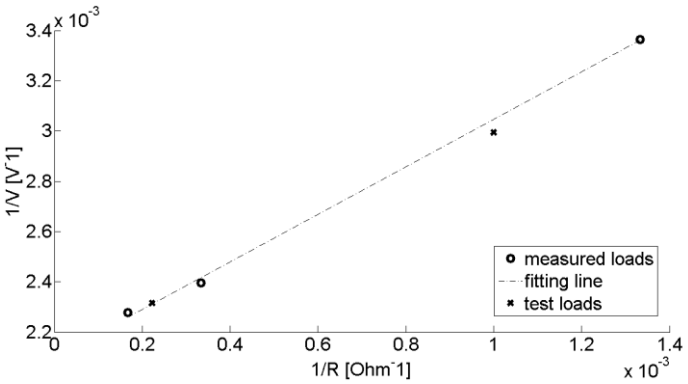

Figure 15. Fitting line between 1/V and 1/R obtained on three measured loads and verified on two test loads - canine power level

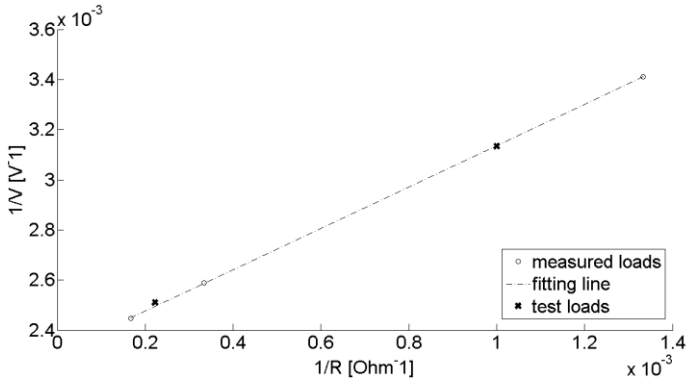

Figure 16. Fitting line between 1/V and 1/R obtained on three measured loads and verified on two test loads - premolar power level

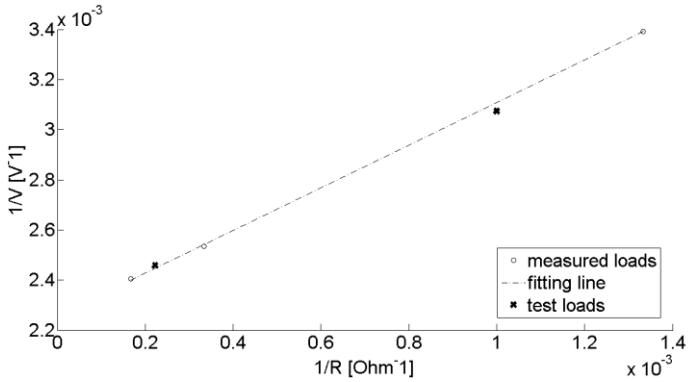

Figure 17. Fitting line between 1/V and 1/R obtained on three measured loads and verified on two test loads - molar power level

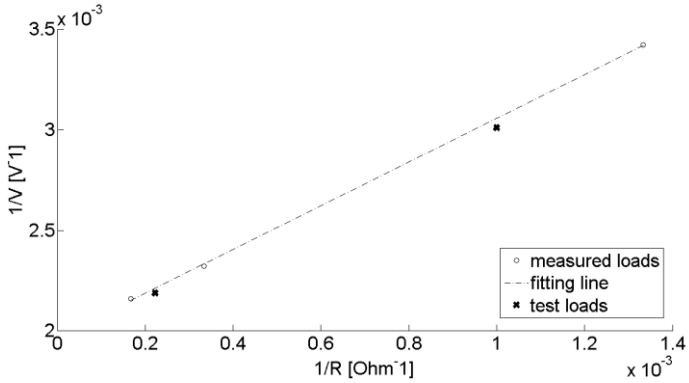

Figure 18. Fitting line between 1/V and 1/R obtained on three measured loads and verified on two test loads - molar power level plus boost

Table 1. Thevenin circuit parameters for the different power levels

Power level	**V_{th} [V]**	**R_{th} [Ω]**
Incisor	435	392
Canine	500	495
Premolar	435	398
Molar	455	408
Molar plus boost	526	594
Average values	**474**	**458**

In order to use the Thevenin equivalent circuit in numerical simulations (as it will be described in Paragraph 2.3), the average values of those obtained for the different power levels were computed (they are reported in the last row of Tab. 1).

As regards the power values, they are reported in Fig. 19-23 for incisor, canine, premolar, molar and molar plus boost levels, respectively.

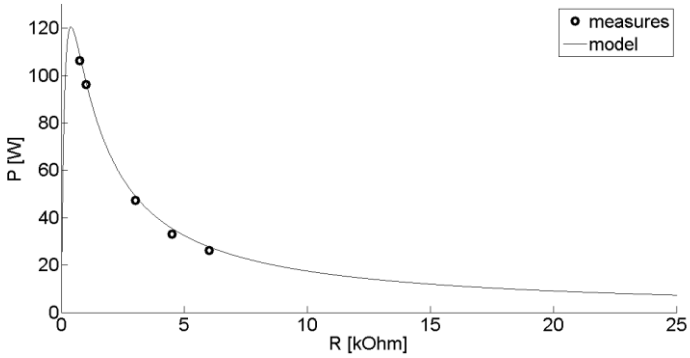

Figure 19. Power curve shape (solid line) with measured power values (circles) - incisor power level

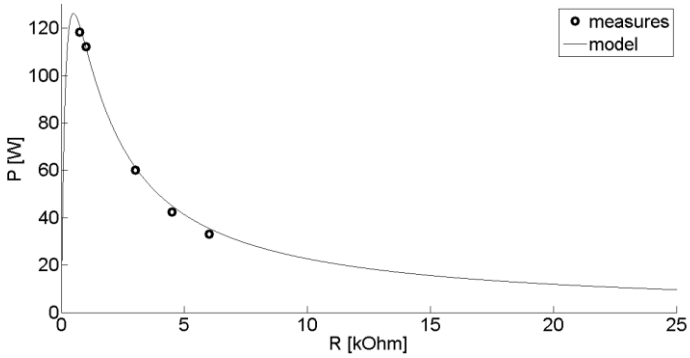

Figure 20. Power curve shape (solid line) with measured power values (circles) - canine power level

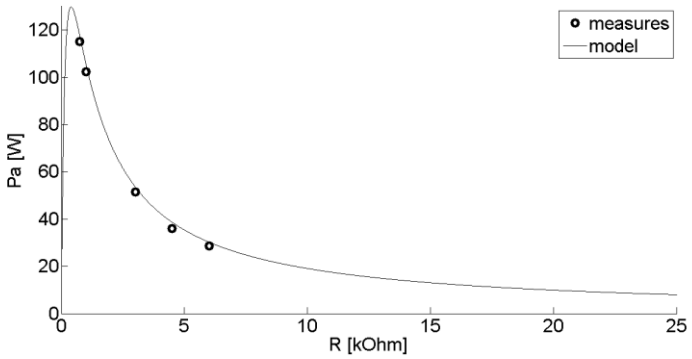

Figure 21. Power curve shape (solid line) with measured power values (circles) - premolar power level

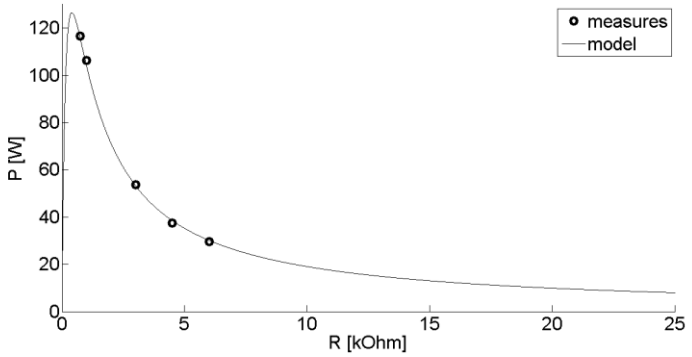

Figure 22. Power curve shape (solid line) with measured power values (circles) - molar power level

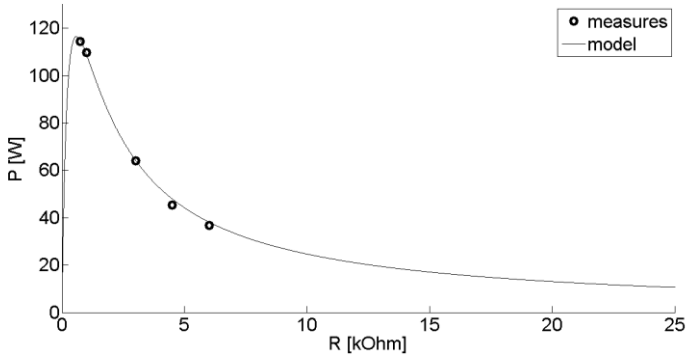

Figure 23. Power curve shape (solid line) with measured power values (circles) - molar plus boost power level

With regard to the nominal power value of the device (i.e. 110 W on a pure resistive load of 1 kΩ, which means a high current, however not dangerous thanks to the very short duration and the frequency of the signal), in Tab. 2 power values on 1 kΩ resistor are reported.

Table 2. Power values on 1 kΩ resistive load

Power level	Measured power [W]
Incisor	96
Canine	112
Premolar	102
Molar	106
Molar plus boost	110
Average value	**105**

So, given the obtained results about the electric parameters of the device, the system can be considered linear, so that the use of Thevenin's theorem is correct.

2.2.3. Discussion and conclusions

Thanks to electrical measurements, a Thevenin's equivalent circuit of Endox® electromedical device was obtained for each available power level (i.e. incisor, canine, premolar, molar and molar plus boost) by considering the RMS value of the signals.
Such parameters were achieved by making the measurements on three resistive loads (i.e. 750 Ω, 3 kΩ and 6 kΩ), then the models were verified by repeating the measurements on two different loads (i.e. 1 kΩ and 4.5 kΩ). From Fig. 14-18 it is possible to infer that the obtained Thevenin model has a good predictive capability, since the residuals are very low (< 2%).
In order to numerically simulate the electromedical device, the average values of these circuits were considered, obtaining a unique model. This consists of a series connection between a sinusoidal voltage generator (V_{th} = 474 V, RMS value, corresponding to a peak value of 474*√2 V) and a resistance (R_{th} = 458 Ω).
The possibility to use this model in numerical simulations makes possible to simulate the therapy and to better understand the underlying acting mechanisms, as it will be described in Paragraph 2.3.
In this way, in the future it would be possible also to modify the therapy in its different aspects (e.g. power, frequency, electrode shape and positioning), looking for the combination providing the best outcome.
Moreover, the power values were measured on the five different considered resistive loads (i.e. 750 Ω, 1 kΩ, 3 kΩ, 4.5 kΩ and 6 kΩ) and they were compared to the power curve shape obtained by means of Thevenin model, for each power level. In Fig. 19-23 it is possible to observe that such values are in agreement with those predicted by the models, so they can be considered reliable to make predictions on the applied therapeutic signals.
As regards the nominal power value of the device, from Tab. 2 it is possible to state that the measured values for the different levels are in agreement with the declared power; in fact,

only for canine level the rating value of 110 W is slightly exceeded, but all the other ones are lower. If the average value is considered, a power of 105 W is obtained. By observing the shape of the power curve obtained from the Thevenin model (Eq. 7), it is possible to note that power decreases for higher loads and this is reasonable, since the power is inversely proportional to the load itself (except for very low loads, inferior to R_{th} parameter, in correspondence of which there is the maximum power transfer).

2.3. Numerical simulation of the therapy

The Finite Element Analysis (FEA), also known as Finite Element Method (FEM), is a numerical tool to find solutions to problems of different nature, from the stress-strain evaluation to the electromagnetic quantities distribution, based on partial differential equations, which are then reduced to algebraic ones [96].
It is the most versatile among the numerical methods when the treated objects show complex geometries and inhomogeneous means [97]. In fact, it divides the problem domain into smaller and simpler homogeneous elements (called "finite elements"), where the equations are solved ("discretization" of the problem, obtained with the so-called "mesh"). Then, the various solution functions are combined in order to obtain the solution in the whole domain, minimizing the global error.
In this way, it is possible to represent sophisticated geometries (also thanks to the development of digital images techniques) including even materials with different properties (e.g. mechanical or electric properties).
FEM was initially developed in the early 1960s to solve structural problems (particularly in civil and aeronautical engineering), but its application fields expanded rapidly also thanks to the major availability of computers with advanced performances.
In 1976 FEA was used for the first time also in implant dentistry [98] and it has become increasingly useful to predict the effects of stress on the implant and on the surrounding bone [99]. Most of the applications are in the mechanical area (they have grown exponentially in the last decade, generating an increasing interest in dental research [100]). They are focused on the behaviour of the implant-bone system when subjected to different mechanical loads, depending on several factors (e.g. the implant dimensions, the surface finishing and the quality of the peri-implant bone); this could improve the shapes of the preparations, since nowadays CAD-CAM technologies in dentistry are spreading [101]. More recently in the literature there are some papers dealing with tooth and electromagnetism, concerning the endodontic treatment and the electronic apex locators [102]–[105].
Given that the potentiality of FEM has been proved to be very high, in this study the technique has been applied in order to simulate the therapy for peri-implantitis based on the application of radio frequency electric current (as described in the introduction of this Chapter), in order to gain additional insight into the underlying mechanisms. In fact, with this kind of numerical simulation it is possible to obtain electric current and field distributions and to observe how they depend on the therapeutic setup configuration (e.g. electrodes positioning). In this way, in the future, the therapy could be modified and improved, and the design of the electromedical device could be adjusted on the basis of the results of the numerical analysis.
In addition, this kind of simulation was done also in the case of a natural tooth root affected by periodontitis, since the therapy is effective in terms of inflammation reduction, as described in Paragraph 1.3, so in the future its application field could be extended in this direction.
Moreover, the same numerical method has been applied also to simulate the bioimpedance measurements, as it will be described in Chapter 3.

2.3.1 Materials and methods

The 3D model was realized in COMSOL Multiphysics® environment [106]. The geometric and the electric properties of biological tissues were taken from the literature, as it will be shown below. As regards the electromedical device, the Thevenin equivalent circuit (described in Paragraph 2.2) was used.

2.3.1.1. COMSOL Multiphysics®

COMSOL Multiphysics® is an advanced solver and numerical simulation software usable in different physics and engineering applications. It can be used with whatever system that can be described by means of partial differential equations. There is also the possibility of considering more than a physic at the same time, coupling different physics phenomena (e.g. to consider the thermal effect associated with the Joule effect due to electrical phenomena).
It provides different modules for the various applications: electromagnetism, mechanics, fluid dynamics and chemistry; in particular, in this thesis mainly the AC/DC module was used. It allows to simulate electric, magnetic and electromagnetic fields in static and low-frequency applications, that is when the system dimensions are far smaller than λ (which is the wavelength, equal to c/f, where c is the waveform speed and f the considered frequency). Both time and frequency domains analyses are possible. The simulations are based on Maxwell's equations and on materials laws (e.g. Ohm's law).
In Fig. 24 there is the typical user interface of the software.

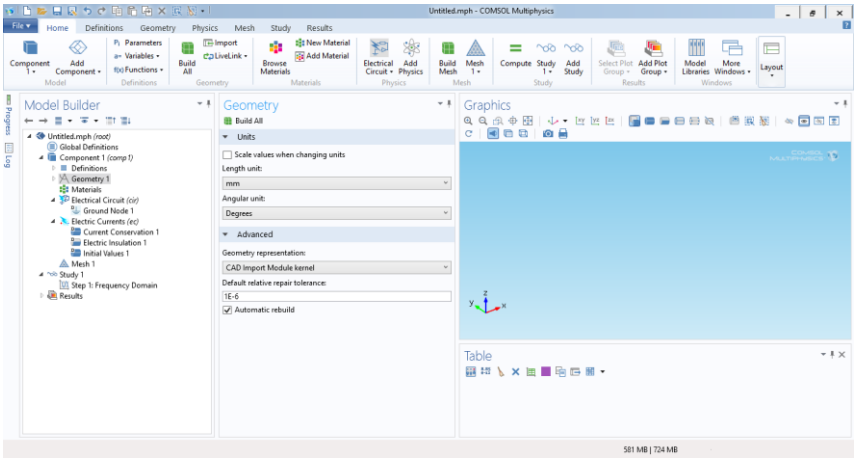

Figure 24. COMSOL Multiphysics® typical user interface

On the left, there is the "Model Builder", with the "model tree", showing all the blocks of the created model:

- the geometry of the model, with all its parts; it can be imported or drawn inside the software itself (the latter is the case);

- the materials, with their required properties, depending on the aim of the model (e.g. for electromagnetic studies, electrical conductivity, relative permittivity and relative permeability are required);
- the used physics; in this case, there are "Electrical circuit" for the simulation of Thevenin equivalent circuit of the therapeutic device and "Electric Currents", used to compute electric field, current and potential distributions (with the hypothesis that, given the low frequency, the inductive effect is negligible);
- the mesh, used to discretize the geometry into finite elements of determined shape (e.g. tetrahedral mesh);
- the studies, in time and/or frequency domains.

The underlying equations are the current density (given by the contribution of conductive and displacement currents, expressed with complex quantities) (Eq. 8) and the current conservation equation (Eq. 9).

$$J = \sigma E + j\omega D \tag{8}$$

$$\nabla \cdot J = 0 \tag{9}$$

By expressing the electric field as the gradient of scalar electric potential ($E = -\nabla V$), through Eq. 9 it is possible to obtain Eq. 10, which is a Laplace equation for complex potential:

$$\nabla \cdot [(\sigma + j\omega\varepsilon_0\varepsilon_r)\nabla V] = 0 \tag{10}$$

Boundary conditions have to be defined: V = 0 V on the passive electrode, $V = V_{th}$ on the active one (V_{th} is the voltage generator, as defined in Paragraph 2.2).

2.3.1.2. Tooth geometry

Natural teeth can be grouped into different types: incisors, canines, premolars and molars, as shown in Fig. 25 [107]. Indeed, there are eight incisors (four maxillary, four mandibular), four canines (two maxillary, two mandibular), eight premolars (four maxillary, four mandibular) and twelve molars (six maxillary, six mandibular). They have different shapes as well as different functions:

- Incisors are necessary to cut food and are important also for phonation and for aesthetic aspects;
- Canines have a sharp surface, suitable to grip and tear food; they play an important role in the facial expression;
- Premolars have a flat biting surface, to crash food;
- Molars are the largest teeth, with a flat biting surface, to chew and grind food.

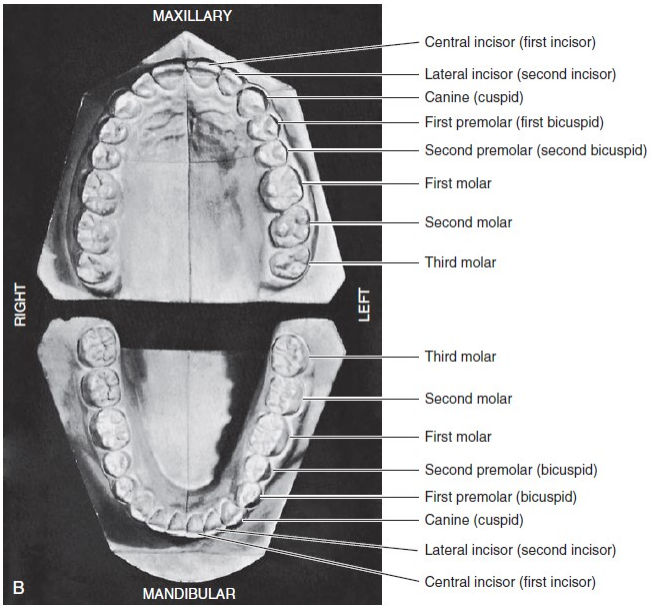

Figure 25. Teeth anatomy chart, with maxillary and mandibular arches

When a natural tooth needs to be substituted by an implant, this one shape has to resemble the natural tooth root one, as shown in Fig. 26. In this way, the implant can behave in a way that is similar to the tooth it replaces, in terms of load, functions and so on.

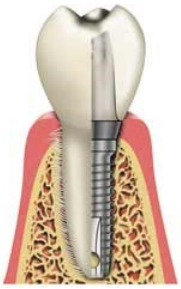

Figure 26. Natural tooth and dental implant comparison: they are similar in shape and dimensions, in order to allow a proper behaviour of the prosthesis

The therapy was simulated on a dental implant placed in replacement of a second premolar tooth root.

The dental implant screwed in the jawbone and the peri-implant tissues affected by peri-implantitis were modelled in a simplified way; a more precise and detailed model should be obtained by means of a reconstruction process based on computed tomography or magnetic resonance tomography volumetric data [108], but the computational load would be very high.

The realized model presents the following tissues: alveolar bone, gingiva (considered more generally as connective tissue) and inflamed gingiva (typical of peri-implantitis, as described in Paragraph 1.1). The dental implant (realized in titanium) dimensions were

similar to those of a second premolar tooth root [107]: 14 mm in length, 4 mm in diameter. For the sake of simplicity, changes in geometric dimensions of the inflamed tissue were not considered, even if the inflammatory process is actually characterized by oedema (i.e. swollen tissue) [109]. The realized geometry is reported in Fig. 27.

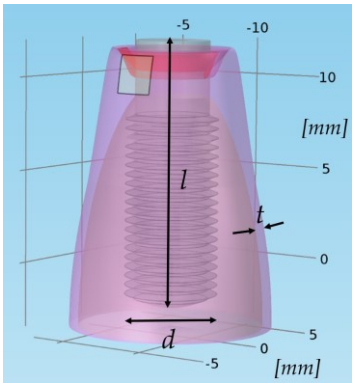

Figure 27. Model geometry of the dental implant screwed in the jawbone: d is the implant diameter (4 mm), l its length (14 mm) and t the gingiva thickness (1 mm)

Then, the simulation was run also on the model of a natural tooth root, related to a premolar. A frontal section of the geometry of the realized 3D model is reported in Fig. 28. In this case, more tissues are present: enamel, dentin, bone, pulp and gingiva.

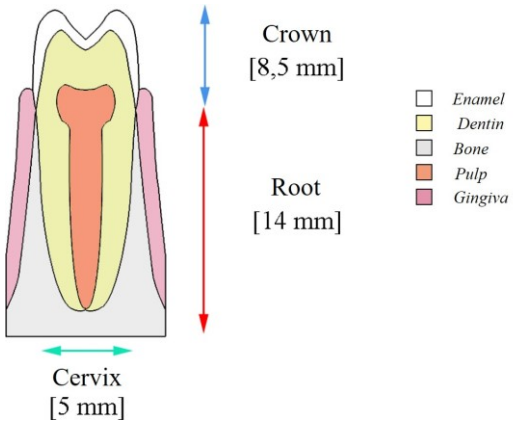

Figure 28. Geometry of a natural premolar tooth root - frontal section

2.3.1.3. Tissues electrical properties

In order to make an electromagnetic simulation, it is necessary to define the electric properties of the involved materials (i.e. enamel, dentin, pulp, gingiva, inflamed gingiva and bone): electrical conductivity (σ), relative permittivity (ε_r) and relative permeability (μ_r). These were taken from the literature [110]–[112]; since these properties are frequency-

dependent, a frequency equal to 312.5 kHz (i.e. the therapy frequency) was considered. With regard to the inflamed gingiva, its electrical conductivity was considered as twice the healthy gingiva one [113], since it is richer in liquid content than the healthy one (hyperaemia and infiltration of the adjacent tissues are typical of the inflammatory process [114]). On the contrary, the relative permittivity was not changed, because, to the best of the author's knowledge, there are no evidences of such parameter changes related to the inflammatory process.
Such biological tissues electric properties are reported in Tab. 3.

Table 3. Biological tissues electric properties at 312.5 kHz

Tissue	**σ [S/m]**	**ε_r [dimensionless]**	**μ_r [dimensionless]**
Enamel	0.021	190	1
Dentine	0.022	190	1
Pulp	0.390	347	1
Gingiva	0.390	245	1
Inflamed gingiva	0.780	245	1
Bone	0.021	190	1

These values were obtained on a limited population [110]–[112] and the inter-individual biological variability is high, nevertheless they are essential to better understand what happens during the therapy.

2.3.1.4. Therapeutic device model

The electromedical therapeutic device was simulated by means of its Thevenin equivalent circuit (obtained with the procedure described in Paragraph 2.2), that is, a series connection between a sinusoidal voltage generator (474 V RMS value, corresponding to a peak value of 474*√2 V) and a 458 Ω resistor.

In the case of the dental implant, this circuit was connected between two electrodes, simulating those used in the clinical trial (as described in Paragraph 2.1):

- The active electrode, which is the implant itself (in real practice, it is screwed into the implant fixture, providing a good electric connection), working as the generator terminal;
- The passive electrode (also called neutral or return electrode), adhering to the gingiva; it is a 4 mm^2 area metallic square surface.

The neutral electrode was placed in different positions, to demonstrate that in this way it is possible to drive the therapeutic current lines.

With regard to the simulation of the treatment in the natural tooth affected by periodontitis, the two electrodes (i.e. 4 mm^2 area metallic square surfaces) were placed in the lingual and

the buccal sides of the gingiva, as reported in Fig. 29, so as to make the electric current pass through the tissue between the two poles.

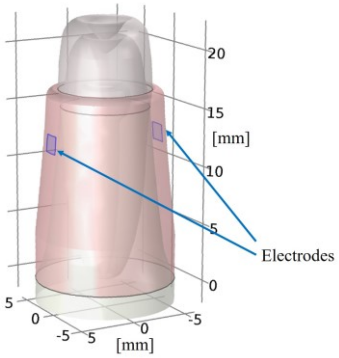

Figure 29. Electrodes positioning in case of natural tooth root treatment (periodontitis)

2.3.1.5. Simulation parameters

Once the geometry was realized, it was discretized with a tetrahedral mesh, denser in the regions near the edges and around the corners. The one related to the dental model implant is shown in Fig. 30; the model has got 340754 tetrahedral, 63325 triangular and 2833 edge elements.

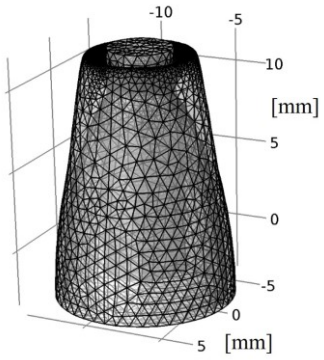

Figure 30. Meshed geometry (tetrahedral mesh) – dental implant model

The mesh concerning the natural tooth root is reported in Fig. 31; it has got 168651 tetrahedral, 17621 triangular and 167 edge elements.

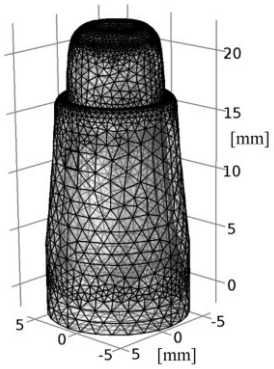

Figure 31. Meshed geometry (tetrahedral mesh) – natural tooth root model

As regards the type of the study, the frequency domain was considered, setting the frequency parameter equal to 312.5 kHz. The simulation was run selecting a stationary solver, for a fully coupled solution.
Results can be presented in different ways: 2D and 3D plots, tables, values obtained from integration or other mathematical operations, selecting the variable of interest (e.g. electric current or field).

2.3.2. Results

The simulation results allow to investigate the distributions of electric current and field, in order to better understand the mechanisms which the therapy is based on.
Results related to the simulations in the case of the dental implant and of the natural tooth root are reported in Paragraphs 2.3.2.1 and 2.3.2.2, respectively.

2.3.2.1. Results – dental implant (peri-implantitis)

In Fig. 32 the distribution of the electric current is reported (surface and arrow plot), while in Fig. 33 there is the distribution of the electric field; in particular, they are frontal sections of the model, passing in the middle of the implant. It is worthy to underline that the active electrode is the implant itself, while the passive one adheres to the gingiva (in Fig. 32-33, it is in correspondence of the red lateral spot, where there the electric current is focused on).

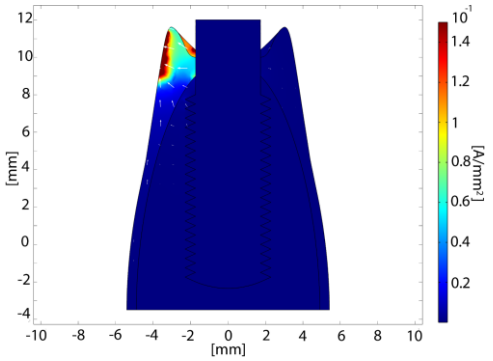

Figure 32. Electric current density distribution (peri-implantitis) - frontal section

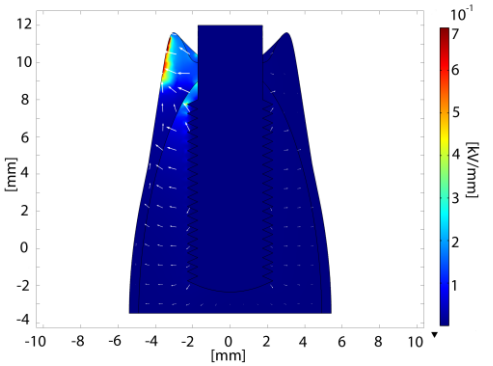

Figure 33. Electric field distribution (peri-implantitis) - frontal section

In Fig. 34 it is possible to observe that moving the neutral electrode along the gingiva surface, it is possible to drive the therapeutic current lines in different areas.

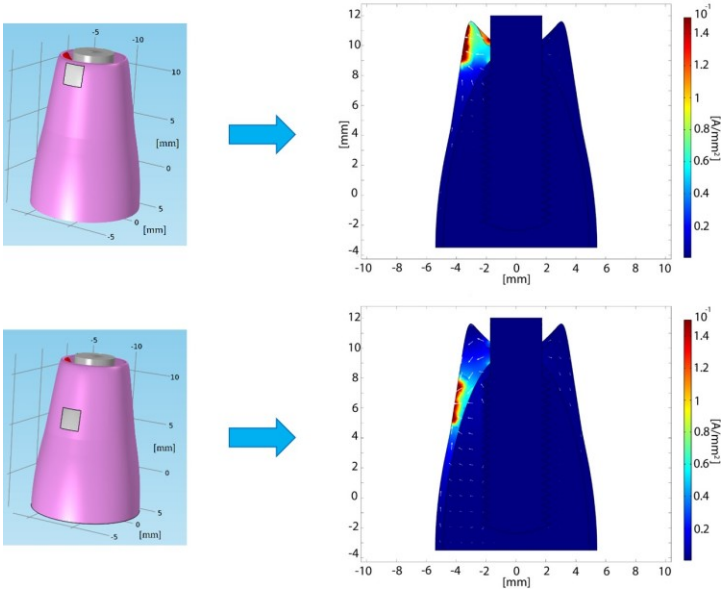

Figure 34. Distribution of electric current lines with different neutral electrode positioning: upper (top) and lower (bottom) positioning allows to drive the electric current lines in different tissue portions

2.3.2.2. Results – natural tooth root (periodontitis)

With regard to the natural tooth root simulation, the distributions of electric current and field are reported in Fig. 35-36, respectively (frontal sections of the model). The two electrodes in Fig. 35-36 are in correspondence of the light spots (due to the higher electric current density) on the sides of the gingiva.

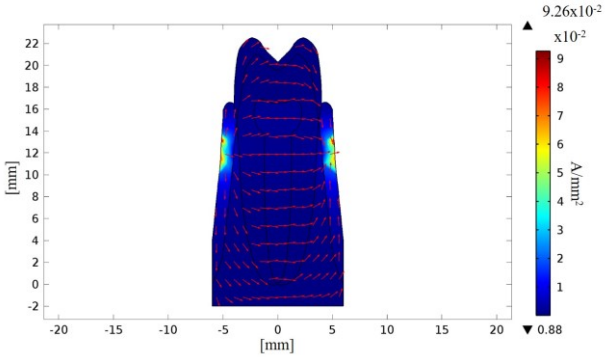

Figure 35. Electric current density distribution (periodontitis) - frontal section

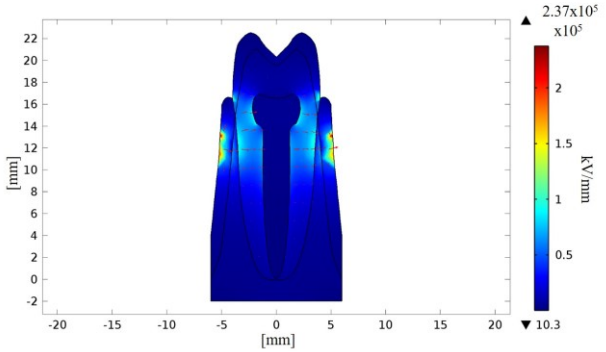

Figure 36. Electric field distribution (periodontitis) - frontal section

2.3.3. Discussion and conclusions

Numerical simulations allow to obtain the electric current and field distributions resulting from the therapeutic procedure, applied to a dental implant screwed in the jawbone affected by inflammation (typical of peri-implantitis disease) or to a natural tooth root with inflamed periodontal tissue (i.e. periodontitis). In this way, it is also possible to try to investigate the mechanisms underlying the different effects of the therapy (i.e. inflammation reduction, bone regeneration).

With regard to the case of peri-implantitis, from Fig. 32 it is possible to infer that the anti-inflammatory effect is probably linked to the electric current passing through the soft tissues (i.e. gingiva). Moreover, the electric current is focused on the inflamed portion of the gingiva, since its electrical conductivity is higher (due to the presence of liquids in the inflamed tissues). The therapy proves to be delimited to a small area and its effects on non-interested areas are minimized. In addition, also moving the return electrode in a proper position permits to drive the therapy in the impaired area, so contributing to localize the therapy (Fig. 34).

On the contrary, from Fig. 33 it is possible to deduce that the bone healing is accelerated by the electric field (stimulation of bone formation by means of pulsed electromagnetic field is well documented in the literature [115], [116]).

Similarly, with regard to the periodontitis case, in Fig. 35 it can be noted that electric current is focused on soft tissue, so that positive effects on the inflammatory process are possible.

In conclusion, it is reasonable to think that such therapy provides positive effects on inflammation thanks to the electric current, while the electric field promotes the bone healing. Moreover, in the future the therapy could be improved by considering the results of simulations made with different configurations, such as by varying the electrodes positioning and/or shape and dimension (geometry and position of the electrodes affect the electric field distribution [117]). This kind of “parametric study” was made concerning the bioimpedance measurements simulations, as it will be described in Chapter 3.

With regard to the electrodes adhering to the gingiva, it is important to consider that the current density is higher at the edges; in addition, there are numerical errors (i.e. geometric singularities) due to edge effects (the electric potential distribution is “smooth”, but its gradient, $E = -\nabla V$, is theoretically infinite). So, the numerical results obtained in edge zones (e.g. regarding current density) cannot be considered reliable (at least 2-3 elements from the edges should not be considered [118]), but the global solution remains correct (the results elsewhere are not polluted at all).

Chapter 3.

Bioimpedance measurements: inflammation detection

Bioimpedance method is a powerful technique, widely applied to monitor the remodelling and changes in the organism under normal and pathological conditions [114]. It is advantageous because it is minimally invasive and the necessary instrumentation is simple, ergonomic, non-invasive, painless and relatively inexpensive [119]. The interest in such measurements is constantly growing, as it is well-documented by the presence of international conferences on this theme, such as the International Conference on Electrical Bio-Impedance (ICEBI, whose latest edition took place in Stockholm in June 2016 [120]). Many different figures are involved in the development of such measurements: biomedical engineers, biophysicists, mathematicians, electrochemists, computer scientists, physiologists, biologists and medical doctors.
Bioimpedance can be defined as the tissue ability to oppose electric current flow [121].
The popularity of bioimpedance measurements in medicine is growing and there are several clinical and laboratory application fields, among which it is possible to highlight the following ones:

- The monitoring of electrode-tissue contact in medical electrode applications (e.g. ECG and EEG) [122], [123];
- Vital sign monitoring, such as Impedance Cardiography (ICG), to monitor cardiodynamic parameters (e.g. heart rate and stroke volume) [124];
- Lung imaging (by means of Electrical Impedance Tomography, EIT [125]) and monitoring (by means of multisine Electrical Impedance Spectroscopy, EIS [126]);
- Skin diagnosis (e.g. skin cancer, dermatitis, skin moisture, sweat activity and hyperhidrosis [127]–[129]);
- Tissue characterization (e.g. estimation of body composition to monitor nutrition and physical training or screening of cancer) [130]–[134];
- The assessment of oxidative stress (linked to vascular inflammatory response) by means of EIS, which could be included in echocardiography, tomography or micro-thermal sensors to assess pre-atherosclerotic lesions (integrating systems in already existent ones allow to broaden their use) [135], [136];
- The monitoring of bronchial, urinary bladder, joints and airway inflammation [137]–[141];
- Biology and biochemistry applications to assess cell size and shape, the state of the cell membranes and the status of intra- and extra- cellular media [142]–[145];

- Dentistry applications, in particular for the measurement of the root canal length [146], [147], for the characterization of hard dental tissues (i.e. enamel and dentin [148], [149]) and, recently, for the detection of caries lesions [150], [151]).

Human tissues impedance values vary with their physiological/pathological state [113], so they can be used with diagnostic aims. In particular, bioimpedance method can be a useful technique to diagnose an impaired site of a tissue when compared with the corresponding healthy area, employed as the control. An approach like this has been used with different aims; for example, in [152] the authors have detected thoracic traumas by comparing the phase angles of bioimpedance measured in both the thorax sides. While in a study made on a mammary gland, the authors have reported a bioimpedance value of the inflamed gland 2-3 fold lower than that of the contralateral one [113]. In fact, tissue inflammation causes an increase of electric conductivity with respect to normal values; this is due to the presence of liquids (hyperaemia, extravasation of plasma and infiltration of the adjacent tissues are typical of the inflammatory process [113], [137]). These results have suggested the use of bioimpedance method as a means to locate inflamed tissues in oral environment [153], which is a common scenario in case of periodontitis or peri-implantitis. This technique would represent an objective means to localise and quantify inflammation, since at present the evaluation of inflammations is done mainly with the naked eye, by observing the redness and the swelling of the gingiva.
Such bioimpedance-based localization procedure could permit to focus the radio frequency alternating current therapy in the impaired area, since the current densities and pathways from an electrical signal are determined to a considerable extent by the electric properties of biological tissues [154]. Thanks to the discrimination between healthy and inflamed tissues, the therapy could be improved, enhancing the effect on the impaired site and minimizing the involvement of the surrounding tissues.
In addition, it is important to assess inflammation phenomena in oral environment, since there is the evidence that titanium-based implants under conditions of biological inflammation present an increased potential for corrosion [155].
A few numerical models were realized in order to simulate this measurement procedure in peri-implant tissues and also in natural tooth roots. The validity of such models was investigated by means of an in vitro model representing a simplified version of the numerical one (Paragraph 3.1.1).
Furthermore, some experimental measurements have been made on patients with dental implants in case of healthy tissues, inflammation and peri-implantitis. Also measurements in natural teeth have been made, paying particular attention to the design of the electrodes used for the measurement (electrodes are particularly important, since they are the site of charge carrier conversion from ions to electrons and vice versa [121]). In this way, it was possible to evaluate the repeatability of the measurement and also the intra- and inter-subject variability.
Bioimpedance measurements were made at a single frequency, which is the one of the electric therapy proposed (Chapter 2), i.e. 312.5 kHz. As it will be discussed in detail in Chapter 4, this frequency avoids both dangerous effects on the patients and also polarization effects on the electrode, caused by direct current; in addition, frequencies in the range of kHz have been demonstrated to be suitable for this aim [156]. Small excitation values were used, in order to have a linear system [121]. A two-electrode system was used,

since there is not the problem of the presence of stratum corneum influencing the result [121].
In addition, to further improve the innovative electric therapy for peri-implantitis, it would be interesting to extend the application of bioimpedance measurements to assess the bone level in dental implants, to evaluate their stability in an objective way. In fact, in the literature there are many works dealing with the determination of the implant stability by means of impedance studies. A correctly osseointegrated implant shows a higher modulus of impedance, because of the bone growth at the interface with the implant itself [157], [158]. Electrical Impedance Spectroscopy demonstrates to be a suitable means to monitor the osteointegration process of a dental implant; an important advantage is the non-invasivity of the technique, contrary to X-rays, which, in addition, are incapable to investigate soft tissues and implant contact layer [159]. In particular, the phase angle of the measured impedance has been proved to be more reliable to infer the implant stability [160].

3.1. Numerical simulation of bioimpedance measurements

Numerical simulations of the bioimpedance measurement procedure was made in COMSOL Multiphysics® environment [106].
In this work, various numerical models were considered, both of dental implants (placed in premolar position) and of healthy tooth roots (i.e. canine, incisor and premolar).
In this way, the author wants to evaluate the feasibility of the detection of inflamed tissue areas [161]. Once such evaluation was made, some experimental measurements were carried out [162].
In the case of dental implants, different electrodes in terms of shape (both square and rounded), dimension and positioning were modelled, sequentially placed on the gingiva along the bone curvature. This was done in order to find the best design for electrodes addressed to bioimpedance measurements in oral environment.
The change in impedance due to the tissue inflammation is judged by comparing the impedance modulus in healthy and inflamed gingiva sides; the percentage difference was then considered, as described in Eq. 11:

$$\Delta Z = \frac{Z_{healthy} - Z_{inflamed}}{Z_{healthy}} \tag{11}$$

It is desired to understand if such impedance changes are adequately pronounced to detect inflamed areas and what precision is required for the measuring instruments.
In the following paragraphs the numerical simulations of bioimpedance measurements in models of implants (Paragraph 3.1.1) and natural tooth roots (Paragraph 3.1.2) are described, together with the variations caused by different electrodes configurations.

3.1.1. Dental implant model: bioimpedance measurements simulation

In this paragraph, the numerical simulation of bioimpedance measurements in dental implant case is described.

3.1.1.1 Materials and methods

As regards the simulation of bioimpedance measurements in the case of a dental implant, a simplified geometry of the tissues surrounding the dental implant was considered (i.e. the same described in Paragraph 2.3.1.2, also reported in Fig. 37), concerning an implant substituting a second premolar tooth root. Since, for the sake of simplicity, no swollen tissue was modelled, it is reasonable to assume that the analysed structure is the worst case situation for the detection of inflamed tissue through impedance measurements (because the swelling would make the impedance change also more evidently).

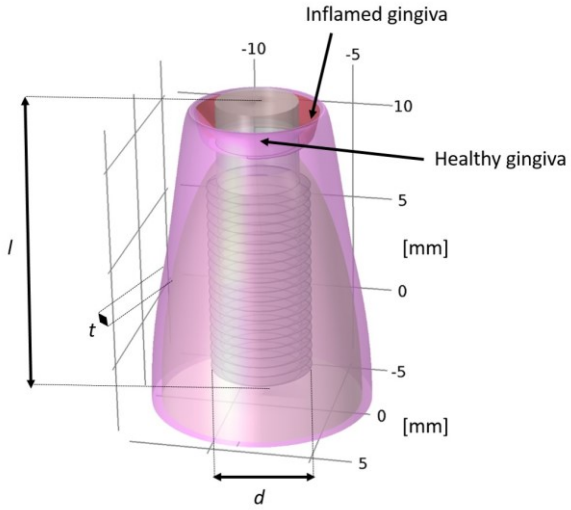

Figure 37. 3D model geometry of the dental implant screwed in the jawbone, with a portion of inflamed gingiva; d is the diameter of the fixture, l its length and t the gingiva thickness along the bone curvature

In order to simulate impedance measurements, two electrodes were modelled:

- Active electrode, which is screwed into the fixture of the implant; hence, the implant itself works as the active electrode;
- Passive electrode (also called "neutral electrode"), adhering to the gingiva. This is a square metallic surface (4 mm^2 in area), sequentially moved vertically along the gingiva, to investigate the method capability of a precise location of the inflammation. In particular, such neutral electrode was placed in four different positions, as it is shown in Fig. 38 A).

In addition, also different neutral electrodes were used, in order to identify the most suitable one for this kind of physiological measurement. In particular, a bigger square electrode (9 mm^2 area) and a rounded one (2 mm in diameter) were tested, as shown in Fig. 38 B) and C), respectively (together with their sequential positioning).

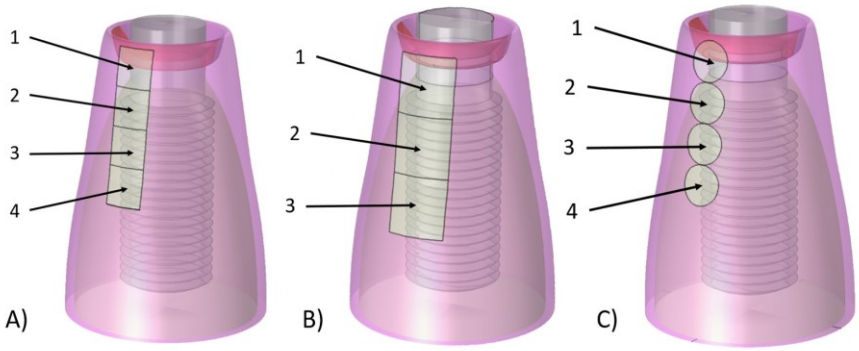

Figure 38. Neutral electrode sequential positioning to locate the inflamed region: A) square electrode (4 mm^2), B) bigger square electrode (9 mm^2) and C) rounded electrode

In order to simulate the measurement, the system is connected in series with an alternating current (AC) sinusoidal generator (Fig. 39). The active electrode is the generator terminal, while the neutral electrode is fixed at 0 V potential (i.e. ground); the generator imposes 1 V voltage (at 312.5 kHz) between the two electrodes, so that a current passes through the tissues.
When the passive electrode is moved along the mucosa, different impedance values will be measured. In particular, it is expected that the value will be lower when the current flows through the inflamed tissue, since it is richer in liquid content than the healthy one (hyperaemia and infiltration of the adjacent tissues are typical of the inflammatory process [114]) and, consequently, it is characterized by a lower conductivity. Higher the inflammation severity, higher the electrical conductivity; in particular, two different levels are considered, with an electrical conductivity double and triple the normal one, as defined in Eq. 12:

$$\sigma_{inflamed} = k * \sigma_{healthy} \tag{12}$$

where the multiplying factor k was considered equal to 2 and 3, depending on the inflammation severity (more severe the inflammation is, higher the k factor will be).

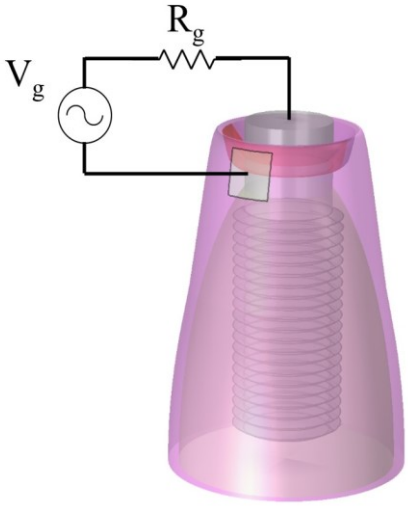

Figure 39. AC sinusoidal generator connected between active and passive electrodes

To evaluate the ability of bioimpedance method in detecting inflammations, both inflamed and healthy tissues were measured in order to be compared. Different inflamed tissue volumes were considered:

- Small, i.e. 2 mm^3 area;
- Medium, i.e. 5 mm^3 area;
- Big, i.e. 13 mm^3 area.

The numerical study is carried out by solving a Laplace equation for complex potential, as described in Paragraph 2.3.1.1. Impedance is then computed as the ratio between the complex voltage on the active electrode to the complex total current.
Finally, to evaluate the presence of inflammation, the percentage variation of the impedance modulus is considered (Eq. 11).

3.1.1.2. Results

Healthy and inflamed tissues impedances were compared and differences of 4÷20% have been found, depending on the considered parameters (i.e. inflammation volume and severity, neutral electrode shape/dimension/position).
In Tab. 4 there are the results related to the model of the tooth with the dental implant, in case of a square electrode placed in correspondence of the inflamed tissue. It can be noted that the reactance is negligible with respect to the resistance, therefore, from here on out, only the impedance modulus will be reported.

Table 4. Impedance value results for tooth with dental implant model - inflamed tissue, square electrode, Z = R + jωX (where R is the resistance, X the reactance)

Electrode position	R [Ω]	X [Ω]	|Z| [Ω]
1	498	-6	498
2	491	-9	491
3	620	-16	621
4	790	-25	791

The results in case of different neutral electrode shapes/dimensions are reported in Tab. 5, while those related to different inflamed volumes are detailed in Tab. 6. Finally, the results of the simulations with different inflammation severity levels are shown in Tab. 7.

Table 5. Impedance values for tooth with dental implant model

Electrode	Electrode position	$\|Z\|_{healthy}$ [Ω]	$\|Z\|_{inflamed}$ [Ω]	ΔZ [%]
Squared	1	558	498	**10.75**
	2	498	491	1.41
	3	622	621	0.16
	4	791	791	0.00
Squared, bigger	1	320	296	**7.50**
	2	402	401	0.25
	3	570	570	0.00
Rounded	1	652	568	**12.88**
	2	602	596	1.00
	3	745	744	0.13
	4	909	909	0.00

Table 6. Impedance values for tooth with dental implant model (k=2; square neutral electrode) – different inflamed volumes (small = 2 mm^3; medium = 5 mm^3; big = 13 mm^3)

Inflamed volume	Electrode position	$\|Z\|_{healthy}$	$\|Z\|_{inflamed}$	ΔZ [%]
Small	1	553	519	**6.15**
	2	493	489	0.81
	3	620	620	0.00
	4	791	791	0.00
Medium	1	558	498	**10.75**

	2	498	491	1.41
	3	622	621	0.16
	4	791	791	0.00
Big	1	551	445	**19.24**
	2	493	471	4.46
	3	621	618	0.48
	4	791	791	0.00

Table 7. Impedance values for tooth with dental implant model (inflamed tissue volume = medium; square neutral electrode) – different inflammation severity levels

Inflammation severity	**Electrode position**	$\|Z\|_{healthy}$	$\|Z\|_{inflamed}$	**ΔZ [%]**
k = 2	1	558	498	**10,75**
	2	498	491	1,41
	3	622	621	0,16
	4	791	791	0,00
k = 3	1	557	463	**16,88**
	2	498	489	1,81
	3	622	621	0,16
	4	791	791	0,00

3.1.1.3. Discussion and conclusions

From the simulations run on the dental implant models, some deductions can be figured out:

- The preferable shape of the electrode is the rounded one, since it allows to obtain a greater ΔZ (see Tab. 5); maybe, this is because in squared electrodes the current density is too high at the edges, making the surface area too sensitive and the bulk less sensitive. With regard to the dimensions, the smaller is the better, because, as it can be seen from the results, it highlights the impedance difference between healthy and inflamed tissues;
- As it can be expected, ΔZ is higher when the inflamed volume is bigger (Tab. 6); more extended the inflammation is, more evident the change in the impedance value will be;
- Higher the inflammation severity level is, more evident the change in impedance value will be (Tab. 7);

- ΔZ is higher when the electrode is nearer to the inflamed zone. Anyway, it is worth considering that in upper position the impedance is lower also because of the greater proximity between the two electrodes (due to the tissue curvature). Anyway, this influence is the same both in the healthy and in the inflamed sides, so it is plausible to think that it does not influence the percentage difference in the impedance modulus.

In conclusion, it can be stated that the numerical simulations demonstrate the feasibility of inflammation localisation by means of bioimpedance measurements (as asserted also in [156]), since the change due to the inflammatory process is adequately pronounced to discriminate between healthy and inflamed tissues (4-20%). The characteristics of the electrodes are very important, because, all other things being equal, they influence the results significantly. Perhaps, it would be useful to calibrate the system on the specific subject before each measurement, in order to evaluate his own variability.
Such kind of measurement can help the clinician to detect inflamed tissue, offering an objective assessment method. This gains also more relevance if it is considered together with the proposed therapy for peri-implantitis; in fact, bioimpedance measurement could quantify both the extension and the severity of the inflammation, suggesting how to personalise the therapeutic dose.
In addition, in the future it would be interesting to extend the application of bioimpedance measurements to assess the bone level in dental implants, to evaluate their stability in an objective way, since (as already said in the introduction of this chapter) a correctly osseointegrated implant shows a higher modulus of impedance [157].

3.1.2. Natural tooth root model: bioimpedance measurements simulation

In this paragraph, numerical simulations of bioimpedance measurements in natural tooth roots surrounded by inflamed tissue are described.

3.1.2.1 Materials and methods

Numerical simulations were run on natural tooth roots models, concerning incisor, canine and premolar teeth, whose geometries (different in terms of shapes and dimensions) are reported in Fig. 40 A), B) and C), respectively [107]. Here, both the electrodes (metallic square surface, 4 mm^2 area, three sequential positions) are adhering to the gingiva, placed in opposed positions. The simulation was repeated in presence and in absence of inflamed tissue, so as to permit the comparison between the two. In this way, not only peri-implantitis but also periodontitis case was considered.

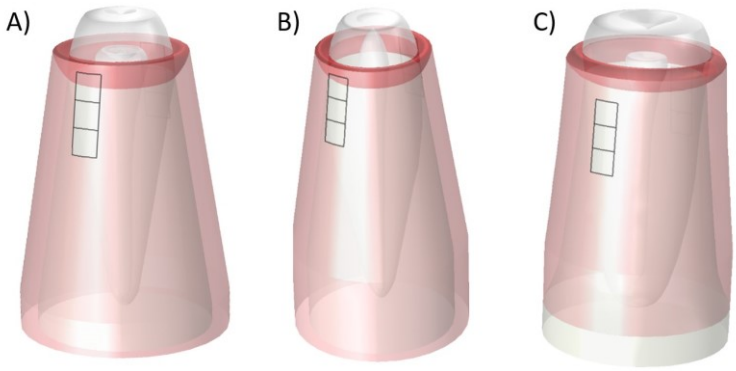

Figure 40. Natural tooth roots models with inflammations concerning incisor (A), canine (B) and premolar (C) teeth – square electrodes

Moreover, the simulations were made also with circular electrodes (2 mm in diameter), placed vertically along the bone curvature (adhering to the gingiva) in 6 different consecutive positions. In this case, only healthy tissues were modelled, to evaluate the impedance values range obtainable from healthy subjects (experimental measurements in healthy tooth roots will be described in Paragraph 3.2.2). Such models are reported in Fig. 41 A), B) and C) for incisor, canine and premolar tooth roots, respectively.

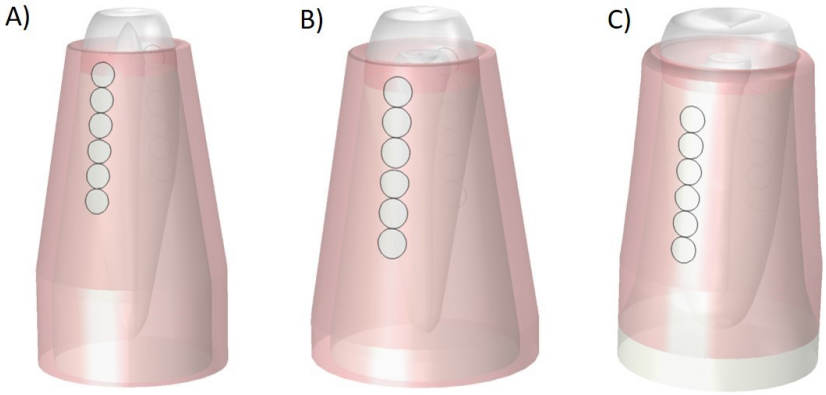

Figure 41. Natural healthy tooth roots models concerning incisor (A), canine (B) and premolar (C) teeth – rounded electrodes

3.1.2.2. Results

With regard to the simulations on natural tooth roots with inflammation, where square electrodes were modelled, the results are reported in Tab. 8.

Table 8. Impedance measurement simulations results on different natural tooth roots (i.e. incisor, canine and premolar) with inflammation, obtained with the electrodes placed in 3 different positions (adhering to the gingiva) along the bone curvature – square electrodes

Tooth	Electrode position	$\|Z\|_{healthy}$ [Ω]	$\|Z\|_{inflamed}$ [Ω]	ΔZ [%]
Canine	1	2668	2362	**12.96**
	2	2255	2154	4.69
	3	2087	2049	1.85
Incisor	1	2574	2302	**11.82**
	2	2176	2090	4.11
	3	2026	1991	1.76
Premolar	1	2717	2309	**17.67**
	2	2254	2137	5.47
	3	2081	2030	2.51

In Tab. 9 there are the bioimpedance measurement simulation results obtained for the healthy tooth roots with circular electrodes.

Table 9. Impedance measurement simulations results on different natural healthy tooth roots (i.e. incisor, canine and premolar), obtained with the electrodes placed in 6 different positions (adhering to the gingiva) along the bone curvature – rounded electrodes

Tooth	Electrode position	|Z| [Ω]
Incisor	1	2877
	2	2480
	3	2327
	4	2331
	5	2250
	6	2243
Canine	1	2956
	2	2570
	3	2415
	4	2392
	5	2302
	6	2268
Premolar	1	2562

	2	2412
	3	2342
	4	2334
	5	2319
	6	2333

3.1.2.3. Discussion and conclusions

From the simulations run on natural tooth roots with inflammation, it is possible to see that changes of 11-18% are reported in the impedance modulus; as it can be expected (similarly to the case of dental implant, Paragraph 3.1.1), ΔZ is higher when the electrodes are placed nearer to the inflamed area.
So, these numerical simulations demonstrate the feasibility of inflammation localisation by means of bioimpedance measurements also in natural teeth, since the change in impedance modulus is up to 18% with respect to the healthy case; this can be useful for example in case of periodontitis, offering an objective assessment method to quantify the severity of the inflammation.
With regard to the simulations run on natural healthy tooth roots, it is possible to observe that the impedance modulus decreases while moving the electrodes downwards. This highlights the importance of making measurements always with the same configuration; otherwise, an important variability would be caused on the results.
Finally, an important parameter influencing the results is the electrical conductivity of biological tissues, whose variability is not negligible.

3.1.3. Experimental validation and self-consistency of the model

The self-consistency and the accuracy of the numerical models were tested by a comparison between simulated results and experimental measurements.
The simulated geometry and the experimental setup are reported in Fig. 42 A) and B), respectively.

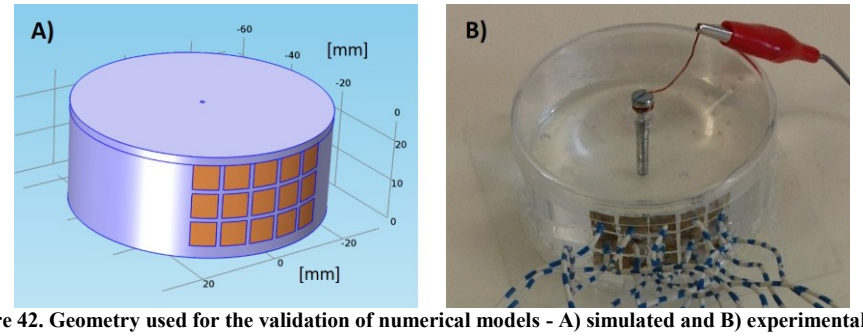

Figure 42. Geometry used for the validation of numerical models - A) simulated and B) experimental ones

The active electrode is a metallic screw fixed in the centre of the model, while the neutral one is splitted into 15 squared metallic electrodes with a side of 6 mm, in order to be able to measure the electric current exiting from each of them (by means of a current probe, i.e. TEK CT-2 by Tektronix [163]). The aim of the array of metallic patches forming the neutral electrode is to provide quantitative information about the current density distribution in the liquid. The system has a cylindrical shape and is filled with water until the edge of the upper electrodes.

Both numerically and experimentally, a sinusoidal signal of 7 V (peak-to-peak value) in amplitude at 312.5 kHz was applied from the active electrode (by means of a waveform generator, i.e. 33120A by Keysight Technologies [164]), in the centre of the cylindrical model.

The measured electric current distribution (Fig. 43) satisfactorily agrees with the simulated one (Fig. 44); these maps were obtained by interpolating the values measured at the 15 electrodes, in order to have a more complete description of the electric current distribution in the area.

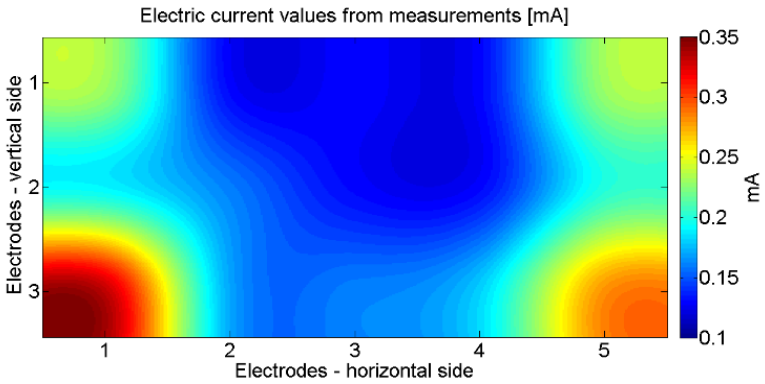

Figure 43. Models validation - Electric current values from measurements

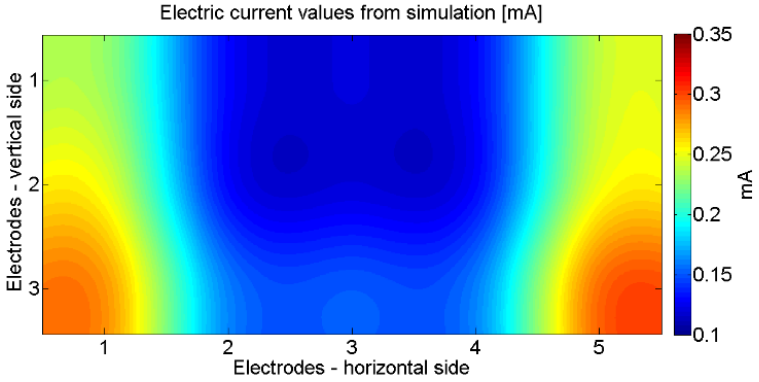

Figure 44. Models validation - Electric current values from simulation

The numeric values related to experimental and numerical results are reported in Tab. 10-11, respectively.

Table 10. Models validation - Electric current values from measurements

Electric current distribution – measurements [mA]				
0.23	0.13	0.13	0.13	0.23
0.19	0.16	0.13	0.13	0.20
0.33	0.17	0.16	0.18	0.28

Table 11. Models validation - Electric current values from simulation

Electric current distribution - simulation [mA]				
0.23	0.13	0.12	0.13	0.24
0.25	0.13	0.12	0.13	0.25
0.28	0.16	0.15	0.16	0.29

The deviations between the two sets of electric current values are acceptable, if it is accounted for the measurement setup resolution (0.02 mA), the instrument accuracy (±3%), the uncertainty of water conductivity value (5÷50 mS/m, depending on ions content and temperature [165]) and numeric errors due to singularities in the simulated geometry (i.e. the edges of the electrodes).

It is worth noting that the current distribution is not uniform, because, according to theory, the current flowing from the active electrode to the central patches of the neutral electrode array experiences a higher impedance path.

The satisfactory agreement between simulation and measurements, both for the current distribution and for the current intensity, makes the model confident for application to the realistic tooth roots models described in this thesis.

3.2. Experimental measurements on patients

After having run different numerical simulations concerning dental implants and natural tooth roots, experimental measurements were made, both on patients with dental implants in different clinical conditions (Paragraph 3.2.1) and on healthy subjects (Paragraph 3.2.2), in order to have some first measurements supporting the numerical models.
Measurements were carried out by means of an LCR meter (Agilent HP, 4285A precision LCR meter, using the auto-balancing bridge technique [121]), equipped with a proper insulation transformer in order to guarantee the electrical safety of the participant. The whole study was carried out by following the principles outlined in the WMA Declaration of Helsinki (Ethical Principles for Medical Research Involving Human Subjects [84]).
The aim of such measurements is to validate the numerical models (Paragraph 3.1), by comparing the impedance modulus in simulation and in experimental conditions. An important role is played by the variability in biological parameters (e.g. electrical conductivity and morphology) and in measurement conditions (e.g. electrodes positioning and contact pressure).
The measurements on the natural healthy tooth roots are intended to start creating a database to determine the physiological range (and also a statistical means of comparison) and the variability of bioimpedance in oral environment, as well as to evaluate the repeatability of the measure. Moreover, intra- and inter-subject variability has a great relevance in physiological measurements, so their evaluation is fundamental.

3.2.1. Measurements on patients

In order to validate the results of the numerical simulations of bioimpedance method, some measurements were made on patients with dental implants, surrounded by healthy or pathological tissues.
This was a pilot study, carried out to understand which the best measurement conditions are and how to define the measurement procedure for future clinical applications, also aimed at improving the proposed electrical therapy for peri-implantitis (Chapter 2). Obviously, it would be desirable to make such bioimpedance measurements on a wider population, to include as many different cases (e.g. in terms of morphology and clinical condition) as possible.

3.2.1.1 Materials and methods

A few experimental measurements were made on patients with dental implants (following the principles outlined in the WMA Declaration of Helsinki - Ethical Principles for Medical Research Involving Human Subjects [84]) in 3 different cases:

- Dental implant surrounded by healthy tissue;

- Dental implant surrounded by inflamed tissue;
- Dental implant with peri-implantitis.

The impedance measurement was made at a single frequency (i.e. 312.5 kHz, which is the frequency of the proposed therapy for peri-implantitis described in Chapter 2) with an LCR meter (Agilent HP, 4285A precision LCR meter [166]) equipped with a proper insulation transformer to guarantee the subject's electrical safety. Two electrodes (made of stainless steel) were used: the active electrode (screw-shaped) screwed in the implant fixture, the passive one (circular, 2 mm in diameter) adhering to the gingiva. The meter was calibrated before the measurements, so as to compensate for cables and electrodes impedances. The measurement setup is reported in Fig. 45.

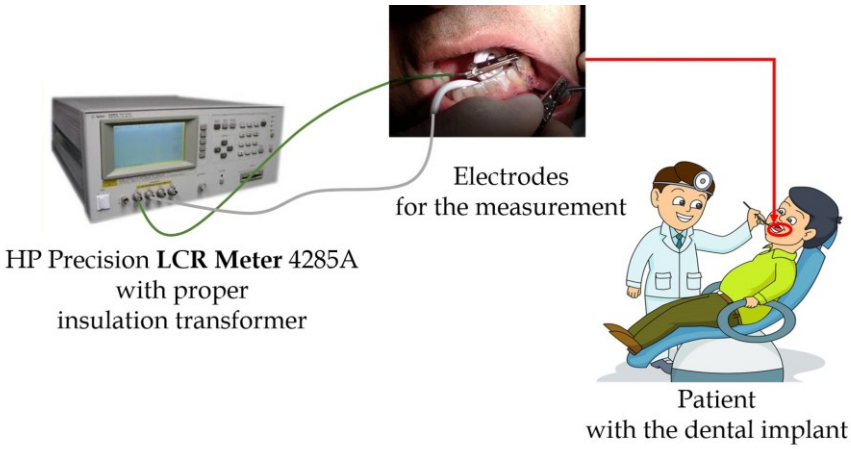

Figure 45. Measurement setup: active electrode screwed into the implant fixture, passive electrode adhering to the gingiva; the two electrodes are connected to an LCR meter equipped with a proper insulation transformer

Three measurements were made on each subject; an equivalent circuit, consisting of a series connection between a resistor (R_s) and a capacitor (C_s), was considered to model the system, as it can be seen in Fig. 46.

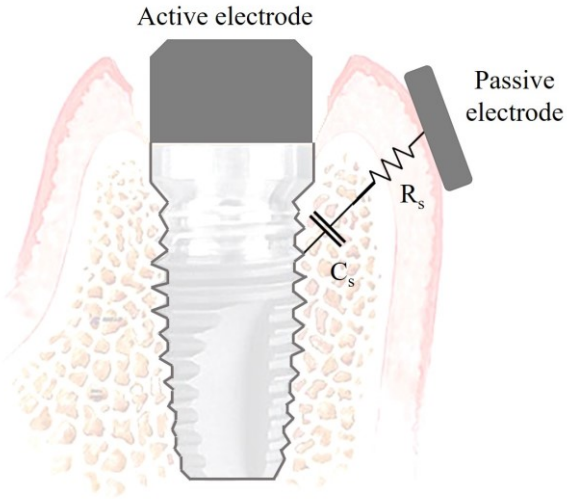

Figure 46. Equivalent circuit of tissues, consisting in a series connection between a resistor, R_s, and a capacitor, C_s

Finally, the impedance modulus was computed and the percentage difference in case of inflammation and peri-implantitis was contemplated with respect to the healthy case.

3.2.1.2. Results

In Tab. 12, the results of the measurements on the three cases are reported. In the last column, there are the mean value and the standard deviation of the impedance modulus, on which the percentage difference with respect to the healthy case is computed.

Table 12. Impedance measurements on different clinical cases: dental implant surrounded by healthy/inflamed tissue, peri-implantitis; system modelled as a series connection between a resistor (R_s) and a capacitor (C_s)

Case	Test	R_s [Ω]	C_s [nF]	Z [Ω]	m±σ |Z| [Ω]
Healthy	**1**	738	1.51	811	**845±35**
	2	791	1.75	843	
	3	789	1.30	881	
Inflammation	**1**	440	1.83	521	**539±15**
	2	468	1.80	547	
	3	463	1.74	548	
Peri-implantitis	**1**	330	3.37	363	**368±12**
	2	352	3.46	382	
	3	334	3.81	360	

3.2.1.3. Discussion and conclusions

The preliminary experimental measurements made on three subjects are in agreement with the simulations results, both for the order of magnitude of the measured impedance (hundreds of Ω, both real and absolute values - with regard to the imaginary part, it strongly depends on the electrode-tissue interface -) and for the variations observed when an inflammatory process is present. The measured ΔZ is even greater (35-56%) than those obtained from simulations; this is attributable to the swelling of the tissue, which is present in the real case but was not represented in the numerical model. In case of peri-implantitis, the impedance decrease is more marked because of the bone loss around the dental implant, which is a characteristic absent in the mere inflammation process. Moreover, a further contribution could be added by a change in the relative permittivity of the inflamed gingiva, which has not been considered in the numerical simulations. The predominant part of bioimpedance is the real one and this is in agreement both with our simulation results and with the literature [167].
As regards the intra-subject variability of the measurement, percentage values equal to 4.1%, 2.8% and 3.3% were found for the healthy, inflammation and peri-implantitis cases, respectively. So, such a measurement procedure can be considered adequately precise, even if in the future it is desirable to have a more handy electrodes system, easy usable by clinicians. Also conductive rubber electrodes (at present introduced for wearable monitoring devices [168]) could be designed for this measurement.
However, given the high intra- and inter- subject biological variability, several further measurements on the different clinical cases (i.e. dental implant surrounded by healthy/inflamed tissue, peri-implantitis) are needed in order to identify which the physiological/pathological ranges are and to evaluate the repeatability of the measurement. In fact, at present, individual measurements cannot be classified: only comparison between healthy and pathologic is possible.
The impedance was measured with a two-electrodes system, but in the future it would be interesting to experiment a four-point method, to verify possible improvements in the results. Such a system is usually applied in order to avoid the influence of the interface effects, mainly due to the skin stratum corneum [121], which in the present case is not present (since the measurement is carried out with the electrodes applied to the gingiva).
Moreover, it could be interesting to investigate not only the modulus, but also the phase of the measured impedance, to evaluate the presence of further information. A comparison between the “performance” of the two quantities in terms of discrimination between healthy and inflamed tissues could be remarkable, even if, from numerical simulation results, it seems that the main information lies in the impedance modulus. This can be better observed in Fig. 47, representing the Bode plot of impedance (considering measurement carried out - with square neutral electrode - on an implant substituting a premolar tooth root, with a medium inflamed volume, as described in Paragraph 3.1.1), for modulus and phase parts.

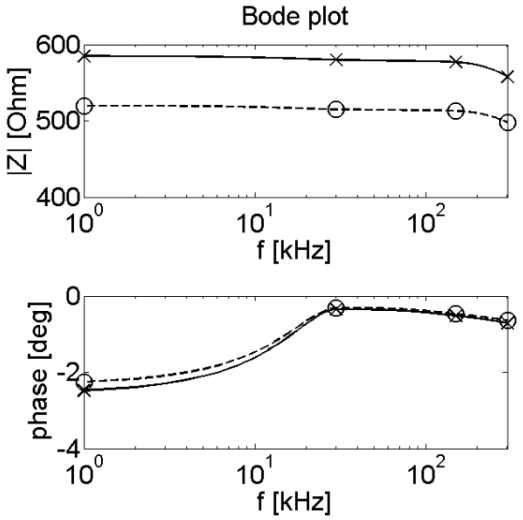

Figure 47. Bode plot: impedance modulus (top) and phase (bottom); markers represent results from numerical simulations (run at different frequency values: 1, 30, 150 and 300 kHz), while lines are obtained by means of cubic interpolation; continuous line is related to healthy tissue, dashed line to inflamed tissue

However, in the future it would be very interesting to carry out multi-frequency measurements also experimentally, to obtain a deeper characterization of different peri-implant tissues (e.g. affected by inflammation or peri-implantitis).

3.2.2 Measurements on healthy subjects

Bioimpedance measurements were carried out also on natural tooth roots, in order to evaluate the repeatability of the measurement and to identify which factors can influence the results. Intra- and inter- subject variability were computed. However, in the future it would be necessary to make a larger study on a wider population, in order to build a bioimpedance database and to establish which are normal and pathological ranges. Moreover, thinking about the possible applicability of the proposed therapy to the case of periodontitis (as discussed in Paragraph 2.3), such values could be useful in order to personalize the therapy according to the inflammation severity.

3.2.2.1 Materials and methods

Three kinds of teeth were considered: incisor, canine and premolar. The impedance measurements were made on three healthy subjects (aged 27±1) and were repeated for four consecutive days; each measure was repeated three times. An LCR meter (Agilent HP, 4285A precision LCR meter [166]), equipped with a proper insulation transformer to

guarantee the subject's electrical safety, was used. The measurement frequency was equal to 312.5 kHz (i.e. the same of the measurements on patients described in Paragraph 3.2.1). The electrodes were realized in stainless steel and had a spherical shape, with a contact area of about 5 mm^2. The meter was calibrated before the measurements, so as to compensate for cables and electrodes impedances. The measurement setup is reported in Fig. 48.

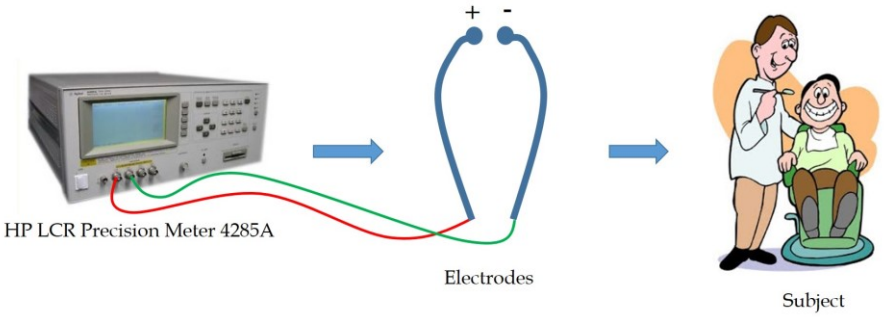

Figure 48. Measurement setup: active and passive electrodes adhering to the gingiva, placed in opposed positions (with respect to the jawbone); the two electrodes are connected to an LCR meter equipped with a proper insulation transformer

3.2.2.2. Results

The impedance absolute values measured in the three subjects related to the three repeated measures on each tooth root each day are reported in Tab. 13.

Table 13. Impedance absolute values measured in incisor, canine and premolar teeth of three healthy subjects in four consecutive days

Absolute impedance values [kΩ]								
Subject 1			Subject 2			Subject 3		
Incisor	Canine	Premolar	Incisor	Canine	Premolar	Incisor	Canine	Premolar
1.5	1.8	1.9	1.2	1.5	2.3	1.6	2.4	1.9
1.2	1.7	2.1	1.4	1.5	1.8	1.7	1.7	2.1
1.6	1.6	1.8	1.4	1.5	2.3	1.5	1.7	1.8
1.4	1.9	2.1	1.3	1.5	1.5	1.3	2.2	1.8
1.1	1.4	2.2	1.2	1.9	1.3	1.9	2.1	1.8
1.4	2.0	1.7	1.4	1.2	1.4	1.5	1.9	2.0
1.4	1.5	1.5	1.2	1.5	1.4	1.7	1.4	1.4
1.4	1.5	1.9	1.4	1.6	1.2	1.3	1.5	1.3
1.4	1.5	1.7	1.1	1.5	1.5	1.4	1.3	1.4

	1.2	1.3	1.4	1.3	1.3	1.2	1.2	1.2	1.3
	1.3	1.5	1.4	1.4	1.3	1.2	1.4	1.4	1.2
	1.3	1.4	1.3	1.3	1.3	1.1	1.3	1.3	1.3
Mean value	1.3	1.6	1.7	1.3	1.5	1.5	1.5	1.7	1.6
Standard deviation	0.1	0.2	0.3	0.1	0.2	0.4	0.2	0.4	0.3

In summary, the results are reported as mean ± standard deviation in Fig. 49-51 for the three subjects.

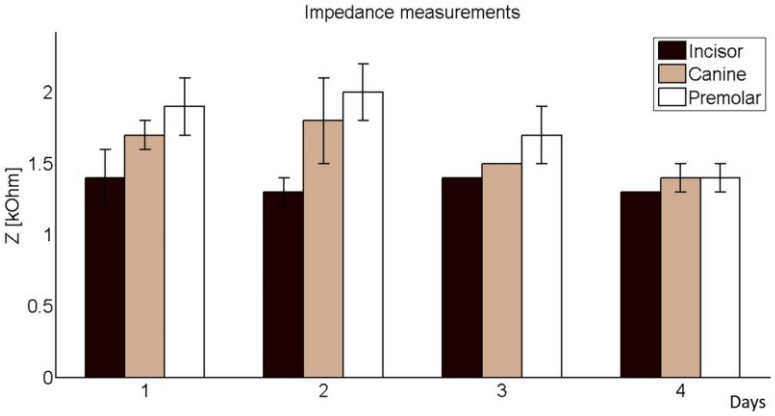

Figure 49. Bioimpedance modulus measurements in subject 1 - summary

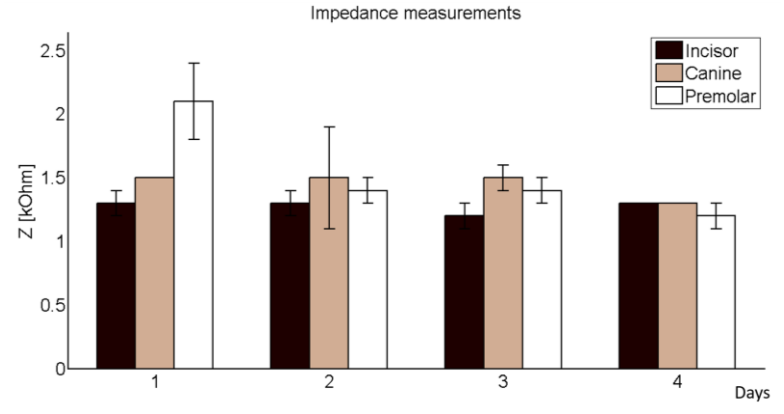

Figure 50. Bioimpedance modulus measurements in subject 2 – summary

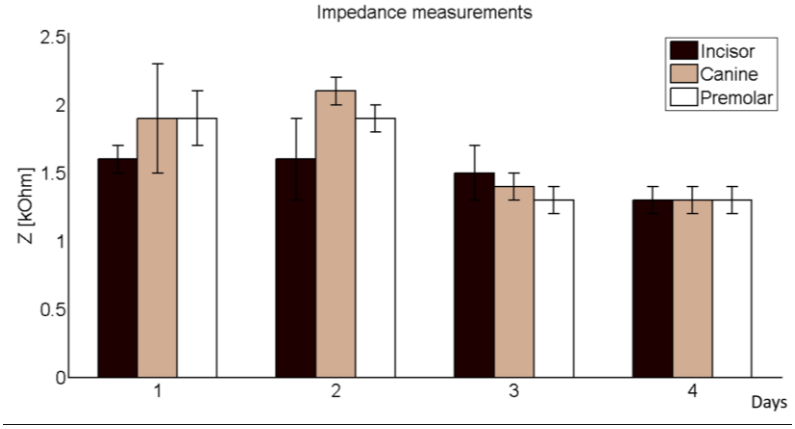

Figure 51. Bioimpedance modulus measurements in subject 3 – summary

Let us now consider the three different teeth kinds; in Fig. 52-54 there are the histograms concerning all the measurements made on the three subjects, for incisor, canine and premolar tooth roots, respectively.

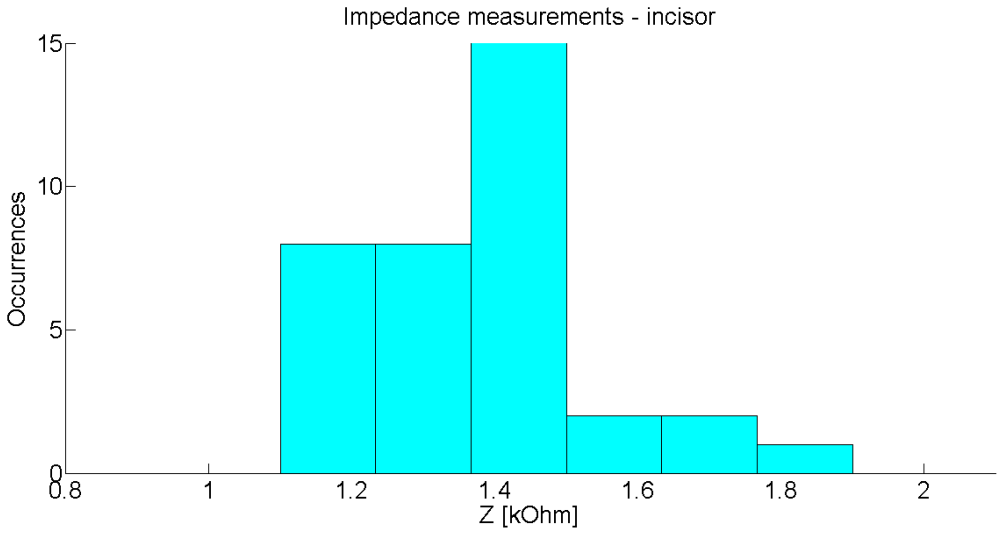

Figure 52. Distribution of absolute impedance measurements on the three subjects - incisor tooth

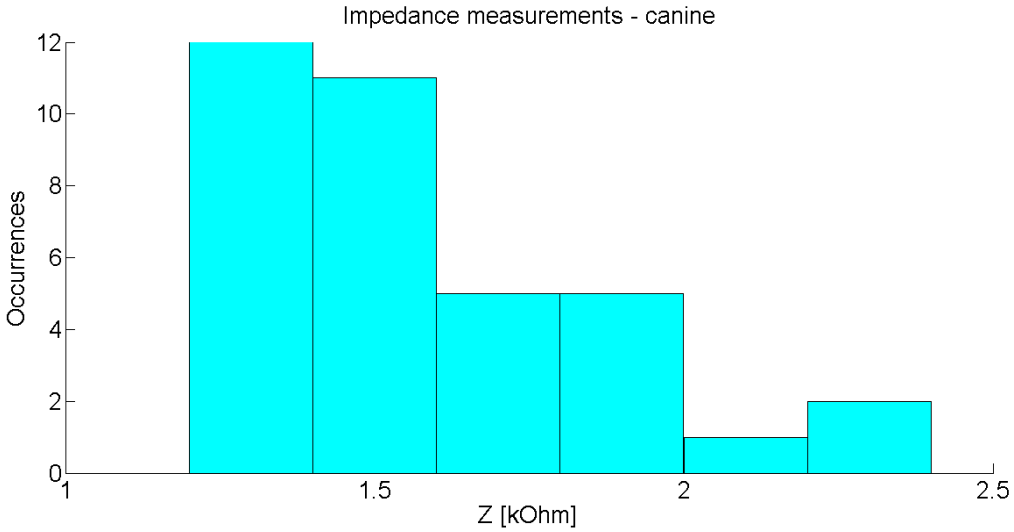

Figure 53. Distribution of absolute impedance measurements on the three subjects - canine tooth

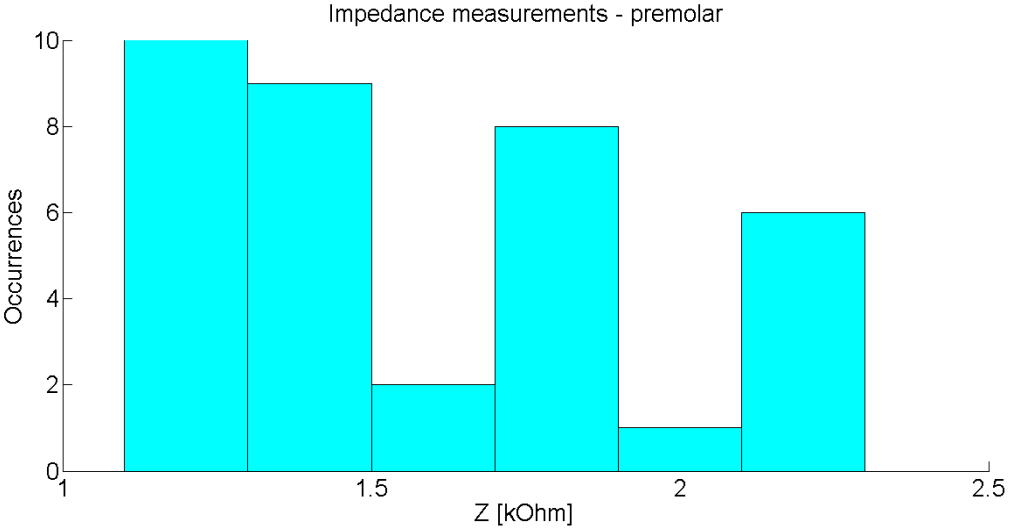

Figure 54. Distribution of absolute impedance measurements on the three subjects - premolar tooth

3.2.2.3. Discussion and conclusions

The bioimpedance measurements were made on three different teeth (i.e. incisor, canine and premolar) in three healthy subjects for four consecutive days. Then, the repeatability of the measurement and the intra- and inter-subject variability were evaluated.
Looking at Tab. 13, it is possible to observe that the order of magnitude of the measured impedance moduli is the same of the simulations described in Paragraph 3.1.2, that is, some kΩ. However, the simulated values are higher than the measured ones. The reasons can be different:

- Biological tissues electrical conductivities: the values used in simulations were taken from the literature [110]–[112], but they were computed on few cases and the biological variability is high [169];
- Actual shape of measured natural tooth roots: the realized models were about single root teeth, but in practice it is possible to have teeth with multiple roots (less bone would be passed by electric current, which would move through the soft tissue, so the resulting impedance would be lower) and the variability in the root canal morphology is high [170], [171];
- Position of the electrode: if it is lower, the impedance decreases (see Tab. 9);
- Actual electrodes surface in contact with gingiva: if it is bigger, the impedance decreases (see Tab. 5).

To support the above hypotheses, the bioimpedance measurement simulation was repeated in the case of a premolar tooth root with a bigger electrode (2 mm in diameter instead of 1.5 mm) in lower position (Fig. 55): the resulting impedance modulus is equal to 1909 Ω instead of 2333 Ω obtained with the smaller electrode in the same position (see Tab. 9). So, a difference in diameter of just 0.5 mm causes a change in the impedance value of ≈ 18%.

Figure 55. Model of premolar tooth root, bigger electrodes placed in lower position

In practice, the contact surface can vary also with the pressure exerted during the measurement (this parameter should be controlled during the measurement, e.g. by loading/unloading a proper spring [172]). A possible design of electrodes controlled in terms of contact pressure is shown in Fig. 56.

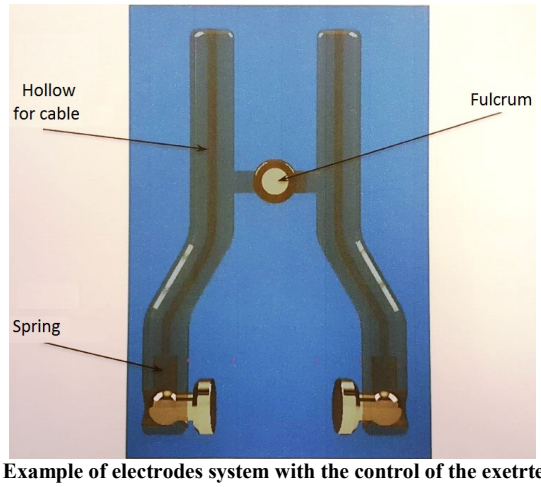

Figure 56. Example of electrodes system with the control of the exetrted pressure by means of loading/unloading a spring

The measurement electrodes has a high influence on the measurement results, so it would be interesting to test different kinds of electrodes (e.g. hydrogel electrodes, with an effective area quite stable [121], or carbonated fiber, adaptable to curved surfaces [173]).
If we compare the impedance values measured in natural tooth roots with the ones obtained from implants, it is possible to note that the former are equal to few kΩ, while the latter to hundreds of Ω. This is reasonable, because in the case of implants there is a metallic volume present, with a very high conductivity, while in natural roots there is hard tissue, so its conductivity is lower and consequently the impedance will be higher.
With regard to the repeatability of the measurement, it obviously depends on several factors, among which there are the contact area between electrode and gingiva (and, so, the pressure exerted during the measurement) and the position of the electrodes along the gingiva curvature.
The intra-subject variability is quite good (< 10%) in the same day, but it varies more (up to 26%) in different days, probably due to a different electrodes positioning.
The inter-subject variability is greater (up to ≈ 20% for premolar tooth).
However, in the future it would be necessary to widen the measured population, in order to build a database of bioimpedance values in natural healthy tooth roots. In this way, it would be possible to make a deeper analysis of bioimpedance variability (the present data are not statistically significant for the size of the sample) and, perhaps, to classify single measurements in healthy/pathological ranges.
In addition, it would be interesting to get more information about the investigated tissues by means of Electrical Impedance Spectroscopy (EIS [174]). Such a technique could be applied to characterize more deeply the oral tissues, since EIS has been demonstrated to provide multiple information [175]–[177], avoiding the undesired interfering effect of electrodes and measurement conditions (e.g. temperature and humidity), which are present in the impedance measurement at a single frequency.

Chapter 4.

Electrical safety of the therapy

The word “safety” comes from the Latin “sine cura”, which means “without worries”. Electric current represents a substantial threat in the medical treatment and care of patients, often physically connected to medical devices over a certain period. Therefore, in electromedical devices, electrical safety aspects are fundamental; it is necessary to consider the electrical safety of patients/operators, the exposition to electromagnetic sources and also the possible interferences with other instrumentation (i.e. electromagnetic compatibility - EMC - aspects).
There are several studies on the hazards of Radio Frequency (RF) and microwave electromagnetic fields to humans [178], [179]. In particular, the quantities to be considered depend on the working frequency:

- at low-frequency: induced currents are considered [180];
- at high-frequency: the heating of the exposed areas (due to the energy absorption) is contemplated [181].

The rules to evaluate such safety issues are meticulously reported in regulations established by specific institutions:

- International Council on Non-Ionizing Radiation Protection (ICNIRP), which furnishes “advice and guidance on the health and environmental effects of Non-Ionizing Radiation (NIR, i.e. radio, microwave, UV and infrared) to protect people and the environment from detrimental NIR exposure” [182];
- Institute of Electrical and Electronic Engineers (IEEE) [183];
- International Electrotechnical Commission (IEC) [184].

ICNIRP and IEEE provide standards in terms of basic restrictions that should never be exceeded in order to avoid health risks. Such limits depend on the intended use of the medical device and also on the working frequency. IEC standards are typically used for EMC tests.
The device designed for the therapy of peri-implantitis is a Class II device, with applied parts of type BF (i.e. floating), working at RF, as it will be said in detail in the Appendix. So, it is necessary to consider mainly three regulations: IEC 60601-1, IEC 60601-2-2 and IEC 60601-1-2, which will be described in Paragraph 4.1.1, 4.1.2 and 4.1.3, respectively.
In order to be able to sell a medical device in European Union, it is necessary to comply with the above cited directives and to obtain a CE marking, which is a mandatory conformity marking, necessary to declare that the instrument meets the legal requirements of the European Community directives that are applicable to such product [185]. There are the indications for specific tests allowing the verification of the product performance in terms of safety requirements and electromagnetic compatibility, as it will be described in

Paragraph 4.1.4. A notified body executes such tests and the technical documentation (e.g. the technical description of the product and its instructions) is compiled. Finally, if all the established limits are observed, the certification marking is obtained.
Among all the required tests, in vitro and in vivo experiments are very important to demonstrate the electric safety of a medical device. In the present study, a preliminary in vitro test was made in order to evaluate the cell vitality after the delivery of the therapeutic signal. This aspect will be discussed in Paragraph 4.2. Before doing the experiment (Paragraph 4.2.2), it was numerically simulated in COMSOL Multiphysics® environment, in order to clarify the setup configuration (Paragraph 4.2.1). In the future, it would be interesting to conduct other in vitro experiments, in order to study the therapeutic effects in terms of inflammation and bacteria growth reduction. In addition, ECIS technology (Electric Cell-substrate Impedance Sensing) could be applied in order to study the activity of cells grown in tissue culture and also their morphology in a non-invasive way (the method is based on impedance measurements) [186].

With regard to the effects on human body, the regulation CEI 64 ("Effects of current passing through the human body" [187, p. 64]) deals with the effects of electric current. The level of danger depends on the amplitude, the frequency and the duration of the stimulus (low frequencies are more dangerous than high frequencies), but also on the complexion of the subject. Moreover, it is necessary to take into account the electric current path: if it crosses the heart (or, more generically, the thorax), it is more dangerous. The main possible consequences are the tetanisation, the respiratory block, the ventricular fibrillation and burns.
Electric currents at frequencies of some kHz (the proposed medical device works at RF) are not able to provoke convulsions, not even cardiac or respiratory arrest. The main effect to be considered is the heating of the exposed tissues: at frequencies higher than 100 kHz, currents of hundreds of mA cause heat sensations, but no cases of ventricular fibrillation are reported in the literature ([187, p. 64]). Depending on the duration of the signal, at amplitude magnitudes of some A it is possible to cause burns; the heat developed because of Joule effect is higher on the entry and exit points. At high frequencies, the danger decreases: the shorter the duration, the higher the stimulus amplitude needs to be in order to cause damages; moreover, the skin effect avoids that the electric current at high frequencies involve vital organs.
In the specific case of the proposed therapy, the electric current is limited between the active and the neutral electrode, so it is focused between the dental implant and the gingiva and no current lines flow until the cardiac muscle. Moreover, such a device does not produce so dangerous current levels: the rating power is 110 W on 1 kΩ (Paragraph 2.2), which corresponds to an electric current of about 300 mA, lower if the load is higher. From numerical simulation results (Paragraph 2.3), a current of 484 mA is reported on a load of 521 Ω (corresponding to a power of 122 W and an energy of 17 J for a therapy duration of 140 ms). In this regard, it is important to take into account that the human electrical resistance depends on several factors:

- the current path;
- the skin conditions: lower resistance in presence of wounds or humidity;
- the contact surface: greater this area, lower the resistance;

- the contact tension: higher the voltage, lower the resistance;
- the contact duration: higher the duration, lower the resistance;
- working frequency: higher the frequency, lower the resistance;
- the kind of tissue: a tissue is a good conductor if it is fat-free, while it is a bad conductor if it is fatty or bony.

Anyway, the results from the conducted in vivo clinical trial (Paragraph 2.1) have already proved the therapy to be electrically safe.
Finally, numerical simulations to investigate the heating aspect was run (Paragraph 4.3), even if edge effects cause numerical errors near the geometric edges, in correspondence of which the results cannot be considered reliable.

4.1. Regulations and standards for electromedical devices: IEC 60601-1

The responsible for the test, the ordinary and the corrective maintenance of medical devices is the clinical engineering.
CEI is the Italian Electrotechnical Committee responsible for technical standardisation in the electrotechnical, electronic and telecommunication fields. It takes part into the activities of the corresponding European standardisation organisation (CENELEC) and international one (IEC, International Electrotechnical Commission) and adopts harmonised European regulations (which, in this way, become Italian laws).
Regulations about medical devices safety and performance in Europe were harmonised in the 1990s. In particular, the Directive 93/42/EEC [188] (amended by means of the Directive 2007/47/EC) defines the criteria to be applied during the design and the realization of medical devices. It establishes the requirements to be met for the placement of a medical device into the European market. According to the World Health Organisation (WHO) [189], a medical device is *any instrument, apparatus, implement, machine, appliance, implant, reagent for in vitro use, software, material or other similar or related article, intended by the manufacturer to be used, alone or in combination, for human beings, for one or more of the specific medical purpose(s) of*:

- *diagnosis, prevention, monitoring, treatment or alleviation of disease;*
- *diagnosis, monitoring, treatment, alleviation of (or compensation for) an injury;*
- *investigation, replacement, modification or support of the anatomy (or of a physiological process);*
- *supporting or sustaining life;*
- *control of conception;*
- *disinfection of medical devices;*
- *providing information by means of in vitro examination of specimens derived from the human body;*

and does not achieve its primary intended action by pharmacological, immunological or metabolic means, in or on the human body, but which may be assisted in its intended function by such means.
In the Annex IX of the Directive 93/42/EEC, there are the rules to classify (according to their complexity and the potential risk for the patient) medical devices in four classes:

- Class I: devices with low risk, mainly non-active and non-invasive; they do not touch the patient or are in contact only through the intact skin, or they are used for channelling or storing for eventual administration;
- Class IIa: device with average risk level, active or not (invasive or not), interacting with the body without dangers;
- Class IIb: device with average/high risk level, non-active (mainly invasive) or active, interacting with the body in a dangerous way;
- Class III: device with high risk level, mainly implantable, containing drugs or interacting with vital functions or invasive with respect to the body orifices.

Many medical devices can be categorized in Class IIa and IIb.

The most important group of standards is represented by IEC 60601-1 – "Medical Electrical Equipment" (often simply referred to as IEC 601). It is a regulation that applies to the safety of medical electrical systems (controlling all the aspects of safety directly or indirectly related to the handling, use or connection to a medical equipment) and defines the necessary requirements to protect the patient, the operator and the surroundings. It includes technical standards aimed at guaranteeing the safety and the effectiveness of medical devices linked to both mechanical and electrical issues. The compliance with IEC 60601-1 has become a requirement for the commercialisation of electrical medical equipment in many countries. The requirements for certain aspects of safety and performance are defined in collateral standards (i.e. 60601-1-X), while those for specific products or specific measurements are described in particular standards (i.e. 60601-2-X).
EIC 60601-1 also defines the requirements for the information to be present on the medical equipment nameplate, which has to constitute an unambiguous identification of the equipment, including the manufacturer's name, the model number, the serial number and the electrical requirements. The labelling has to be easily readable during the whole life of the device and must not unstick itself (neither partially).
During the functional life of medical equipment, visual inspection is one of the most important part of the general safety inspections, since in most cases it allows the technicians to detect possible faults. It concerns the housing enclosure, the cabling, markings and labellings and the integrity of mechanical parts.

With regard to the power sources, according to IEC 60601-1 it is possible to identify three different classes:

- Class I: beyond the basic insulation, the protection against electric shock has an additional safety ground (protectively earthed), connected to the internal/external conductive parts of power source;
- Class II: beyond the basic insulation, the protection against electric shock has an additional insulation layer (double insulation or reinforced insulation).
- Internal power source (e.g. a battery).

Moreover, such regulation defines an applied part as a *part of medical electrical equipment that in normal use necessarily comes into physical contact with the patient for medical electrical equipment or a medical electrical system to perform its function.*
It can be, for example, a cable or an electrode intended, in its normal use, to come into contact with the patient. It is possible to distinguish three main types of applied parts:

- B: it provides protection against electric shock with particular attention to leakage current and patient auxiliary current; it is not suitable for direct cardiac application;
- BF: it has a floating applied part; it provides a higher protection against electric shock and it is suitable for direct cardiac application;
- CF: it has an insulated floating applied part, with the highest protection level against electric shock.

Each of these can be defibrillation-proof applied part, for a total of six parts, as shown in Fig. 57.

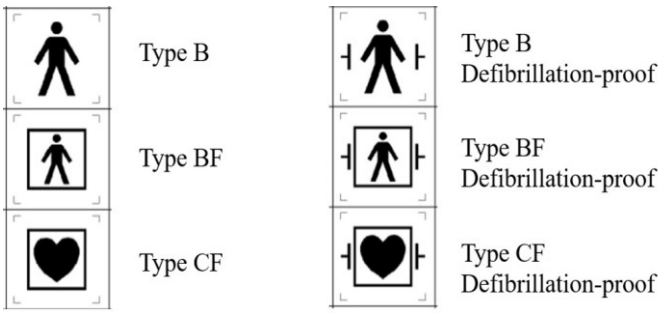

Figure 57. Medical devices - applied parts types

It is important to periodically test the integrity of the low resistance connection between the earth conductor and any metal conductive parts (this is commonly referred to as "Earthbond testing" or "Groundbond testing"). The test current has to be applied (by means of a dedicated probe) between the Earth pin and the main supply plug and any accessible part.

In general, three kinds of electric current have to be taken into account:

- Leakage current, without a functioning effect, which flows through the patient body (connected through an applied part) because of a voltage caused by an external source; all leakage measurements have to be carried out using normal (NC) and single fault conditions (SFC). There are three kinds of leakage currents:
    - Earth leakage, flowing down the protective Earth conductor of the mains inlet leads; the test circuit is reported in Fig. 58;

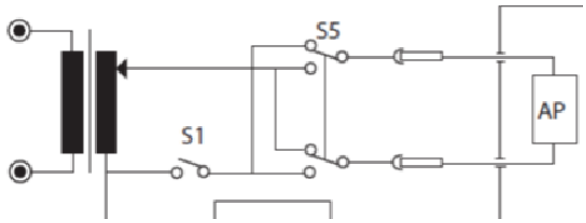

Figure 58. Test circuit for Earth leakage (NC: S1 closed, S5 normal and then reversed; SFC: S1 open, S5 in normal and then reversed) – the relays operate the SFC

    - Enclosure leakage, flowing to the Earth through a person touching the medical equipment (or part of it); the test circuit is reported in Fig. 59;

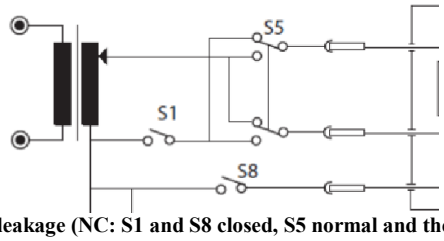

Figure 59. Test circuit for Enclosure leakage (NC: S1 and S8 closed, S5 normal and then reversed; SFC: S1 open, S8 closed, S5 in normal and then reversed) – the relays operate the SFC

- Applied part (or patient) leakage, flowing to the Earth through a person via the applied part by applying an unintended voltage from an external source. It is the most important leakage current; both supply open and Earth open cases are considered. The test circuit is reported in Fig. 60.

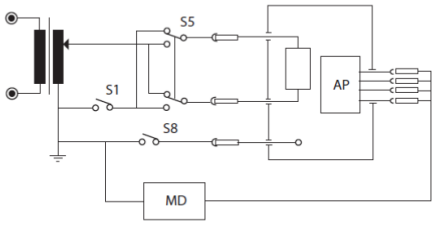

Figure 60. Test circuit for Patient leakage (NC: S1 and S8 closed, S5 normal and then reversed; SFC, supply open: S1 open, S8 closed, S5 in normal and then reversed; SFC, Earth open: S1 closed, S8 open, S5 in normal and then reversed) – the relays operate the SFC

The prescribed limits for leakage currents are reported in Fig. 61.

Excluding power cord	< 0.1 Ω					
Including power cord	< 0.2 Ω					
	Type B Applied Parts		**Type BF Applied Parts**		**Type CF Applied Parts**	
Leakage Current Type	**NC**	**SFC**	**NC**	**SFC**	**NC**	**SFC**
Earth Leakage (General)	0.5mA	1mA	0.5mA	1mA	0.5mA	1mA
Enclosure Leakage	0.1mA	0.5mA	0.1mA	0.5mA	0.1mA	0.5mA
Patient Leakage (dc)	0.01mA	0.05mA	0.01mA	0.05mA	0.01mA	0.05mA
Patient Leakage (ac)	0.1mA	0.5mA	0.1mA	0.5mA	0.01mA	0.05mA
Patient Leakage (F-Type)	NA	NA	NA	5mA	NA	0.05mA
Patient Leakage (Mains on SIP/SOP)	NA	5mA	NA	NA	NA	NA
Patient Auxiliary Current (dc)	0.01mA	0.05mA	0.01mA	0.05mA	0.01mA	0.05mA
Patient Auxiliary Current (ac)	0.1mA	0.5mA	0.1mA	0.5mA	0.01mA	0.05mA

Figure 61. IEC 60601-1 test limits - Earthbond test limits at 25 A, 50 Hz
(NC = Normal Condition; SFC = Single Fault Condition)

- Auxiliary current, which is the current flowing through the patient in normal conditions but no aimed to physiological effects (i.e. the current used to make measurement); the test circuit is reported in Fig. 62;

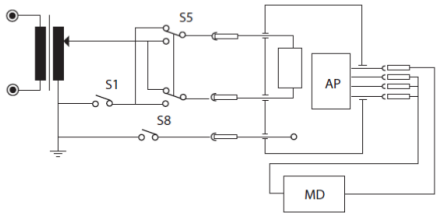

Figure 62. Test circuit for Patient auxiliary current (NC: S1 and S8 closed, S5 normal and then reversed; SFC, supply open: S1 open, S8 closed, S5 in normal and then reversed; SFC, Earth open: S1 closed, S8 open, S5 in normal and then reversed) – the relays operate the SFC

- Electric current aimed at producing some physiological effects on the patient. There are no limits on it, what matters is that the advantage is greater than the risk (or the risk does not exist at all).

In order to reduce the risks caused by the electric shock for the patient, every medical device must be equipped with at least two Means Of Protection (MOP), so that the imposed limits are not overtaken.
The regulation IEC 60601-1 is related not only to electrical aspects, but concerns also the sterilisation method (which has to be described in the device instruction manual) and the protection against harmful ingress of water. Moreover, it deals with mechanical hazards, caused by phenomena such as moving parts, scraping surfaces, sharp sides and edges, instability, vibrations and noise. With regard to mechanical strength, the device has to pass specific impact tests. Finally, this regulation regards the protection against radiations and against too high temperature values.

As disclosed in the introduction of this chapter, the proposed device is a Class II device, with applied parts of type BF; so, besides the general regulation IEC 60601-1, it is necessary to consider other two standards: the collateral standard IEC 60601-1-2 and the particular standard IEC 60601-2-2, which will be described in Paragraph 4.1.1 and 4.1.2, respectively. They are related to electrical safety aspects and to the tests called for an electromedical device of this kind, which can be considered similar to an electrosurgical knife (both for the working frequency and for the amplitude of the used signal - but not for the signal supply duration -).

4.1.1. IEC 60601-1-2

As previously said, the directive IEC 60601-1 deals with medical electrical equipment. IEC 60601-1-2 ("General requirements for basic safety and essential performance - Collateral Standard: Electromagnetic disturbances - Requirements and tests") is a collateral standard discussing the electromagnetic compatibility aspects, that is, the unintentional generation, propagation and reception of electromagnetic energy, which may cause interferences or damages in medical equipment. The international Technical Committee 77 (TC77) of IEC works full-time on EMC issues.
In particular, IEC 60601-1-2 defines the tests for basic safety and essential performance of a medical electrical device in presence of electromagnetic disturbances/emissions.
"Basic safety" refers to the absence of unacceptable risk: it is not possible to have absolute safety, the aim is to reach an acceptable risk level. "Essential performance" refers to those functions considered essentials, where loss or degradations beyond the fixed limits results in an unacceptable risk; they are defined by the manufacturer, complying with his risk acceptability criteria.
This directive is the basis for particular standards, such as IEC 60601-2-2 (which will be described in Paragraph 4.1.2).

Two devices are considered electromagnetically compatible when they work well also in presence of the other one and EMC ensures the correct working of different equipment items in the same electromagnetic environment.
In particular, three aspects have to be considered:

- **Emission**, which is the generation (deliberated or accidental) of electromagnetic energy by a source and its release in the surrounding environment. There are both conductive and radiated emissions; EMC studies possible countermeasures to minimize the unwanted emissions;
- **Susceptibility**, which is the tendency of a device to malfunction in the presence of unwanted emissions (i.e. radio frequency interference, RFI); **immunity** is the opposite of susceptibility, which is the ability of the device to work well even in the presence of RFI;
- **Coupling**, which is the interference (continuous, pulse or transient) mechanism (conductive, inductive, capacitive or radiative) between the emission source and the device.

EMC can act on all the above mentioned aspects, that is, by quieting the interference sources, by inhibiting the coupling mechanisms or by reinforcing the victim device. Obviously, the first steps consist in the identification of the source, the victim and the coupling mechanism.
The EMC aim is to control the interference and to reduce the associated risks to acceptable levels.
Immunity test levels are specified by the directive on the basis of the intended use of the device. Different issues are taken into account: ESD (i.e. electrostatic discharge), radiated and conducted emissions (induced by RF fields), electrical fast transient, bursts, surge and magnetic field.
Tests to be conducted are described and criteria on the identification of immunity pass/fail are defined; acceptable degradations (i.e. not resulting in unacceptable risks) have to be specified. Test conditions, that is, ambient temperature, humidity and atmospheric pressure, have to be as similar as possible to normal ones. During such immunity tests, the device is expected to keep performing its intended use and to remain safe.
Not only the use in hospital is considered (i.e. professional healthcare facility environment), but also different environments: home healthcare environment (e.g. homes, schools and shops) and special environment (e.g. military areas).
The environment of use has to be included in the instructions of the medical device, together with its expected essential performance, the list of cables and transducers.
With regard to the labeling of the medical device, the standard establishes that the instructions have to include the environment of use.

4.1.2 IEC 60601-2-2

IEC 60601-2-2 (entitled “Medical electrical equipment – Particular requirements for the basi safety and essential performance of high frequency surgical equipment and high frequency surgical accessories”) is a set of particular requirements for basic safety and essential performance of high frequency surgical equipment and high frequency surgical

accessories. It amends and supplements IEC 60601-1 and it refers to electrosurgical knife, which, as previously said, is similar to the medical device proposed in this thesis (and described more in detail in the Appendix).
Some of the prescriptions can be applied to the designed device, because of its similarity with electrosurgical knife operation.

4.2. Evaluation of cell vitality

The main requirement for a medical device, even before its effectiveness, is its electrical safety.
In the present study, the first test made in this investigation field was an in vitro test to evaluate the cell vitality after the treatment, made in different experimental configurations and with different therapeutic doses, as it will be described in detail in Paragraph 4.2.2.
At first, such test setup was numerically simulated in COMSOL Multiphysics® environment in order to define the experimental parameters. Such models are described in Paragraph 4.2.1.
This had to be only a pilot study, to be repeated not only in cell cultures, but also in stem and dental-derived stem cells cultivated in scaffolds, in order to evaluate the bone regeneration after the therapeutic signal administration and the anti-bacterial and anti-inflammatory effects by means of microtomography. However, the other steps have not been carried out yet, because of the lack of an adequate laboratory and high cost. In the future, it would be interesting to complete them.

4.2.1. Numerical simulation of in vitro tests

In this paragraph, there is the description of the numerical simulation of in vitro tests. The different configurations are reported in Materials and methods section and the results obtained with different therapeutic doses are finally described.

4.2.1.1. Materials and methods

The in vitro test consisted in experimenting the proposed treatment with different doses (one, two or three repetitions, as it will be described in Paragraph 4.2.2) in cells cultured in DMEM (i.e. standard cell culture media [190]). Cell cultures were grown in Petri dishes, gathered together in groups of six (three tests, three controls). The geometric model is reported in Fig. 63.

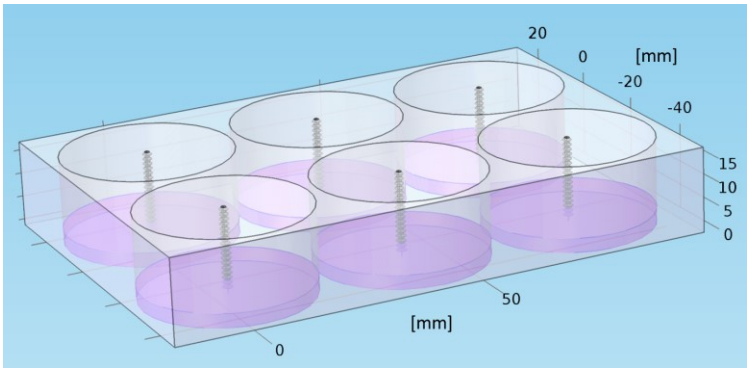

Figure 63. Petri dishes gathered in groups of six: three tests, three controls

A single dish is reported in Fig. 64; the dimensions are 36 mm in diameter and 18 mm in height. The neutral electrode is a screw fixed in the centre of the dish, while the neutral electrode is a metallic foil adhering to the lateral surface of the cylinder. At the bottom of the container, there is the culture media with the cells in suspension.

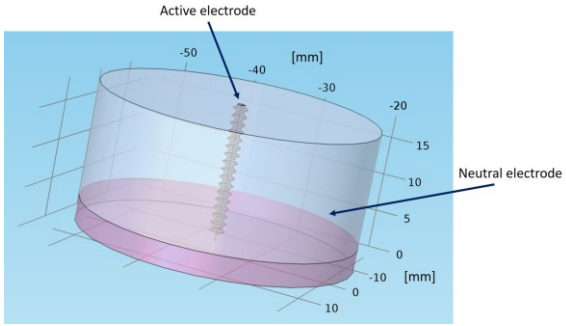

Figure 64. Petri dish with active and neutral electrode (central screw and metallic lateral surface of the cylinder, respectively)

The electric properties of DMEM liquid were measured (at 312.5 kHz, that is the device working frequency) in laboratory by means of an LCR meter (Agilent HP, 4285A precision LCR meter [166]) and are reported in Tab. 14.

Table 14. DMEM liquid electrical properties: electric conductivity (σ) and relative dielectric permittivity (ε_r)

DMEM electrical properties	
Electric conductivity [S/m]	1.21
Relative dielectric permittivity [dimensionless]	5524

The equivalent circuit of the therapeutic device (Paragraph 2.2) is connected between active and neutral electrodes.
Three different configurations are considered:

1. Direct connection between therapeutic device and cell culture (Fig. 65 A));
2. Connection with the interposition of a resistive load of 1.5 kΩ (Fig. 65 B));

3. Connection with the interposition of a resistive load of 9 kΩ (Fig. 65 C)).

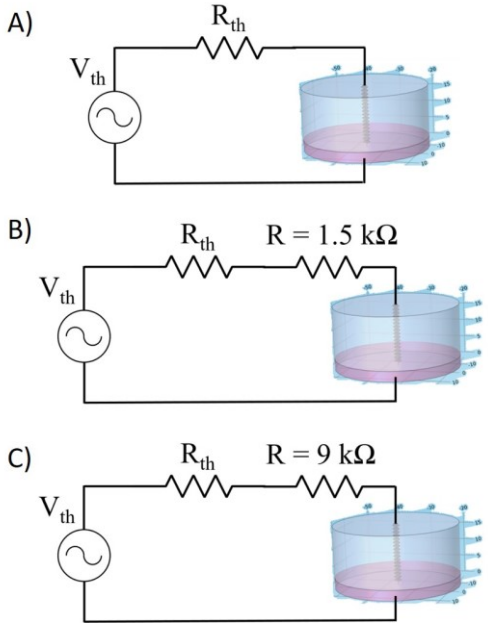

Figure 65. Experimental configurations: A) direct connection between therapeutic device and cell culture; B) interposition of a resistive load of 1.5 kΩ; C) interposition of a resistive load of 9 kΩ

In the second and third cases, the voltage difference between active and neutral electrode will be reduced, so also the electric field will be lower. In this way, it is possible to take into account the effect of different therapeutic doses.

4.2.1.2. Results

The results are reported by considering a single Petri dish; in fact, there are no influences between two adjacent recipients, as illustrated in Fig. 66-67 for what regards electric current density and field distributions, respectively, and in Fig. 68 for the electric field intensity at the mean height of DMEM liquid (frontal view of two adjacent Petri dishes).

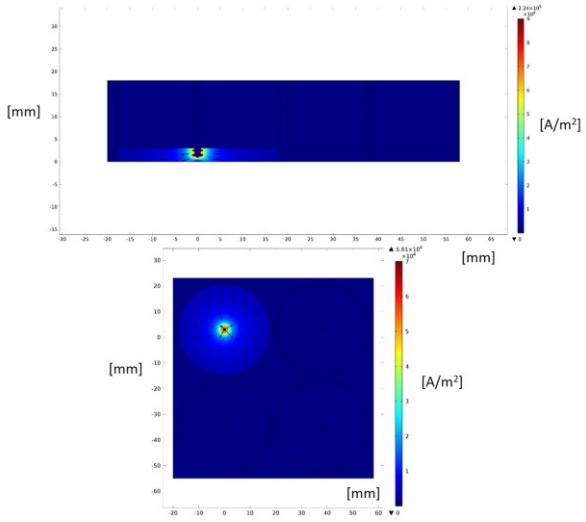

Figure 66. Electric current density distribution - adjacent Petri dishes (frontal side view, top; top view, bottom)

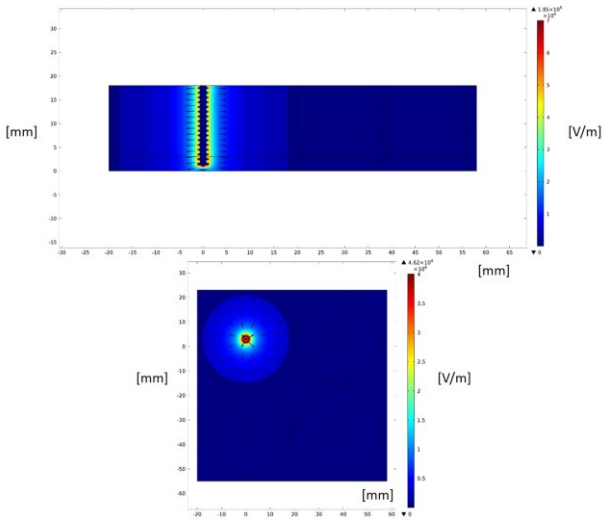

Figure 67. Electric field distribution - adjacent Petri dishes (frontal view, top; view from above, bottom)

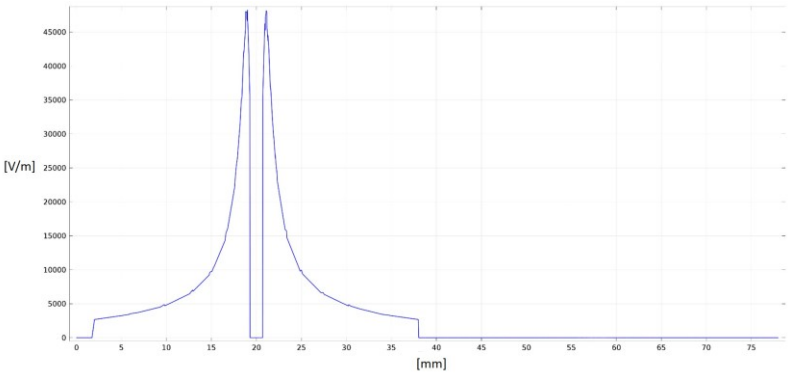

Figure 68. Electric field distribution at the mean height of DMEM liquid in two adjacent Petri dishes - frontal view

In fact, it is possible to note that the plastic walls between two Petri dishes does not allow the current to pass (Fig. 66), while the electric field lines are confined by the metallic neutral electrode (Fig. 67-68).

The results concerning electric current density and field distributions are reported in Fig. 69-71 for configurations 1, 2 and 3, respectively.

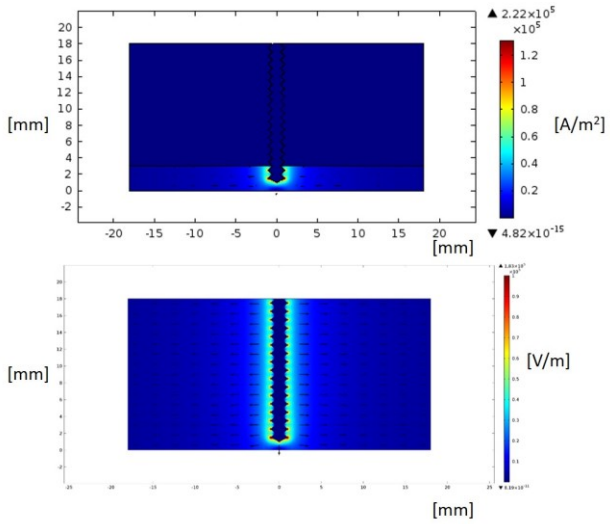

Figure 69. Configuration 1 - electric current density (top) and electric field (bottom) distributions - frontal view

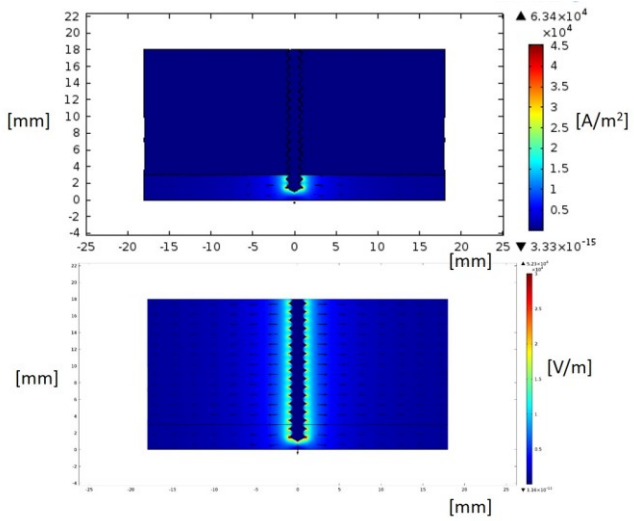

Figure 70. Configuration 2 - electric current density (top) and electric field (bottom) distributions - frontal view

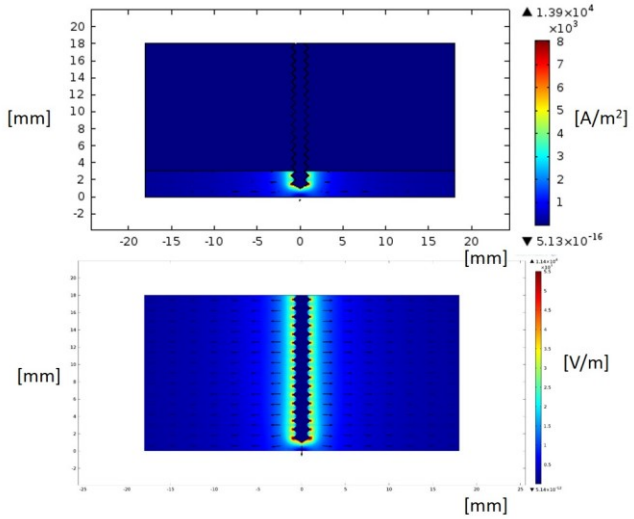

Figure 71. Configuration 3 - electric current density (top) and electric field (bottom) distributions - frontal view

Absolute impedance value of the Petri dish system was equal to 144 Ω. The electric current values passing the system and the potential difference between active and neutral electrodes in the three configurations are reported in Tab. 15. As it was expectable, higher the resistive load connected in series, lower the current passing through the system and the electric potential difference between the two electrodes.

Table 15. Electric current passing the system in the three different configurations

Configuration	Current [mA]	Electric potential [V]
1	1115	160
2	319	46
3	70	10

4.2.1.3. Discussion and conclusions

The realized numerical 3D models allow to observe the electric current density and electric field distributions when the treatment is made on a cell culture. By modifying the experimental configuration (i.e. by connecting in series different resistive loads), it is possible to evaluate the effect of different therapeutic doses. In fact, higher the load in series, lower the electric potential difference between the active and the neutral electrodes, so lower the electric current and field.
In addition, from the results it is possible to state that the used recipients are suitable for such tests, because there are no interferences between adjacent dishes and so the resulting differences are attributable to the different treatments.

4.2.2. In vitro tests

The first pilot study was made at the Department of Experimental Medicine (DIMES) in Naples. The experimental protocol is described in Materials and Methods section, then the results are reported.

4.2.2.1. Materials and methods

The present in vitro study was made on dental pulp derived cells, cultured in Petri dishes (as described in Paragraph 4.2.1).
The experimental protocol adopted in this in vitro study considered three different configurations (reported in Paragraph 4.2.1) and three different therapy modalities (also in the clinical practice, according to the severity of the pathology, the treatment can be repeated up to a maximum of three times, as reported in Paragraph 2.1):

- One burst of the therapeutic signal (i.e. single emission, with a time duration of 140 ms);
- Two repetitions of the therapeutic signal;
- Three repetitions of the therapeutic signal.

So, three groups of six Petri dishes (each including three tests and three controls) were used in the study, to apply the three different therapy modalities. The configuration of each group is reported in Fig. 72.

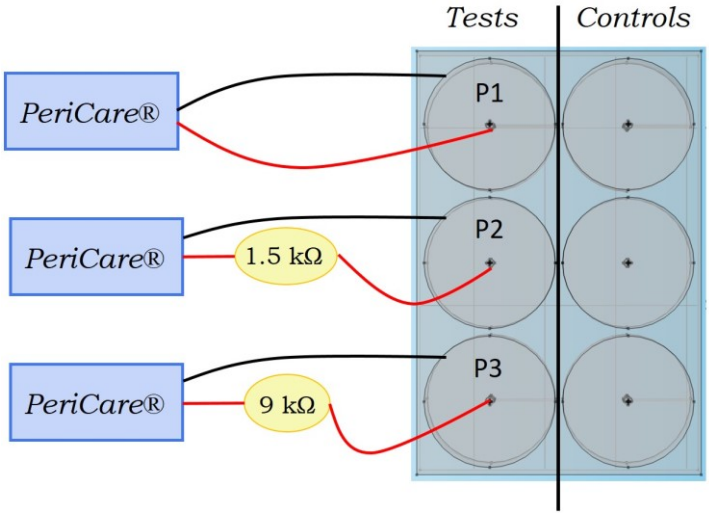

Figure 72. Group of 6 Petri dishes: 3 tests (with the three different configurations: P1, direct connection between the therapeutic device and the cells culture; P2, interposition of a resistive load of 1 kΩ; P3, interposition of a resistive load of 9 kΩ) and 3 controls

The evaluation of the cell vitality was made 24 hours after the treatment by means of annexin/propidium iodide kit and also by means of flow cytometric analysis.

4.2.2.2. Results

The biological results concerning the cell vitality are reported in terms of histograms in Fig. 73-75 for the three different therapy modalities (i.e. one burst, two and three repetitions), respectively.

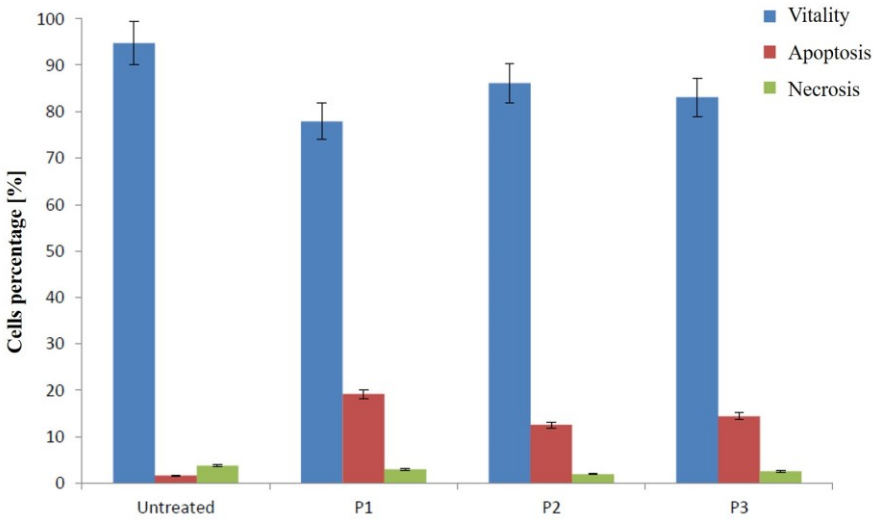

Figure 73. Vitality evaluation - one burst therapy modality

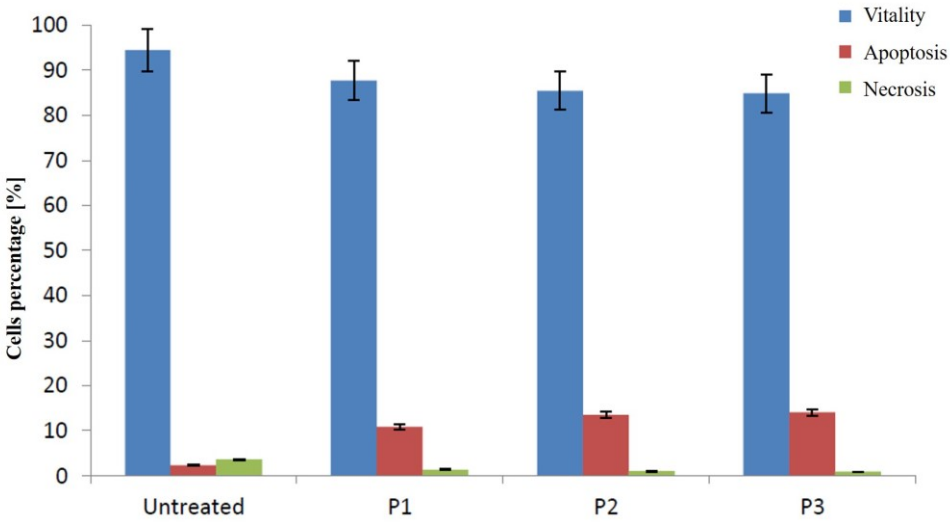

Figure 74. Vitality evaluation - two repetitions therapy modality

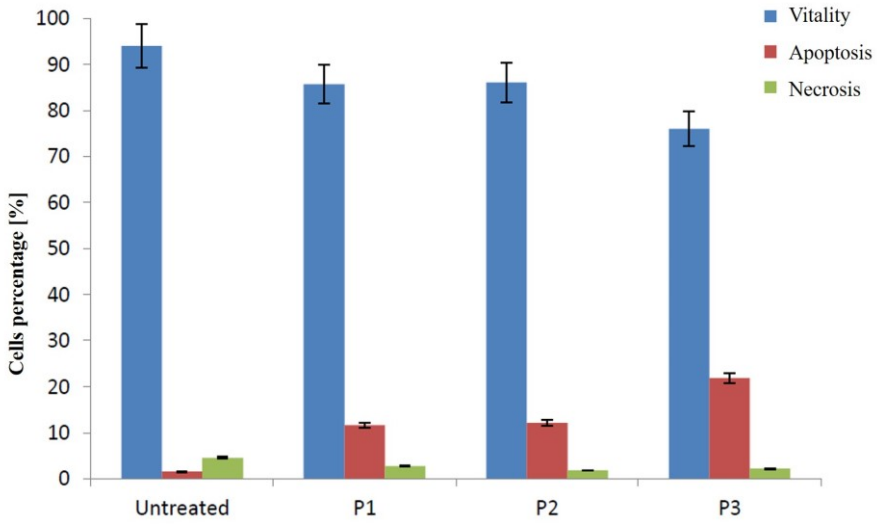

Figure 75. Vitality evaluation - three repetitions therapy modality

4.2.2.3. Discussion and conclusions

The in vitro study allowed to evaluate the cell vitality after the treatment, administered in different conditions, both in the therapeutic dose (i.e. by means of different connections between the therapeutic device and the cell cultures) and in the repetitions of the therapeutic signals (up to three times).
The resulting cell vitality is very high: about 85% for the tests versus 94% of the controls. The main negative effect caused by the administered treatment was apoptosis (i.e. a process of programmed cell death, highly controlled, conferring advantages during an organism's lifecycle [191]), but does not cause a significant increase in necrosis (i.e. a form of traumatic cell death resulting from acute cellular injury [191]).
So, it is possible to state that the applied therapeutic doses do not cause strong consequences on the cell vitality. Only the dish P3 in the group treated with three repetitions the vitality is a bit lower with respect to the average one.
Anyway, it would be important to consider the fact that in the colture medium neither electric current nor electric field distribution is uniform, so it is not possible to state that every cells have been exposed to the same dose. In the future, it could be interesting to make the exposition by means of a capacitor, in order to obtain a uniform distribution.
In conclusion, this pilot study provided noteworthy results, but, as already said in the introduction of Paragraph 4.2, it needs to be repeated, also to study the differentiation capacity of the treated cells and the effects of different therapeutic doses.
In addition, other kinds of in vitro tests should be made in order to gather different information on the therapeutic effects of the treatment on different cell populations.

4.3. Numerical simulation of thermal effects

The therapy is given by means of two electrodes placed in the oral environment, hence it is important to consider also possible effects on nerves (trigeminal nerve and its branches, in particular) and on the cardiac activity. Anyway, since the working frequency is 312.5 kHz, there are nor nerve stimulation effects (absent above 300 kHz [192] – the same precaution is adopted in electrosurgical knife, to avoid stimulation effects) nor the risk of interferences with the heart (nearly absent for frequencies higher than 4 kHz [55]).
As regards electrocution risks, it can be asserted that the dangerous signals are those whose duration is less than 10 ms, included in the critical period of the cardiac cycle (i.e. the vulnerable period).
At frequencies of hundreds of kHz, the heating effect is the only relevant one. In order to evaluate possible thermal effects of the proposed therapy, numerical simulations were run in COMSOL Multiphysics® [118] environment.
In particular, an electromagnetic study is carried out in order to evaluate the electric field distribution; then, the Joule effect is used to couple the electromagnetic physics to the thermal one, so obtaining the temperature distribution.
As it will be described in detail in Materials and Methods section (Paragraph 4.3.1), the geometric model represents a dental implant screwed in the jawbone and the surrounding jaw, to evaluate the therapy influence on the surrounding tissues.
In the results, it is fundamental to take into account the numerical errors due to singularities (i.e. edge effects): temperature values resulting from the simulations cannot be considered reliable for some mesh elements from the edge. Anyway, the global results are not influenced by such phenomena, so they can be evaluated.

4.3.1. Materials and methods

In this paragraph, there is the description of the numerical simulations of the therapy run on a model representing a dental implant substituting a premolar tooth root and the surrounding tissues.

A simplified geometry of the tissues surrounding the dental implant was considered (i.e. the same described in Paragraph 2.3.1.2, to which the lateral jawbone has been added).
In order to simulate the therapeutic signal administration, two electrodes were modelled:

- Active electrode, which is screwed in the fixture of the implant;
- Passive electrode, adhering to the gingiva.

The geometry of the model is reported in Fig. 76.

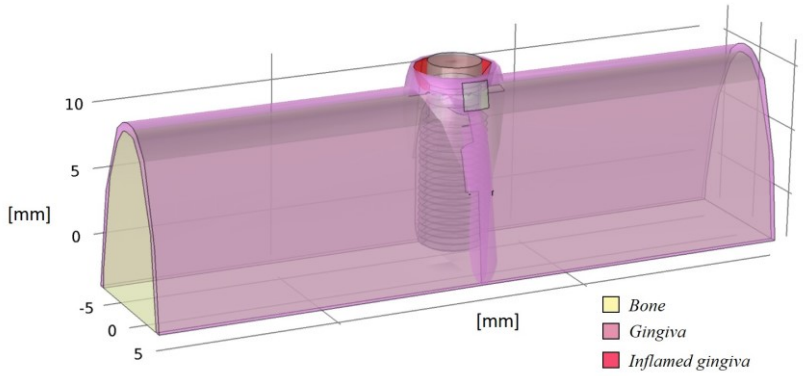

Figure 76. Geometry of the model representing a dental implant screwed in the jawbone and the surrounding tissues

The geometric and the electric properties of biologic tissues are the same used in the simulations described in Paragraph 2.3.1.2. As regards the thermal properties, they were taken from the literature [193]–[196] and they are reported in Tab. 16.

Table 16. Biological tissues thermal properties

Tissue	Density ρ [kg/m^3]	Thermal capacity Q [J/(kg*K)]	Thermal conductivity k [W/(m*K)]
Dental pulp (connective tissue)	1027	2372	0.39
Dentine/Enamel (bone-cortical)	1908	1313	0.32
Bone (cancellous)	1178	2274	0.31
Gingiva (connective tissue)	1027	2372	0.39

The first step in the simulation was the electromagnetic study (COMSOL Multiphysics® AC/DC module), conducted in the same manner described in Paragraph 2.3.1. Once obtained the electric potential distribution (and so also the electric field and the density current ones), thanks to the multiphysics option of the software, the thermal study was carried out in the time domain (COMSOL Multiphysics® Bioheat transfer module), considering an interval equal to the duration of the treatment (i.e. 140 ms). In this way, the temperature distribution can be obtained. In particular, the heat equation is considered (Eq. 13):

$$\rho C_p \frac{\partial T}{\partial t} + \nabla \cdot (-k\nabla T) + \rho C_p u \nabla T = \rho_b C_b \omega_b (T_b - T) + Q_{met} + Q_{ext} \quad (13)$$

where:

- ρ is the tissue density (Tab. 16);
- ρ_b is the blood density (i.e. 1000 W/m^3 [197]);
- C_p is the thermal capacity at constant pressure;
- C_b is the blood thermal capacity (i.e. 3639 J/(kg·K) [198]);
- T is the temperature [K];
- T_b is the blood temperature (i.e. 37°C = 310.15 K [199]);
- ω_b is the blood perfusion rate (0.0036 s^{-1} [200]);
- Q_{met} is the metabolic source (negligible);
- Q_{ext} represents the electromagnetic heating.

Both for the electromagnetic and for the thermal studies, the simulation was run selecting a direct solver, for a fully coupled solution.

4.3.2. Results

The distributions of the electric current and of the electric field are reported in Fig. 77-78, respectively, in a frontal section of the model, so as to observe possible influences in the surrounding tissues.

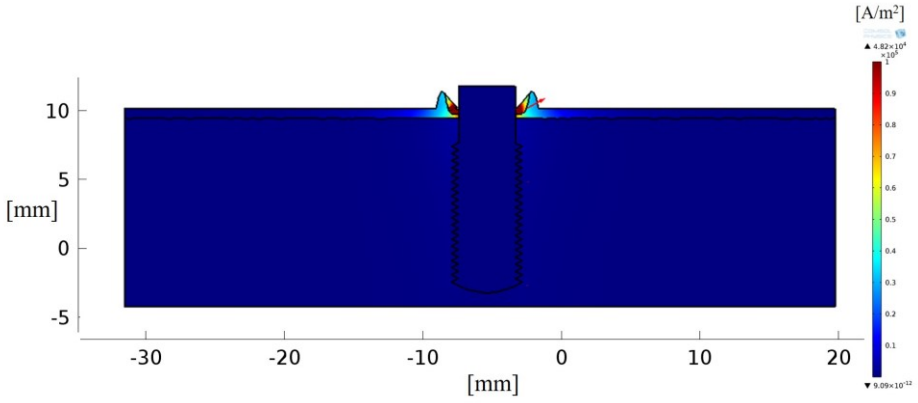

Figure 77. Electric current density distribution - frontal section

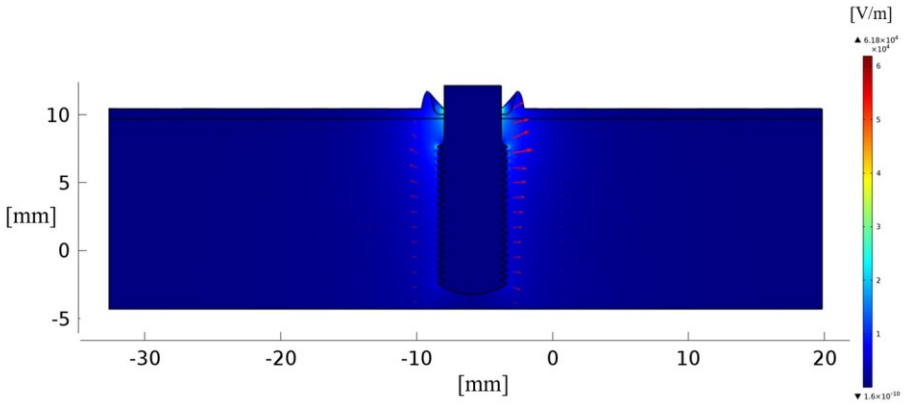

Figure 78. Electric field distribution - frontal section

In Fig. 79 the temperature distribution is shown.

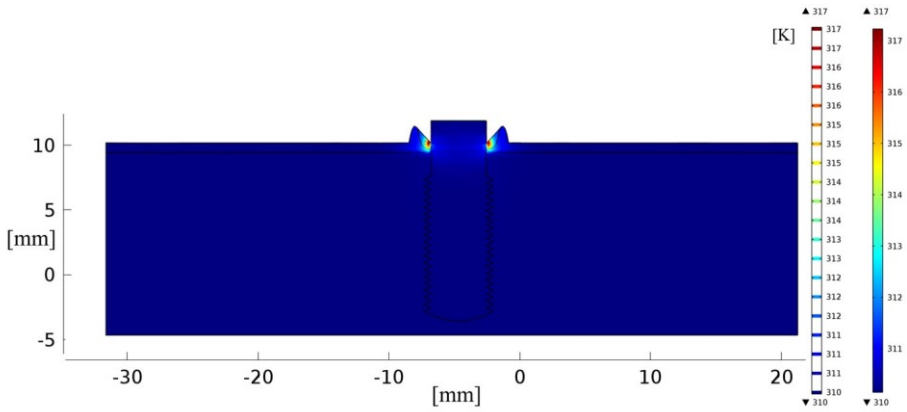

Figure 79. Temperature distribution - frontal section

It is possible to note that the edge effects causing spikes in the electric field distribution (in particular, in the edge between the gingiva and the implant surface) affect also the electric current distribution, since $J = \sigma E$ (Eq. 8). So, the numerical errors come back in the temperature distribution results.
If we move from such edges, the temperature rise is not elevated, as shown in Fig. 80.

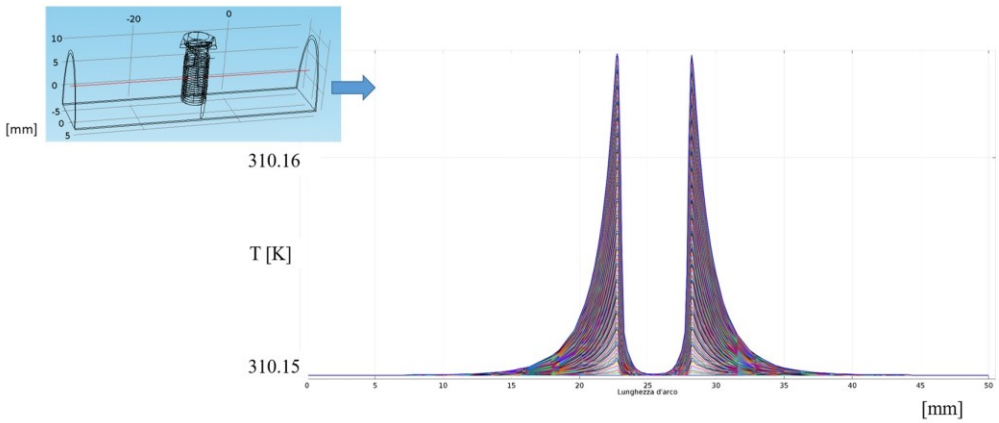

Figure 80. Temperature increase during the treatment (the coloured lines correspond to the various time instants) – transversal line (the red one in the picture on the left)

4.3.3. Discussion and conclusions

The coupling between electromagnetic and thermal physics in COMSOL Multiphysics® environment allows to analyse the temperature distribution associated with the Joule effect caused by the treatment.
In spite of the presence of edge effects, it is possible to observe that, while moving far from the source (i.e. the implant itself), the thermal effect gradually becomes weaker, so that, also thanks to the blood perfusion, the tissues are maintained at the physiological temperature of 37°C. The global temperature increase in the tissues surrounding the treated dental implant is lower than 1°C (except for the area near the electrodes edges, where the electric current density is higher), so it can be considered acceptable.
The edge effect can be diminished by reducing the size of the mesh elements; anyway, it was not possible to do this further, because of computational issues. Besides, edge effects partly exist in reality, so it is normal to have a different distribution of the electric current density (and, consequently, of temperature) near the geometric boundaries (important because they can cause burns), even if numerical errors due to singularities produce not reliable results.
In conclusion, this simulation confirms that the proposed therapy for peri-implantitis does not cause dangerous heating effects on the surrounding tissues.

Chapter 5.

Discussion and conclusions

This doctoral study project started from the clinical evidence of a radio frequency electric current-based therapy for peri-implantitis experimented in a clinical trial (Paragraph 2.1). Such therapy, which can be included in the electric treatments and electromagnetic stimulation (Paragraph 1.3), is able to inhibit bacteria, to stimulate bone regeneration and to block the inflammatory process. The analysis of the available follow-up data has demonstrated that there are no complications associated to the treatment, whose sessions are fast and painless, allowing an immediate benefit for the implant recovery. Therefore, the outcomes are significant and in the future the clinical trial will be broaden, in order to get more data to evaluate, so as to support both the efficiency and the safety of the proposed therapy for peri-implantitis.

The initial medical device used for the therapy (i.e. Endox® Endodontic system) has been electrically characterized (Paragraph 2.2), providing the Thevenin's equivalent circuit (i.e. a series connection between a sinusoidal voltage generator (V_{th} = 474 V, RMS value, corresponding to a peak value of 474*√2 V) and a resistor (R_{th} = 458 Ω).

Then, the obtained model has been used in numerical simulations run in COMSOL Multiphysics® environment (Paragraph 2.3), in order to simulate the therapy and to better understand the underlying mechanisms. In fact, the numerical results provide the electric current and field distributions obtained with the administration of the therapy to a dental implant screwed in the jawbone affected by inflammatory process (characteristic of peri-implantitis) or to a natural tooth root with inflamed periodontal tissues (i.e. periodontitis). It is possible to infer that probably the anti-inflammatory effect is associated to the electric current (focused in the inflamed portion of the gingiva), while the bone remodelling effect is due to the electric field (whose lines cross both soft and hard tissues).

Moreover, it can be observed that the therapeutic signal proves to be limited to a small area, minimizing the effects on the surrounding tissues. The electromagnetic signal can be driven also by moving the neutral electrode, in order to focus the treatment in the impaired area, which can be localized thanks to bioimpedance measurements (Chapter 3).

The feasibility of this approach has been at first evaluated by means of numerical simulations, both on dental implant and on natural tooth root models.

With regard to the simulations run on dental implant models, it is possible to state that the neutral electrode should be preferably small and round-shaped. As it can be expected, more the inflammation is severe and big, more easily its detection is. The computed change in impedance appears to be adequately pronounced (i.e. 4-20%, depending on the different parameters) to discriminate between healthy and inflamed tissues. This would be an objective method helping the clinician to detect, locate and quantify an inflammation and it

would be quite important, if it is considered that nowadays the inflammation diagnosis is mainly made with the naked eye (i.e. by observing the redness and the swelling). In the future, it would be interesting to expand the application field of such a measure to assess the bone level and so the implant stability (given that a correctly osseointegrated implant shows a higher impedance modulus).
As regards the simulations run on natural tooth root models, in the presence of inflammation changes of 11-18% in the impedance modulus have been observed. So, also in this case, inflammation localisation seems to be possible and it could be useful in case of periodontitis. In addition, it can be noted that in these simulations the computed impedance modulus decreases while moving the electrodes downwards. This stresses the importance of the measurement configuration to guarantee the repeatability of the results.
After having verified the feasibility of bioimpedance measurements for inflamed tissues localisation, experimental measures have been carried out, both in patients with dental implants (in different conditions, i.e. healthy, with inflammation and affected by peri-implantitis) and on healthy subjects (in order to evaluate the measurement repeatability). Concerning the measures in patients, the results appear to be in agreement with the numerical ones, that is, a measured impedance in the order of hundreds of Ohm (both real and absolute values, while the imaginary part - negligible - strongly depends on the electrode-tissue interface). Also the variation observed in the presence of an inflammatory process is consistent with the simulated one, even if in the experimental case it is even greater (i.e. 35%) due to the tissue swelling, which was not represented in numerical models for the sake of simplicity. In case of peri-implantitis, the impedance variation is even more evident (i.e. 56%) because of the bone loss around the dental implant. The repeatability of the measure in patients resulted satisfying (≈ 2-4%), even if in the future it is auspicable to design a more handy electrodes system to be comfortably used by clinicians. In order to obtain a sort of database of physiological/pathological bioimpedance ranges, several further measurements on the different cases are needed (in fact, at present only the comparison between healthy and pathologic is possible, but not the classification of individual measurements).
With regard to the measurements on healthy subjects, three different teeth have been considered (i.e. incisor, canine and premolar) and the measures have been repeated for four consecutive days in three subjects. The order of magnitude of the measured impedance modulus is the same of the numerical results (i.e. some kΩ), even if the former are lower. This can be due to the variability of tissues electrical conductivity, to the different morphology of tooth roots, to possible variations in electrode positioning and also to the actual electrode surface in contact with tissue. The influence of the electrode area and position has been confirmed by means of proper simulations. So, the measurement arrangement (e.g. electrodes positioning and electric contact with tissues) is extremely important, therefore in the future it would be fundamental to design a precise electrode system (e.g. by using conductive rubber, hydrogel or carbonated fiber, adaptable to curved surfaces) easy to use by clinicians.
Considering the repeatability of the measurement, it has been reported an intra-subject variability < 10% in a same day, but higher (i.e. up to 26%) in different days, maybe due to the variation in the electrodes positioning. The values computed for the inter-subject variability was higher (up to ≈ 20% for the premolar tooth). Anyway, in the future it would be interesting to make a kind of measurement campaign aimed at creating a database of

bioimpedance values in healthy natural tooth roots. Also the application of EIS (Electrical Impedance Spectroscopy) could be interesting in this field, in order to study the response in different frequency ranges.
Later, the safety aspects of the electromedical device have been considered (Chapter 4), paying particular attention to the electric hazards. The regulation of interest (i.e. IEC 60601-1) have been examined, underlining the aspects related to the handling, use or connection to a medical equipment and the requirements to protect the patient, the operator and the surroundings. Also the electromagnetic compatibility aspects have been taken into account (i.e. collateral standard IEC 60601-1-2), defining the tests to be carried out in order to prove the conformity of the device. As particular standard, that related to surgical knife has been considered (i.e. IEC 60601-2-2), since the working frequency and the signal amplitude are similar (on the contrary, the duration is much shorter, otherwise the cutting effect would be caused).
In vitro tests have been carried out in order to evaluate the cell vitality after the treatment administration (Paragraph 4.2). Different therapeutic doses and repetitions of the treatment have been considered and the effects have been evaluated.
At first, numerical simulations have been run to define the optimal test arrangement. The results show the electric current and field distributions and also confirm that the chosen plastic container for the cell cultures (i.e. Petri dishes) are suitable, since no interferences between adjacent dishes have been observed.
The experimental results have shown a very high cell vitality after the treatment (i.e. $\approx 85\%$ for the tests versus 94% of the controls). The main negative effect of the treatment was apoptosis, but there was not a significant increase in necrosis. Important findings were obtained, but in the future it will be necessary to repeat the tests to study also the effects in the differentiation capability of the treated cells in relation to different administered therapeutic doses. In addition, these trials should be made also in stem and dental-derived cells cultivated in scaffolds, to evaluate the bone regeneration effect.
To conclude the safety aspects evaluation, the thermal effects have been numerically simulated to analyse the temperature distribution caused by the Joule effect associated to the therapeutic signal. From the results (omitting those related to the elements close to sharp edges - edge effects are associated to numerical errors due to singularities -) it is possible to observe that the temperature distribution is not influenced by the treatment and the tissues are maintained at the physiological temperature of 37°C. The global temperature increase in the implant surroundings is lower than 1°C, which can be considered acceptable. So, it can be asserted that the proposed therapy for peri-implantitis does not produce dangerous heating effects on the surrounding tissues.
The prototype of a new device specifically designed for peri-implantitis, named PeriCare® (Appendix), is in the realization phase. It includes both a diagnostic and a therapeutic part, the former for the inflamed tissues detection, the latter for the real therapy. The CE marking process is underway: the technical file is being compiled and the tests for the device conformity verification are being planned.
Then, a clinical trial with PeriCare® will be started. It is expected that the device will be placed into the market during this year.

Appendix: PeriCare® prototype

PeriCare® is the name of the electromedical device whose intended use is specific for the treatment of peri-implantitis. The considered aspects are two:

- Therapeutic aim: the treatment of peri-implant tissues affected by peri-implantitis by means of radio frequency electric current (effective against inflammation, bacterial infection and bone loss);
- Diagnostic aim: localization and quantification of inflamed tissues by means of bioimpedance measurements.

The prototype is being completed and its technical file is being written up, in order to have the device classified by a notified body, who inspects also the manufacturer, its potential third party (who must be certified in compliance with ISO 13485, "Quality management for medical devices" [201]) and the control mechanism between the two. Then, the notified body will carry out annual inspections.
As already said in Chapter 4, the certification process is being started and the required tests are being defined and designed. Once these steps are completed and the CE marking is obtained, a clinical trial with PeriCare® device will be begun (after the permission will have been granted by the Ministry of Health). The efficacy and the electrical safety of the supplied treatment has already been demonstrated through the clinical trial described in Paragraph 2.1 (whose results are reported in [79]).

The theoretical block diagram of the prototype of the new device is reported in Fig. 81.

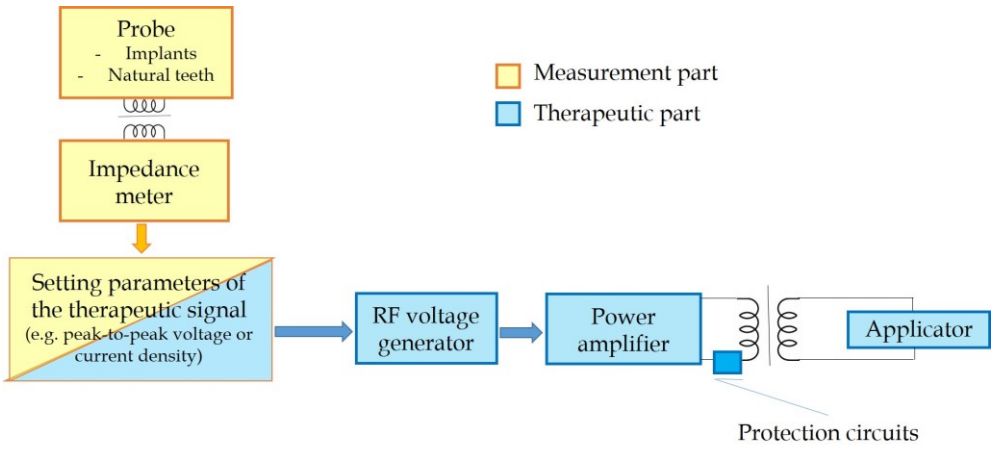

Figure 81. Theoretical block diagram of the prototype of the new device

In the block diagram, the therapeutic part is indicated in blue, while the measurement one in yellow. With regard to the latter, probes (i.e. electrodes) specific for the measurement on

implant/natural tooth roots are being developed, according to the findings made in this doctoral project (Chapter 3). The impedance meter allows the impedance modulus to be assessed, in order to make speculations about the inflammatory state of the tissues and also to monitor the course of the pathology after one or more therapeutic sessions.
Depending on the measured bioimpedance values, the therapeutic signal can be set (this can be done manually only in the prototype of the device in order to tune the treatment to the pathological conditions of the peri-implant tissues, while in the commercalised apparatuses it will be automatically fixed). The device includes different MOPs (indicated in general terms as “Protection circuits”) controlled by a microprocessor, in order to protect the patient and the operator against electric hazards. The applicator is being designed in a way that is suitable to focus the therapy on the inflamed tissues and to guarantee an optimum electric contact.

User instruction manual

According to the European directive 93/42/EEC, the user instruction manual has to include several information, which can be summarized in the following main points:

- The information reported in the medical device label (e.g. manufacturer, maintenance indications and cautions);
- The expected performance and the undesirable adverse effects;
- The instructions for the installation of the device and the useful verification procedures;
- The description of potential risks;
- Possible interferences with other medical devices;
- Instructions about cleaning and sterilisation;
- Possible contraindications to the use of the device;
- The precision of the measurement instrumentation.

In the specific case, PeriCare® manual (which is still being amended) presents two main parts: the instructions for the use of the device and some general information. The prototype described in the manual also provides for the electric potential difference measurement, in order to verify its possible usefulness in the characterisation of pathologic tissues. Moreover, in addition to the real therapeutic signal, an initial analgesia is considered, in order to avoid possible pain to the patient.

Instruction for use

PeriCare® device includes a control unit, a 7” LCD display, a touch screen keyboard, a handpiece with two electrodes, an impedance meter and a voltmeter, as shown in Fig. 82.

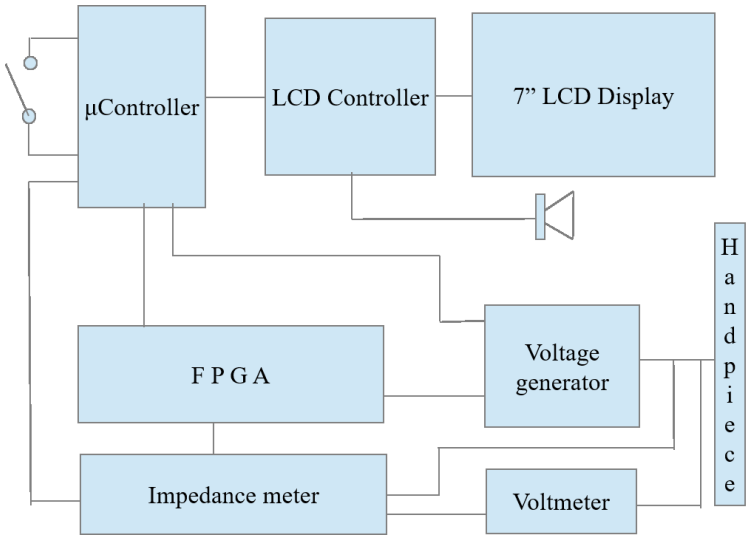

Figure 82. PeriCare® block diagram

PeriCare® device can measure both the electric potential difference and the electrical impedance between the two electrodes of the handpiece. The measurement range is equal to 100 µV – 1 V for the electric potential and to 50 Ω - 50 kΩ for the impedance absolute value. The impedance measurement can be made by using an electric potential difference of 100 mV – 1 V (it depends on the signal quality). In particular, low voltages are used for patients with severe inflammations or those who are particularly sensitive to voltage and have a very low pain threshold.

When the device is turned on, the product name and the release will be shown on the display. It will be possible to adjust the screen brightness (by means of “+” and “-” buttons) and to choose the language.

Moreover, it is possible to display the therapies previously administered to a certain patient (who can be selected through the button “Patient”), with the related data measured in such therapeutic sessions.

The starting screen is reported in Fig. 83 (where INQBA is the manufacturer’s name).

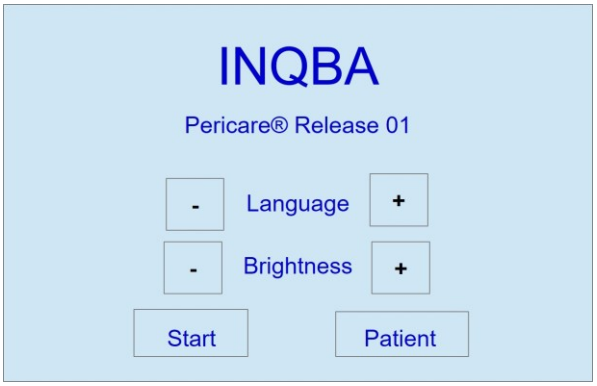

Figure 83. PeriCare® starting screen

By pushing the "Start" button, after a short sound, the screen "Setting of the measurement times" will be shown, as reported in Fig. 84. A progressive number is assigned to each treated patient; in addition, it is possible to select a patient previously treated by means of "+" and "-" buttons and in this case the "Therapeutic session" number will be progressively increased with respect to the latest treatment (this case will be described more in detail at the end of this paragraph).

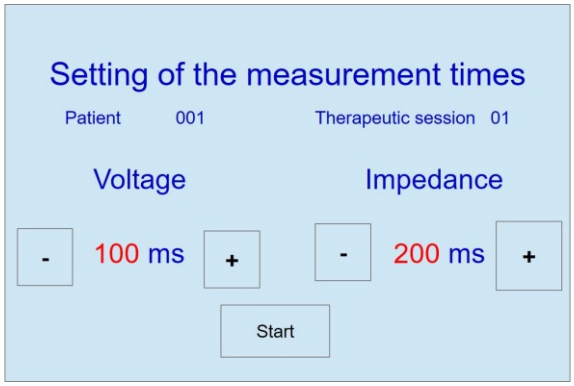

Figure 84. Setting of the measurement times screen - example

The measurement times of voltage and impedance can be set by pressing "+" and "-" buttons; such intervals can be varied from a minimum of 100 ms to a maximum of 300 ms, with steps of 10 ms.
Then, pressing the "Start" button, the device will get ready to make the measurements; later, the "auto-calibration" phase will start, while showing the screen reported in Fig. 85. It is very important not to wait more than 3 minutes between the measurement time setting and the measurement itself, since the made auto-calibration has a limited time duration.
The measurement procedure consists in a series of measures:

- The measurement of the electric potential difference between the electrodes for the set time duration;

- The measurement (in DC, Direct Current) of the resistance between the electrodes for the set time duration;
- The measurement (at 5 kHz) of the impedance between the electrodes for the set time duration.

Figure 85. Measurement execution screen

During the measurement procedure, a modulated sound is emitted; when the sound stops, the measured values (i.e. voltage, resistance and impedance) will be shown. These values are the average between the multiple measurements made during the set measurement time intervals. In addition, three bars will be shown, for voltage, resistance and impedance, respectively. These bars will be green if the measured values can be considered physiological; otherwise, they will be yellow if the values are little far from the physiological range and red if the difference is high, as shown in Fig. 86. If the measured resistance value is lower than 150 **Ω**, a continuous sound will be emitted to highlight an abnormal condition.

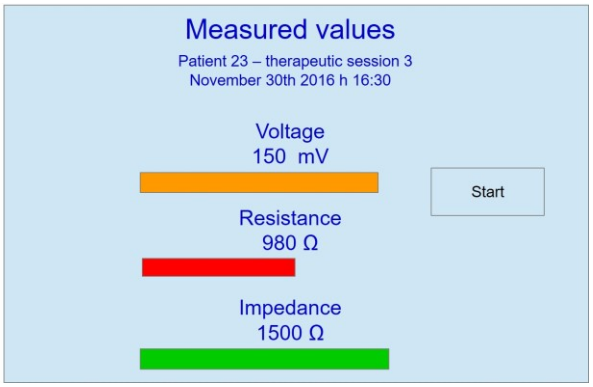

Figure 86. Measurement results screen - example

When pressing the "Start" button, it will be passed to the next phase. Depending on the measured values of electric potential and impedance, power and duration values of the therapy to be applied will be recommended, together with the induced analgesia. These

values will be proposed in two consecutive screens and it will be possible to modify them through "+" and "-" buttons (both for what regards the analgesia and the therapy).
The therapeutic signal amplitude can be regulated between a minimum of 20% and a maximum of 90%, with increments/decrements of 5%. Also the burst duration can be adjusted, between a minimum of 20 ms and a maximum of 210 ms, with increments/decrements of 10 ms.
The analgesic signal can be regulated between a minimum of 3% and a maximum of 15%, while the duration can be adjusted between a minimum of 5 ms and a maximum of 25 ms.
A typical screen during this setting phase is reported in Fig. 87.

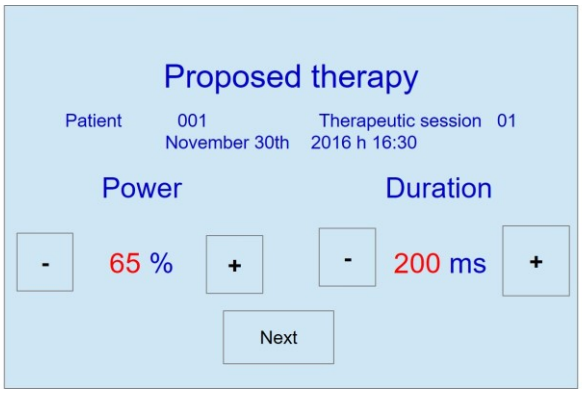

Figure 87. Therapy parameters setting screen - example

Once that power and duration of the therapeutic signal have been set, by pressing the "Next" button it is possible to go to the next screen to regulate the analgesic signal parameters (Fig. 88).

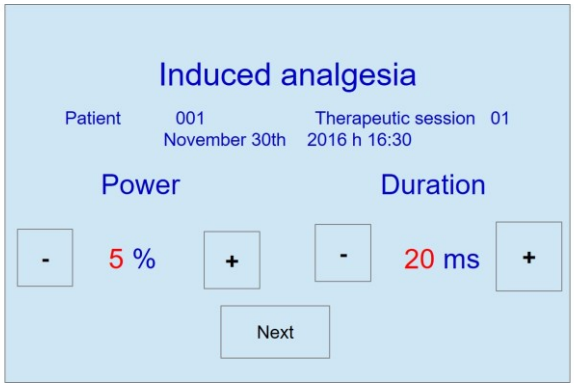

Figure 88. Analgesia parameters setting screen - example

By pressing the "Start therapy" button, the device will produce a voltage with a variable duty cycle and a peak-to-peak amplitude equal to 1200 V, with a maximum peak current of 5 mA (the current is limited by proper resistors placed in the circuitry, in order to avoid too high intensities on the tissues). During this phase, a sound will be emitted for the whole

therapy duration, to inform that a high voltage is being produced; in addition, a red led on the device will be lighted.
The resulting screen is reported in Fig. 89.

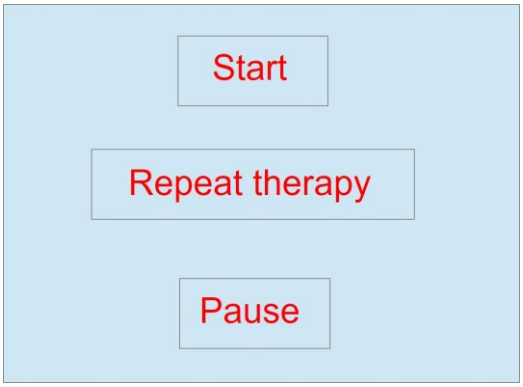

Figure 89. Screen after the therapy administration

By pressing the "Start" button, the procedure will be restarted.
By pressing the "Repeat therapy" button, it will be possible to regulate the power and the duration of the therapy and of the analgesia (Fig. 87-88).
By pressing the "Pause" button, the device will be put in low energy consumption modality, from which it is possible to exit simply by touching the display.
If during the measurement phase the "Pain" button (hand-held by the patient) is pressed, the measurement is immediately interrupted and the measured value is shown with the "Pain" indication, as reported in Fig. 90.

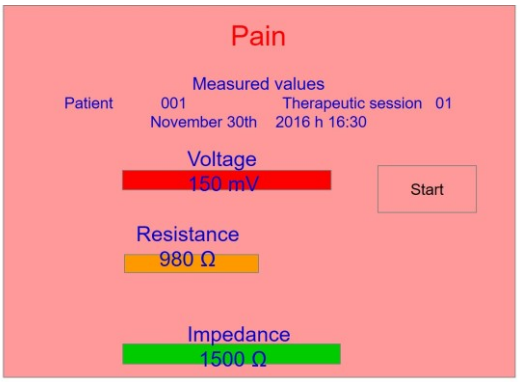

Figure 90. Measurement results screen in case of pain indication - example

However, even if there is the pain indication, the measurements are made with the minimum time duration. This allows to have information on the actual inflammatory status of the tissue.
Then, it is possible to proceed with the setting of the therapy parameters (Fig. 87). In this case, the suggested therapeutic values are minima, to avoid further pain to the patient.

When switching on the device, if it is desired to treat a patient who has already been treated in the past, it is necessary to press the "Patient" button (Fig. 83), instead of the "Start" one. So, the screen shown in Fig. 91 would appear. The patient can be selected by means of "+" and "-" buttons and it is also possible to visualize the therapeutic sessions administred for the selected patient, as well as the measured values and the therapeutic parameters, as shown in Fig. 92, by pressing the "Next" button.

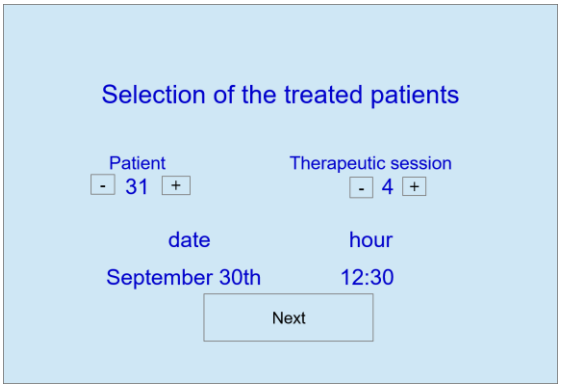

Figure 91. Treated patients selection screen

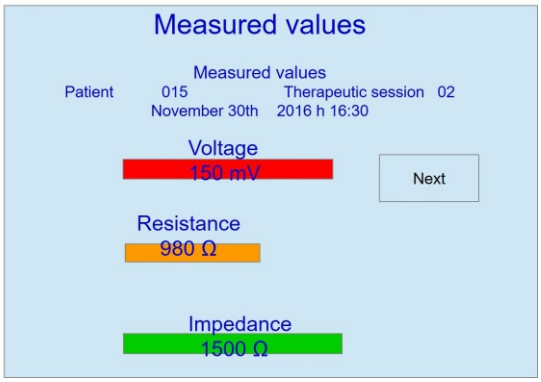

Figure 92. Measured values for a treated patient screen - example

By pressing again the "Next" button, it is possible to see the therapeutic signal parameters, as shown in Fig. 93.

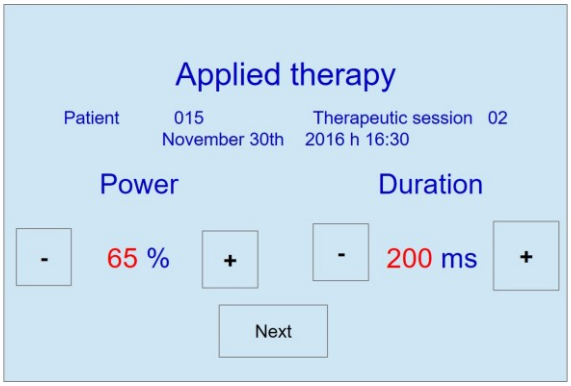

Figure 93. Therapy parameters for a treated patient screen - example

Then, by pressing again the "Next" button, it is possible to see the analgesia parameters, as shown in Fig. 94.

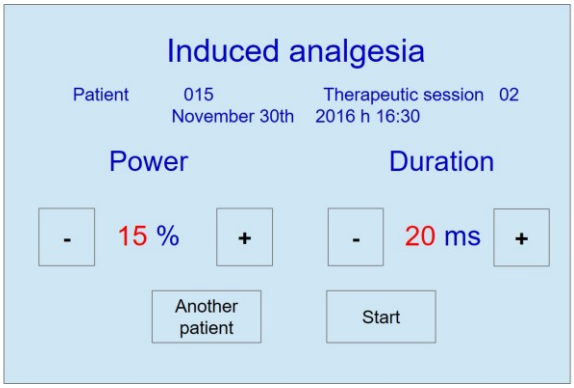

Figure 94. Analgesia parameters for a treated patient screen - example

Finally, by pressing again the "Another patient" button, the initial screen is returned to treat another patient or to administer another therapy session to the same patient. By pressing the "Start" button, it is possible to start a new therapeutic session.

General information

The device functioning is guaranteed by a lithium-ion rechargeable battery. The low energy consumption mode is guaranteed for 24 hours or about 50 consecutive therapeutic sessions. When the battery level is at ≈ 30%, the device will emit a short acoustic signal every 2 minutes, to draw attention to the necessity of recharging the battery.
If the battery level is lower than 20%, the device will show the screen in Fig. 95. Anyway, it is possible to make another two therapeutic sessions by pressing the "Later" button. However, it will be necessary to recharge the batteries in order to not compromise the device functioning.

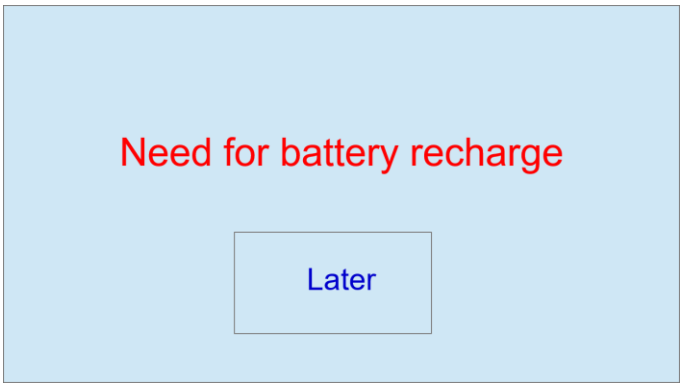

Figure 95. Battery low level (< 20%) screen

After about 10 minutes of inactivity, the device enters in "Pause" modality (low energy consumption).
It is advisable to turn off the device when it is not used, by means of the specific switch, to avoid the batteries running out.
After having made a series of 1500 therapeutic sessions, the device will stop, requiring a maintenance intervention to make the necessary calibration procedures; the screen which appears is reported in Fig. 96.
The same screen is shown if a malfunctioning of the device is noticed.
If this screen is shown because of the reached therapeutic sessions limit, by pressing the "Later" button it will be possible to make other 100 therapeutic sessions before the device definitively stops.
On the contrary, if such screen is shown because of a malfunctioning of the device, observed during the operation, the device will stop immediately. The device will have to be sent for the maintenance to a centre qualified to operate on the device and to release the calibration certification of the internal parameters.

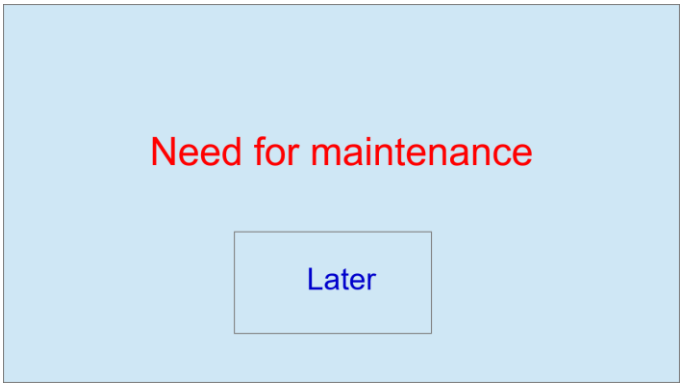

Figure 96. Required maintenance screen

List of tests for CE marking

In order to enter the European market, a medical device must have the CE marking, which means that the product meets high safety, health and environmental requirements, established in all the relevant European medical devices directives (i.e. in PeriCare® case, the ones identified in Paragraph 4.1.1).
To demonstrate the conformity of a medical device, it is necessary to identify the proper assessment route.
First of all, the class of the device has to be determined. As previously said, PeriCare® is a Class II device, with applied parts of type BF (the most similar device already existent is the surgical knife).
Several charcateristics of the device have to be assessed in order to verify the conformity to the appropriate directives; among these, the main are:

- Mechanical and structural safety;
- Protection resistance;
- Insulation resistance;
- Earth/enclosure/patient leakage currents;
- Auxiliary currents in the patient.

It is necessary that the manufacturer completes a self-certification for what regards the quality control of the design and of the fabrication process. Then, it is compulsory that a notified body controls and approves the quality system of the fabrication, the final product and the tests (regulation ISO 9001 – "Quality management systems - requirements" [202]). The final product is examined and verified about the conformity to the type description in the CE certification.

Electromagnetic Compatibility tests

Electromagnetic compatibility (EMC) tests are fundamental to verify that the product meets the applicable standards.
Radio frequency (RF) testing is conducted mainly indoor, in a properly calibrated and maintained test chamber (e.g. anechoic, reverberation or TEM cell); sometimes, numerical simulations are used to test virtual models.
During the testing, many documents are produced and they will be necessary to obtain the CE marking.
The tests to be carried out are different:

- Emission tests: both radiated and conducted emissions are considered.
  In particular, the measurement of radiated emissions are carried out by means of a specific spectrum analyser (i.e. EMI Test Receiver or EMI Analyzer), including bandwidths and detectors specified by international EMC standards. Antennas (e.g. dipole, biconical, log-periodic, double ridged guide and conical log-spiral)

are used as transducers; radiated emissions must be measured in all the directions around the emitting device (DUT, Device Under Test).
On the other hand, the conducted emissions (along cables and wiring) are measured by means of the LISN (Line Impedance Stabilisation Network) or the AMN (Artificial Mains Network) and the RF current clamp; in case of pulse emissions, an oscilloscope can be used, to obtain the waveform in the time domain;

- Susceptibility tests: both radiated field and conducted voltage/current susceptibility are investigated. The former one involves a high-powered source of pulse energy and a radiating antenna, while the latter implicates a high-powered signal/pulse generator and a current clamp (or another transformer). The DUT is tested against powerline disturbances (e.g. surges, lightning strikes and switching noise); in addition, with a spark generator ("ESD pistol", where ESD stands for "electrostatic discharge"), electrostatic discharge testing is performed.

Quality manual

The Quality Manual has to describe the objectives, the procedures and the methods used to guarantee the satisfaction of the fundamental requirements considered by the directive. It can be organised following the structure illustrated in ISO 9001 [202], which provides for different aspects:

- Management responsibilities;
- Organization of the Quality System;
- Verification of the agreements;
- Development of new products;
- Documents management;
- Provisions management;
- Products provided by the customer;
- Identification and traceability;
- Manufacturing process management;
- Tests and trials;
- Test, measure and trial instruments;
- Trials status;
- Not complying products management;
- Corrective actions;
- Movement, packaging and delivering;
- Documents recording quality information;
- Internal inspections;
- Personnel training;
- Technical assistance;
- Statistical techniques.

Technical file

To submit the device to the tests for the CE marking, the technical file has to be realized, following the indications in the directive 93/42/CEE. To comply with such regulation, the manufacturer has to provide the supervisory bodies with a complete technical documentation related to the company (e.g. personal data, company history, product kinds and possible clinical trials) and with the realized products. This document must include several information:

- A global index;
- A general description of the device, possible different versions included;
- The intended use and the risk classification;
- The applicable regulations;
- The risk analysis: it takes into account the safety requirements, the description of the hazard, the technical and the practical remedies; for all the dangerous parameters, it is necessary to provide the maximum acceptable defectiveness and a statistical criterium for the data assessment;
- The user instruction manual;
- The labelling;
- The technical description;
- The technical documentation: it includes the product specifications, drawings, block diagrams, hardware description, circuit diagrams, layout, software validation and flow chart (i.e. software architecture), components characteristics, sterilization procedures, computations, simulations and statystical analyses;
- The design verification;
- The experimental-clinical validation;
- The declaration of conformity;
- The quality system;
- Notes about modifications.

It is fundamental to identify the device class according to the Annex IX of the Directive 93/42/EEC, reporting all the applicable rules and the motivations for the made choice.
Also the realizing cycle of the device has to be described, together with the list of productions and trials, the quality plan and, if possible, the device master records. The critical points of the fabrication process have to be highlighted, explaining how the risks have been reduced. If the device has sterile parts, it is necessary to attach the file related to the sterilisation validation process (as an alternative, it can be included in the Quality Manual).
The manufacturer has to provide a copy of the conformity declaration (the original has to be conserved by the manufacturer and provided to the competent authorities), guaranteeing that the device has been designed and realized complying with the applicable regulations.
The documentation related to the realization procedures has to be kept in the Device Master Record. It is preferable to have an identification system of the lots or of the single devices.
In the technical file it is possible to attach also a report of the complaints register.
Finally, it is possible to include the information about the technical assistance procedures.

Certification process

The CE marking of a product is required in order to be authorized to sell it in EEA (European Economic Area, formed by the European Union - EU -, Iceland, Lichtenstein and Norway). This marking confirms that the product meets EU safety, health and environmental requirements.

European Commission establishes different steps to get the CE marking:

1. Identification of the European requirements for the product to be commercialized, as described in directives for medical devices;
2. Control of the product compliance with the specific requirements; if the manufactuer follow the harmonised EU standards (whose use is, however, voluntary) in the production process, the product is presumed to be in conformity with the requirements;
3. Control of the necessity of a test to be carried on by a notified body (i.e. a special conformity assessment body);
4. Product test to verify the compliance with technical requirements; moreover, the possible risks must be estimated and documented;
5. Technical dossier compilation, including the documents proving the conformity to technical requirements;
6. CE marking and declaration of conformity.

When all these stages are completed, it is possible to affix the CE marking on the product, so that it is visible, legible and indelible. In addition, the identification number of the notified body must be put on the product. Finally, the manufacturer has to sign an EU declaration of conformity related to the legal requirements.

In the specific case of PeriCare® device, the step 1 has been completed (i.e. the directives of interest have been identified, Paragraph 4.1). Technical requirements have been pinpointed according to the applicable regulations (step 2). A suitable notified body (step 3) will carry out the specific tests in order to verify the product compliance (step 4). As regards step 5, the technical file is being compiled with the information already had (e.g. the general description of the device, intended use and applicable regulations). At the end of the certification process, the CE marking will be obtained and the declaration of conformity will be signed by the manufacturer.
Hopefully, the process will be completed in the next few months, so as to be able to start soon the clinical trials with PeriCare® device and to place it into the market.

References

[1] L. Gaviria, J. P. Salcido, T. Guda, and J. L. Ong, "Current trends in dental implants," *J. Korean Assoc. Oral Maxillofac. Surg.*, vol. 40, no. 2, pp. 50–60, Apr. 2014.

[2] P. I. Brånemark *et al.*, "Osseointegrated implants in the treatment of the edentulous jaw. Experience from a 10-year period," *Scand. J. Plast. Reconstr. Surg. Suppl.*, vol. 16, pp. 1–132, 1977.

[3] C. E. Misch, *Dental Implant Prosthetics*. Elsevier Health Sciences, 2014.

[4] M. M. Bornstein, S. Halbritter, H. Harnisch, H.-P. Weber, and D. Buser, "A retrospective analysis of patients referred for implant placement to a specialty clinic: indications, surgical procedures, and early failures," *Int. J. Oral Maxillofac. Implants*, vol. 23, no. 6, pp. 1109–1116, Dec. 2008.

[5] C. E. Misch, *Contemporary Implant Dentistry*. Elsevier Health Sciences, 2007.

[6] "The National Institutes of Health (NIH) Consensus Development Program: Dental Implants." [Online]. Available: https://consensus.nih.gov/1988/1988DentalImplants069html.htm. [Accessed: 08-Jun-2016].

[7] L. Vidyasagar and P. Apse, "Dental implant design and biological effects on bone-implant interface," *Stomatologija*, vol. 6, no. 2, 2004.

[8] A. Gulsahi, "Bone Quality Assessment for Dental Implants," in *Implant Dentistry - The Most Promising Discipline of Dentistry*, I. Turkyilmaz, Ed. InTech, 2011.

[9] M. D. McNutt and C.-H. Chou, "Current trends in immediate osseous dental implant case selection criteria," *J. Dent. Educ.*, vol. 67, no. 8, pp. 850–859, Aug. 2003.

[10] D. C. Smith, "Dental implants: materials and design considerations," *Int. J. Prosthodont.*, vol. 6, no. 2, pp. 106–117, Apr. 1993.

[11] R. B. Osman and M. V. Swain, "A Critical Review of Dental Implant Materials with an Emphasis on Titanium versus Zirconia," *Materials*, vol. 8, no. 3, pp. 932–958, Mar. 2015.

[12] G. R. Parr, L. K. Gardner, and R. W. Toth, "Titanium: the mystery metal of implant dentistry. Dental materials aspects," *J. Prosthet. Dent.*, vol. 54, no. 3, pp. 410–414, Sep. 1985.

[13] M. Niinomi, "Mechanical properties of biomedical titanium alloys," *Mater. Sci. Eng. A*, vol. 243, no. 1–2, pp. 231–236, Mar. 1998.

[14] L. Le Guéhennec, A. Soueidan, P. Layrolle, and Y. Amouriq, "Surface treatments of titanium dental implants for rapid osseointegration," *Dent. Mater.*, vol. 23, no. 7, pp. 844–854, Jul. 2007.

[15] "Dental Implants Market by Product Type, Material, Stage, Connectors & End User - 2020 | MarketsandMarkets." [Online]. Available: http://www.marketsandmarkets.com/Market-Reports/dental-implants-prosthetics-market-695.html. [Accessed: 29-Feb-2016].

[16] P. Madianos *et al.*, "EFP Delphi study on the trends in Periodontology and Periodontics in Europe for the year 2025," *J. Clin. Periodontol.*, vol. 43, no. 6, pp. 472–481, 2016.

[17] M. Labanca, "Cost effectiveness in implant dentistry," *Implants*, vol. 4, 2012.

[18] American Academy of Implant Dentistry, “Dental Implants Facts and Figures.” .
[19] L. J. A. Heitz-Mayfield, “Peri-implant diseases: diagnosis and risk indicators,” *J. Clin. Periodontol.*, vol. 35, no. 8 Suppl, pp. 292–304, Sep. 2008.
[20] J. Lindhe, J. Meyle, and on behalf of Group D of the European Workshop on Periodontology, “Peri-implant diseases: Consensus Report of the Sixth European Workshop on Periodontology,” *J. Clin. Periodontol.*, vol. 35, pp. 282–285, Sep. 2008.
[21] A.-M. Roos-Jansåker, C. Lindahl, H. Renvert, and S. Renvert, “Nine- to fourteen-year follow-up of implant treatment. Part II: presence of peri-implant lesions,” *J. Clin. Periodontol.*, vol. 33, no. 4, pp. 290–295, Apr. 2006.
[22] R. a. G. Khammissa, L. Feller, R. Meyerov, and J. Lemmer, “Peri-implant mucositis and peri-implantitis: clinical and histopathological characteristics and treatment,” *SADJ J. South Afr. Dent. Assoc. Tydskr. Van Suid-Afr. Tandheelkd. Ver.*, vol. 67, no. 3, pp. 122, 124–126, Apr. 2012.
[23] T. Albrektsson and F. Isidor, “Consensus report: implant therapy,” in *Proceedings of the 1st European Workshop on Periodontology*, 1994, pp. 365–369.
[24] N. U. Zitzmann and T. Berglundh, “Definition and prevalence of peri-implant diseases,” *J. Clin. Periodontol.*, vol. 35, pp. 286–291, Sep. 2008.
[25] “Medical Dictionary,” *TheFreeDictionary.com*. [Online]. Available: http://medical-dictionary.thefreedictionary.com. [Accessed: 08-Jun-2016].
[26] M. A. Atieh, N. H. M. Alsabeeha, C. M. Faggion, and W. J. Duncan, “The frequency of peri-implant diseases: a systematic review and meta-analysis,” *J. Periodontol.*, vol. 84, no. 11, pp. 1586–1598, Nov. 2013.
[27] A. Mombelli and N. P. Lang, “The diagnosis and treatment of peri-implantitis,” *Periodontol. 2000*, vol. 17, no. 1, pp. 63–76, Jun. 1998.
[28] J. Prathapachandran and N. Suresh, “Management of peri-implantitis,” *Dent. Res. J.*, vol. 9, no. 5, pp. 516–521, 2012.
[29] N. P. Lang, A. C. Wetzel, H. Stich, and R. G. Caffesse, “Histologic probe penetration in healthy and inflamed peri-implant tissues,” *Clin. Oral Implants Res.*, vol. 5, no. 4, pp. 191–201, Dec. 1994.
[30] S. Schou, P. Holmstrup, K. Stoltze, E. Hjørting-Hansen, N.-E. Fiehn, and L. T. Skovgaard, “Probing around implants and teeth with healthy or inflamed peri-implant mucosa/gingiva. A histologic comparison in cynomolgus monkeys (Macaca fascicularis),” *Clin. Oral Implants Res.*, vol. 13, no. 2, pp. 113–126, Apr. 2002.
[31] S. Jepsen, A. Rühling, K. Jepsen, B. Ohlenbusch, and H. K. Albers, “Progressive peri-implantitis. Incidence and prediction of peri-implant attachment loss,” *Clin. Oral Implants Res.*, vol. 7, no. 2, pp. 133–142, Jun. 1996.
[32] C. Fransson, J. Wennström, and T. Berglundh, “Clinical characteristics at implants with a history of progressive bone loss,” *Clin. Oral Implants Res.*, vol. 19, no. 2, pp. 142–147, Feb. 2008.
[33] L. Kullman, A. Al-Asfour, L. Zetterqvist, and L. Andersson, “Comparison of radiographic bone height assessments in panoramic and intraoral radiographs of implant patients,” *Int. J. Oral Maxillofac. Implants*, vol. 22, no. 1, pp. 96–100, Feb. 2007.
[34] T. Albrektsson, G. Zarb, P. Worthington, and A. R. Eriksson, “The long-term efficacy of currently used dental implants: a review and proposed criteria of success,” *Int. J. Oral Maxillofac. Implants*, vol. 1, no. 1, pp. 11–25, 1986.

[35] Z. Cao, Y. Chen, Y. Chen, Q. Zhao, X. Xu, and Y. Chen, "Electromagnetic irradiation may be a new approach to therapy for peri-implantitis," *Med. Hypotheses*, vol. 78, no. 3, pp. 370–372, Mar. 2012.
[36] C. Fransson *et al.*, "Severity and pattern of peri-implantitis-associated bone loss," *J. Clin. Periodontol.*, vol. 37, no. 5, pp. 442–448, May 2010.
[37] M. Esposito, J. M. Hirsch, U. Lekholm, and P. Thomsen, "Biological factors contributing to failures of osseointegrated oral implants. (II). Etiopathogenesis," *Eur. J. Oral Sci.*, vol. 106, no. 3, pp. 721–764, Jun. 1998.
[38] M. Quirynen, M. De Soete, and D. van Steenberghe, "Infectious risks for oral implants: a review of the literature," *Clin. Oral Implants Res.*, vol. 13, no. 1, pp. 1–19, Feb. 2002.
[39] G. Alsaadi, M. Quirynen, A. Komárek, and D. van Steenberghe, "Impact of local and systemic factors on the incidence of oral implant failures, up to abutment connection," *J. Clin. Periodontol.*, vol. 34, no. 7, pp. 610–617, Jul. 2007.
[40] A. Leonhardt, S. Renvert, and G. Dahlén, "Microbial findings at failing implants," *Clin. Oral Implants Res.*, vol. 10, no. 5, pp. 339–345, Oct. 1999.
[41] S. S. Socransky and A. D. Haffajee, "Periodontal microbial ecology," *Periodontol. 2000*, vol. 38, pp. 135–187, 2005.
[42] M. M. Fürst, G. E. Salvi, N. P. Lang, and G. R. Persson, "Bacterial colonization immediately after installation on oral titanium implants," *Clin. Oral Implants Res.*, vol. 18, no. 4, pp. 501–508, Aug. 2007.
[43] G. E. Salvi, G. R. Persson, L. J. A. Heitz-Mayfield, M. Frei, and N. P. Lang, "Adjunctive local antibiotic therapy in the treatment of peri-implantitis II: clinical and radiographic outcomes," *Clin. Oral Implants Res.*, vol. 18, no. 3, pp. 281–285, Jun. 2007.
[44] S. Renvert, A.-M. Roos-Jansåker, and N. Claffey, "Non-surgical treatment of peri-implant mucositis and peri-implantitis: a literature review," *J. Clin. Periodontol.*, vol. 35, no. 8 Suppl, pp. 305–315, Sep. 2008.
[45] E. S. Karring, A. Stavropoulos, B. Ellegaard, and T. Karring, "Treatment of peri-implantitis by the Vector system," *Clin. Oral Implants Res.*, vol. 16, no. 3, pp. 288–293, Jun. 2005.
[46] S. Renvert, J. Lessem, G. Dahlén, C. Lindahl, and M. Svensson, "Topical minocycline microspheres versus topical chlorhexidine gel as an adjunct to mechanical debridement of incipient peri-implant infections: a randomized clinical trial," *J. Clin. Periodontol.*, vol. 33, no. 5, pp. 362–369, May 2006.
[47] S. Renvert, J. Lessem, C. Lindahl, and M. Svensson, "Treatment of incipient peri-implant infections using topical minocycline microspheres versus topical chlorhexidine gel as an adjunct to mechanical debridement," *J. Int. Acad. Periodontol.*, vol. 6, no. 4 Suppl, pp. 154–159, Oct. 2004.
[48] F. Schwarz, A. Sculean, D. Rothamel, K. Schwenzer, T. Georg, and J. Becker, "Clinical evaluation of an Er:YAG laser for nonsurgical treatment of peri-implantitis: a pilot study," *Clin. Oral Implants Res.*, vol. 16, no. 1, pp. 44–52, Feb. 2005.
[49] F. Schwarz, K. Bieling, E. Nuesry, A. Sculean, and J. Becker, "Clinical and histological healing pattern of peri-implantitis lesions following non-surgical treatment with an Er:YAG laser," *Lasers Surg. Med.*, vol. 38, no. 7, pp. 663–671, Aug. 2006.

[50] F. Schwarz, K. Bieling, M. Bonsmann, T. Latz, and J. Becker, “Nonsurgical treatment of moderate and advanced periimplantitis lesions: a controlled clinical study,” *Clin. Oral Investig.*, vol. 10, no. 4, pp. 279–288, Dec. 2006.
[51] N. Claffey, E. Clarke, I. Polyzois, and S. Renvert, “Surgical treatment of peri-implantitis,” *J. Clin. Periodontol.*, vol. 35, no. 8 Suppl, pp. 316–332, Sep. 2008.
[52] A. Leonhardt, G. Dahlén, and S. Renvert, “Five-year clinical, microbiological, and radiological outcome following treatment of peri-implantitis in man,” *J. Periodontol.*, vol. 74, no. 10, pp. 1415–1422, Oct. 2003.
[53] “Weiner’s Pain Management: A Practical Guide for Clinicians,” *CRC Press*, 31-Aug-2005. [Online]. Available: https://www.crcpress.com/Weiners-Pain-Management-A-Practical-Guide-for-Clinicians/Boswell-Cole/p/book/9780849322624. [Accessed: 15-Jun-2016].
[54] R. Becker and G. Selden, *The Body Electric: Electromagnetism And The Foundation Of Life*. HarperCollins, 1998.
[55] R. H. Odell and R. E. Sorgnard, “Anti-inflammatory effects of electronic signal treatment,” *Pain Physician*, vol. 11, no. 6, pp. 891–907, Dec. 2008.
[56] “Program | BioEM 2016 Conference.” [Online]. Available: http://www.bioem2016.org/program#plenary. [Accessed: 10-Jun-2016].
[57] L. Gatta *et al.*, “Effects of In Vivo Exposure to GSM-Modulated 900 MHz Radiation on Mouse Peripheral Lymphocytes,” *Radiat. Res.*, vol. 160, no. 5, pp. 600–605, 2003.
[58] “What is an inflammation?,” *PubMed Health*, Jan. 2015.
[59] A. B. Gapeyev, T. P. Kulagina, A. V. Aripovsky, and N. K. Chemeris, “The role of fatty acids in anti-inflammatory effects of low-intensity extremely high-frequency electromagnetic radiation,” *Bioelectromagnetics*, vol. 32, no. 5, pp. 388–395, Jul. 2011.
[60] A. B. Gapeev, K. V. Lushnikov, I. V. Shumilina, and N. K. Chemeris, “Pharmacological analysis of anti-inflammatory effects of low-intensity extremely high-frequency electromagnetic radiation,” *Biofizika*, vol. 51, no. 6, pp. 1055–1068, Dec. 2006.
[61] A. B. Gapeyev, E. N. Mikhailik, and N. K. Chemeris, “Features of anti-inflammatory effects of modulated extremely high-frequency electromagnetic radiation,” *Bioelectromagnetics*, vol. 30, no. 6, pp. 454–461, Sep. 2009.
[62] M. A. Rojavin and M. C. Ziskin, “Medical application of millimetre waves,” *QJM Mon. J. Assoc. Physicians*, vol. 91, no. 1, pp. 57–66, Jan. 1998.
[63] A. G. Pakhomov and P. R. Murthy, “Low-intensity millimeter waves as a novel therapeutic modality,” *IEEE Trans. Plasma Sci.*, vol. 28, no. 1, pp. 34–40, Feb. 2000.
[64] O. V. Betskii, N. D. Devyatkov, and V. V. Kislov, “Low intensity millimeter waves in medicine and biology,” *Crit. Rev. Biomed. Eng.*, vol. 28, no. 1–2, pp. 247–268, 2000.
[65] V. I. Popov, V. V. Rogachevskii, A. B. Gapeyev, R. N. Khramov, N. K. Chemeris, and E. E. Fesenko, “Degranulation of dermal mast cells caused by the low-intensity electromagnetic radiaiton of extremely high frequency,” *Biophysics*, vol. 46, no. 6, pp. 1041–1046, 2001.
[66] A. B. Gapeyev, E. N. Mikhailik, and N. K. Chemeris, “Anti-inflammatory effects of low-intensity extremely high-frequency electromagnetic radiation: frequency and power dependence,” *Bioelectromagnetics*, vol. 29, no. 3, pp. 197–206, Apr. 2008.

[67] K. V. Lushnikov, J. V. Shumilina, E. Y. Yakushev, A. B. Gapeyev, V. B. Sadovnikov, and N. K. Chemeris, "Comparative Study of Anti-Inflammatory Effects of Low-Intensity Extremely High-Frequency Electromagnetic Radiation and Diclofenac on Footpad Edema in Mice," *Electromagn. Biol. Med.*, vol. 24, no. 2, pp. 143–157, Jan. 2005.
[68] D. Soghomonyan, K. Trchounian, and A. Trchounian, "Millimeter waves or extremely high frequency electromagnetic fields in the environment: what are their effects on bacteria?," *Appl. Microbiol. Biotechnol.*, vol. 100, no. 11, pp. 4761–4771, 2016.
[69] H. Tadevosyan, V. Kalantaryan, and A. Trchounian, "Extremely high frequency electromagnetic radiation enforces bacterial effects of inhibitors and antibiotics," *Cell Biochem. Biophys.*, vol. 51, no. 2–3, pp. 97–103, 2008.
[70] H. Torgomyan, V. Kalantaryan, and A. Trchounian, "Low intensity electromagnetic irradiation with 70.6 and 73 GHz frequencies affects Escherichia coli growth and changes water properties," *Cell Biochem. Biophys.*, vol. 60, no. 3, pp. 275–281, Jul. 2011.
[71] A. Arakaki, M. Takahashi, M. Hosokawa, T. Matsunaga, and T. Tanaka, "Bacterial inactivation by applying an alternating electromagnetic field using PAMAM dendron-modified magnetic nanoparticles," *Electrochemistry*, vol. 84, no. 5, pp. 324–327, 2016.
[72] R. Armanino, "Method employing electric fields to selectively kill microbes in a root canal preparation," US20110039226 A1, 17-Feb-2011.
[73] "The classic: Fundamental aspects of fracture treatment by Iwao Yasuda, reprinted from J. Kyoto Med. Soc., 4:395-406, 1953," *Clin. Orthop.*, no. 124, pp. 5–8, May 1977.
[74] C. A. L. Bassett, R. J. Pawluk, and R. O. Becker, "Effects of Electric Currents on Bone In Vivo," *Nature*, vol. 204, no. 4959, pp. 652–654, Nov. 1964.
[75] D. R. Grana, H. J. A. Marcos, and G. A. Kokubu, "Pulsed electromagnetic fields as adjuvant therapy in bone healing and peri-implant bone formation: an experimental study in rats," *Acta Odontológica Latinoam. AOL*, vol. 21, no. 1, pp. 77–83, 2008.
[76] C. A. Bassett, "Fundamental and practical aspects of therapeutic uses of pulsed electromagnetic fields (PEMFs)," *Crit. Rev. Biomed. Eng.*, vol. 17, no. 5, pp. 451–529, 1989.
[77] K. Chang, W. Hong-Shong Chang, Y.-H. Yu, and C. Shih, "Pulsed electromagnetic field stimulation of bone marrow cells derived from ovariectomized rats affects osteoclast formation and local factor production," *Bioelectromagnetics*, vol. 25, no. 2, pp. 134–141, Feb. 2004.
[78] X. L. Griffin, F. Warner, and M. Costa, "The role of electromagnetic stimulation in the management of established non-union of long bone fractures: what is the evidence?," *Injury*, vol. 39, no. 4, pp. 419–429, Apr. 2008.
[79] Cosoli, G., Scalise, L., Tricarico, G., Tomasini, E. P., and Cerri, G., "An innovative therapy for peri-implantitis based on radio frequency electric current: numerical simulation results and clinical evidence," presented at the 38th Annual International Conference on the IEEE Engineering in Medicine and Biology Society.
[80] "Endox Endodontic System." [Online]. Available: http://www.endox.com/indexeng.htm. [Accessed: 16-Jun-2016].
[81] "Learn About Clinical Studies - ClinicalTrials.gov." [Online]. Available: https://clinicaltrials.gov/ct2/about-studies/learn. [Accessed: 16-Jun-2016].

[82] Tricarico, G. and Rustichelli, F., “Retrospective clinical evaluation of periimplantitis through the use of high frequency alternating current,” *Clin. Oral Implant Res.*, vol. 23, no. 81, 2012.
[83] Tricarico, G. and Cosoli, G., “Retrospective Clinical Evaluation of Peri-Implantitis Theraphy through the Use of Radio Frequency Alternating Current,” presented at the Unified Scientific Approaches towards Regenerative Orthopaedics and Dentistry, 2015.
[84] “WMA Declaration of Helsinki - Ethical Principles for Medical Research Involving Human Subjects,” 19-Oct-2013. [Online]. Available: http://www.wma.net/en/30publications/10policies/b3/. [Accessed: 16-Jun-2016].
[85] N. Garg and A. Garg, *Textbook of Endodontics*. JP Medical Ltd, 2013.
[86] Vögele, H. and Hickel, R., “Treatment of Acute Pulpitis with HFAC - A Clinical Study,” presented at the 31° Congresso Nazionale Società Italiana di Microbiologia, 2003.
[87] “IEC 60601,” *Wikipedia, the free encyclopedia*. 28-Dec-2015.
[88] “CE marking,” *Wikipedia, the free encyclopedia*. 19-May-2016.
[89] “Direttiva CEE 93/42 sui dispositivi medici,” *Wikipedia*. 18-Apr-2016.
[90] I. Tsesis, *Complications in Endodontic Surgery: Prevention, Identification and Management*. Springer, 2014.
[91] Haffner, C. *et al.*, “Endox Endodontic System A preliminary report about first experiences,” *ZWR Dtsch. Zahnarzteblatt*, vol. 12, pp. 764–767, 1997.
[92] M. Lendini, E. Alemanno, G. Migliaretti, and E. Berutti, “The effect of high-frequency electrical pulses on organic tissue in root canals,” *Int. Endod. J.*, vol. 38, no. 8, pp. 531–538, Aug. 2005.
[93] A. R. Aranda-Garcia *et al.*, “Antibacterial effectiveness of several irrigating solutions and the Endox Plus system - an ex vivo study,” *Int. Endod. J.*, vol. 45, no. 12, pp. 1091–1096, 2012.
[94] C. Haffner, M. Folwaczny, K. Galler, and R. Hickel, “Accuracy of electronic apex locators in comparison to actual length—an in vivo study,” *J. Dent.*, vol. 33, no. 8, pp. 619–625, Sep. 2005.
[95] U.A.Bakshi and A.V.Bakshi, *Circuit Theory*. Technical Publications, 2009.
[96] J. Reddy, *An Introduction to the Finite Element Method*. McGraw-Hill Education, 2005.
[97] S. R. H. Hoole, *Computer-aided analysis and design of electromagnetic devices*. Elsevier, 1989.
[98] A. M. Weinstein, J. J. Klawitter, S. C. Anand, and R. Schuessler, “Stress analysis of porous rooted dental implants,” *J. Dent. Res.*, vol. 55, no. 5, pp. 772–777, Oct. 1976.
[99] J. P. Geng, K. B. Tan, and G. R. Liu, “Application of finite element analysis in implant dentistry: a review of the literature,” *J. Prosthet. Dent.*, vol. 85, no. 6, pp. 585–598, Jun. 2001.
[100] A. Diarra, V. Mushegyan, and A. Naveau, “Finite element analysis generates an increasing interest in dental research: A bibliometric study,” *Open Dent. J.*, vol. 10, pp. 35–42, 2016.
[101] A. A. Ştefiu *et al.*, “Modelling and finite element method in dentistry,” *Romanian Biotechnol. Lett.*, vol. 20, no. 4, pp. 10579–10584, 2015.

[102] D. Krizaj, J. Jan, and V. Valencic, “Modeling AC current conduction through a human tooth,” *Bioelectromagnetics*, vol. 25, no. 3, pp. 185–195, Apr. 2004.
[103] J. Jan and D. Križaj, “Accuracy of root canal length determination with the impedance ratio method,” *Int. Endod. J.*, vol. 42, no. 9, pp. 819–826, 2009.
[104] D. Križaj, J. Jan, and T. Žagar, “Determination of the root canal length using impedance ratio method,” presented at the IFMBE Proceedings, 2007, vol. 17 IFMBE, pp. 703–706.
[105] D. Križaj, J. Jan, and V. Valenčič, “Numerical computation of impedances of a human tooth for estimation of the root canal length,” *IEEE Trans. Biomed. Eng.*, vol. 49, no. 7, pp. 746–748, 2002.
[106] “COMSOL Multiphysics,” *Wikipedia, the free encyclopedia*. 30-Nov-2015.
[107] S. J. N. D. MS, *Wheeler’s Dental Anatomy, Physiology and Occlusion, 9e*, 9 edizione. St. Louis, Mo: Saunders, 2009.
[108] A. Boryor, A. Hohmann, M. Geiger, U. Wolfram, C. Sander, and F. G. Sander, “A downloadable meshed human canine tooth model with PDL and bone for finite element simulations,” *Dent. Mater. Off. Publ. Acad. Dent. Mater.*, vol. 25, no. 9, pp. e57-62, Sep. 2009.
[109] B. W. Zweifach, L. Grant, and R. T. McCluskey, *The Inflammatory Process*. Academic Press, 2014.
[110] C. Gabriel, S. Gabriel, and E. Corthout, “The dielectric properties of biological tissues: I. Literature survey,” *Phys. Med. Biol.*, vol. 41, no. 11, pp. 2231–2249, 1996.
[111] S. Gabriel, R. W. Lau, and C. Gabriel, “The dielectric properties of biological tissues: II. Measurements in the frequency range 10 Hz to 20 GHz,” *Phys. Med. Biol.*, vol. 41, no. 11, pp. 2251–2269, 1996.
[112] S. Gabriel, R. W. Lau, and C. Gabriel, “The dielectric properties of biological tissues: III. Parametric models for the dielectric spectrum of tissues,” *Phys. Med. Biol.*, vol. 41, no. 11, pp. 2271–2293, 1996.
[113] Y. V. Tornuev *et al.*, “Bioimpedancemetry in the diagnostics of inflammatory process in the mammary gland,” *Bull. Exp. Biol. Med.*, vol. 156, no. 3, pp. 381–383, Jan. 2014.
[114] A. V. Rodin, V. G. Pleshkov, S. D. Leonov, and S. M. Bazhenov, “Experimental study of the diagnostic potentialities of bioimpedance measurement in acute intestinal obstruction,” *Bull. Exp. Biol. Med.*, vol. 155, no. 6, pp. 810–813, Oct. 2013.
[115] P. Diniz, K. Shomura, K. Soejima, and G. Ito, “Effects of Pulsed Electromagnetic Field (PEMF) Stimulation on Bone Tissue Like Formation Are Dependent on the Maturation Stages of the Osteoblasts,” *Bioelectromagnetics*, vol. 23, no. 5, pp. 398–405, 2002.
[116] B. Chalidis, N. Sachinis, A. Assiotis, and G. Maccauro, “Stimulation of bone formation and fracture healing with pulsed electromagnetic fields: biologic responses and clinical implications,” *Int. J. Immunopathol. Pharmacol.*, vol. 24, no. 1 Suppl 2, pp. 17–20, Mar. 2011.
[117] H. Guo, Q. Qiao, and Z. Wang, “Electrical field analysis of extracellular electrical stimulation of optic nerve with spiral cuff electrode,” in *2011 4th International Conference on Biomedical Engineering and Informatics (BMEI)*, 2011, vol. 2, pp. 946–949.
[118] *COMSOL Multiphysics®*. .

[119] D. V. Belik and K. D. Belik, “Improvement of the information value of multifrequency impedancometry for detection of small tumor arrays,” *Biomed. Eng.*, vol. 41, no. 4, pp. 157–161, Jul. 2007.
[120] “Home - ICEBI and EIT Conferences 2016.” [Online]. Available: http://www.icebi2016.org/. [Accessed: 12-Jul-2016].
[121] “Bioimpedance and Bioelectricity Basics, 2nd Edition | Orjan Martinsen, Sverre Grimnes | ISBN 9780080568805.” [Online]. Available: http://store.elsevier.com/Bioimpedance-and-Bioelectricity-Basics/Orjan-Martinsen/isbn-9780080568805/. [Accessed: 12-Jul-2016].
[122] X. Zheng *et al.*, “Electrode Impedance: An Indicator of Electrode-Tissue Contact and Lesion Dimensions During Linear Ablation,” *J. Interv. Card. Electrophysiol.*, vol. 4, no. 4, pp. 645–654.
[123] “Electrode-Tissue Impedance Measurement CMOS ASIC for Functional Electrical Stimulation Neuroprostheses - Semantic Scholar.” [Online]. Available: https://www.semanticscholar.org/paper/Electrode-Tissue-Impedance-Measurement-CMOS-ASIC-Uranga-Sacrist%C3%A1n/308a24786a3920e64fcef1f7eb15aba1ccc8147d. [Accessed: 29-Jul-2016].
[124] G. Cybulski, *Ambulatory Impedance Cardiography: The Systems and their Applications*. Springer Science & Business Media, 2011.
[125] I. Frerichs, “Electrical impedance tomography (EIT) in applications related to lung and ventilation: a review of experimental and clinical activities,” *Physiol. Meas.*, vol. 21, no. 2, p. R1, 2000.
[126] B. Sanchez *et al.*, “In vivo electrical bioimpedance characterization of human lung tissue during the bronchoscopy procedure. A feasibility study,” *Med. Eng. Phys.*, vol. 35, no. 7, pp. 949–957, Jul. 2013.
[127] P. Aberg, I. Nicander, J. Hansson, P. Geladi, U. Holmgren, and S. Ollmar, “Skin cancer identification using multifrequency electrical impedance--a potential screening tool,” *IEEE Trans. Biomed. Eng.*, vol. 51, no. 12, pp. 2097–2102, Dec. 2004.
[128] S. C. Kim, H. S. Park, S. M. Kim, and J. K. Park, “Impedance changes according to the degree of atopi dermatitis in mice,” *Conf. Proc. Annu. Int. Conf. IEEE Eng. Med. Biol. Soc. IEEE Eng. Med. Biol. Soc. Annu. Conf.*, vol. 2011, pp. 2526–2529, 2011.
[129] I. Nicander and S. Ollmar, “Electrical bioimpedance related to structural differences and reactions in skin and oral mucosa,” *Ann. N. Y. Acad. Sci.*, vol. 873, pp. 221–226, Apr. 1999.
[130] S. F. Khalil, M. S. Mohktar, and F. Ibrahim, “The Theory and Fundamentals of Bioimpedance Analysis in Clinical Status Monitoring and Diagnosis of Diseases,” *Sensors*, vol. 14, no. 6, pp. 10895–10928, Jun. 2014.
[131] C. T.-S. Ching *et al.*, “A preliminary study of the use of bioimpedance in the screening of squamous tongue cancer,” *Int. J. Nanomedicine*, vol. 5, pp. 213–220, 2010.
[132] T.-P. Sun *et al.*, “The use of bioimpedance in the detection/screening of tongue cancer,” *Cancer Epidemiol.*, vol. 34, no. 2, pp. 207–211, Apr. 2010.

[133] C. Tsigos, C. Stefanaki, G. I. Lambrou, D. Boschiero, and G. P. Chrousos, “Stress and inflammatory biomarkers and symptoms are associated with bioimpedance measures,” *Eur. J. Clin. Invest.*, vol. 45, no. 2, pp. 126–134, Feb. 2015.
[134] U. G. Kyle *et al.*, “Bioelectrical impedance analysis--part I: review of principles and methods,” *Clin. Nutr. Edinb. Scotl.*, vol. 23, no. 5, pp. 1226–1243, Oct. 2004.
[135] F. Yu *et al.*, “Electrochemical impedance spectroscopy to assess vascular oxidative stress,” *Ann. Biomed. Eng.*, vol. 39, no. 1, pp. 287–296, Jan. 2011.
[136] F. Yu, X. Dai, T. Beebe, and T. Hsiai, “Electrochemical Impedance Spectroscopy to Characterize Inflammatory Atherosclerotic Plaques,” *Biosens. Bioelectron.*, vol. 30, no. 1, pp. 165–173, Dec. 2011.
[137] J. R. Villa Asensi, “The monitoring of bronchial inflammation by bioimpedance,” *Allergol. Immunopathol. (Madr.)*, vol. 37, no. 1, pp. 1–2, Feb. 2009.
[138] R. H. Smallwood, A. Keshtkar, B. A. Wilkinson, J. A. Lee, and F. C. Hamdy, “Electrical impedance spectroscopy (EIS) in the urinary bladder: the effect of inflammation and edema on identification of malignancy,” *IEEE Trans. Med. Imaging*, vol. 21, no. 6, pp. 708–710, Jun. 2002.
[139] D. G. Peroni, A. Bodini, A. Loiacono, G. Paida, L. Tenero, and G. L. Piacentini, “Bioimpedance monitoring of airway inflammation in asthmatic allergic children,” *Allergol. Immunopathol. (Madr.)*, vol. 37, no. 1, pp. 3–6, Feb. 2009.
[140] R. L. Alvarenga and M. N. Souza, “Assessment of knee osteoarthritis by bioelectrical impedance,” in *Proceedings of the 25th Annual International Conference of the IEEE Engineering in Medicine and Biology Society, 2003*, 2003, vol. 4, p. 3118–3121 Vol.4.
[141] A. Keshtkar, “Review Article: Application of Electrical Impedance Spectroscopy in Bladder Cancer Screening,” *Iran. J. Med. Phys.*, vol. 10, no. 1, pp. 1–21, Jan. 2013.
[142] J. Wang, “Electrochemical biosensors: Towards point-of-care cancer diagnostics,” *Biosens. Bioelectron.*, vol. 21, no. 10, pp. 1887–1892, Apr. 2006.
[143] M. Y. Jaffrin and H. Morel, “Body fluid volumes measurements by impedance: A review of bioimpedance spectroscopy (BIS) and bioimpedance analysis (BIA) methods,” *Med. Eng. Phys.*, vol. 30, no. 10, pp. 1257–1269, Dec. 2008.
[144] S. Reitinger, J. Wissenwasser, W. Kapferer, R. Heer, and G. Lepperdinger, “Electric impedance sensing in cell-substrates for rapid and selective multipotential differentiation capacity monitoring of human mesenchymal stem cells,” *Biosens. Bioelectron.*, vol. 34, no. 1, pp. 63–69, Apr. 2012.
[145] E. Sarró *et al.*, “Electrical impedance spectroscopy measurements using a four-electrode configuration improve on-line monitoring of cell concentration in adherent animal cell cultures,” *Biosens. Bioelectron.*, vol. 31, no. 1, pp. 257–263, Jan. 2012.
[146] M. H. Nekoofar, M. M. Ghandi, S. J. Hayes, and P. M. H. Dummer, “The fundamental operating principles of electronic root canal length measurement devices,” *Int. Endod. J.*, vol. 39, no. 8, pp. 595–609, Aug. 2006.
[147] T. Marjanović, I. Lacković, and Z. Stare, “Comparison of electrical equivalent circuits of human tooth used for measuring the root canal length,” *Autom. – J. Control Meas. Electron. Comput. Commun.*, vol. 52, no. 1, May 2011.
[148] J. Sword, D. H. Pashley, S. Foulger, F. R. Tay, and R. Rodgers, “Use of electrochemical impedance spectroscopy to evaluate resin-dentin bonds,” *J. Biomed. Mater. Res. B Appl. Biomater.*, vol. 84, no. 2, pp. 468–477, Feb. 2008.

[149] M. Andrei, C. Pirvu, and I. Demetrescu, “Electrochemical impedance spectroscopy in understanding the influence of ultrasonic dental scaling on the dental structure-dental filling interface,” *Eur. J. Oral Sci.*, vol. 122, no. 6, pp. 411–416, Dec. 2014.
[150] A. P. Morais, A. V. Pino, and M. N. Souza, “A fractional electrical impedance model in detection of occlusal non-cavitated carious,” in *2010 Annual International Conference of the IEEE Engineering in Medicine and Biology*, 2010, pp. 6551–6554.
[151] D. Mortensen, K. Dannemand, S. Twetman, and M. K. Keller, “Detection of non-cavitated occlusal caries with impedance spectroscopy and laser fluorescence: an in vitro study,” *Open Dent. J.*, vol. 8, pp. 28–32, 2014.
[152] Buendia, R., Granhed, H., and Sjoqvist, B.-A., “Towards thoracic trauma detection using bioimpedance,” presented at the International Conference on Electrical Bio-Impedance (ICEBI), Stockholm, 2016.
[153] G. Cosoli, L. Scalise, G. Tricarico, P. Russo, and G. Cerri, “Bioimpedance measurements in dentistry to detect inflammation: numerical modelling and experimental results,” *Physiol. Meas.*, 2017.
[154] D. Miklavčič, N. Pavšelj, and F. X. Hart, “Electric Properties of Tissues,” in *Wiley Encyclopedia of Biomedical Engineering*, John Wiley & Sons, Inc., 2006.
[155] R. L. W. Messer, G. Tackas, J. Mickalonis, Y. Brown, J. B. Lewis, and J. C. Wataha, “Corrosion of machined titanium dental implants under inflammatory conditions,” *J. Biomed. Mater. Res. B Appl. Biomater.*, vol. 88B, no. 2, pp. 474–481, Feb. 2009.
[156] G. Cosoli, L. Scalise, G. Cerri, P. Russo, G. Tricarico, and E.P. Tomasini, “Bioimpedancemetry for the Assessment of Periodontal Tissue Inflammation: a Numerical Feasibility Study,” *Computer Methods in Biomechanics and Biomedical Engineering*, (in press), 2017.
[157] “Monitoring of Fixture Osteointegration after BAHA(R) Implantation.” [Online]. Available: https://www.tripdatabase.com/doc/1063218-Monitoring-of-Fixture-Osteointegration-after-BAHA-R--Implantation-#content. [Accessed: 14-Jul-2016].
[158] P. Arpaia, F. Clemente, and A. Zanesco, “Low-Invasive Diagnosis of Metallic Prosthesis Osseointegration by Electrical Impedance Spectroscopy,” *IEEE Trans. Instrum. Meas.*, vol. 56, no. 3, pp. 784–789, Jun. 2007.
[159] P. Arpaia, F. Clemente, and C. Romanucci, “An instrument for prosthesis osseointegration assessment by electrochemical impedance spectrum measurement,” *Measurement*, vol. 41, no. 9, pp. 1040–1044, Nov. 2008.
[160] S. Ghosal, B. Goswami, R. Ghosh, and P. Banerjee, “Determination of Stability of Dental Implant from Impedance Studies Using Resonance Frequency Analysis,” in *2011 Second International Conference on Emerging Applications of Information Technology (EAIT)*, 2011, pp. 71–74.
[161] Cosoli, G., Salise, L., Russo, P., Tricarico, G., and Cerri, G., “Numerical Modelling of Bioimpedance Measure in Dentistry,” presented at the 16th International Conference on Electrical Bio-Impedance (ICEBI), Stockholm, 2016.
[162] G. Cosoli, L. Scalise, E. P. Tomasini, P. Russo, G. Cerri, and G. Tricarico, “Measure of Bioimpedance to Detect Tissue Inflammation,” presented at the 16th International Conference on Electrical Bio-impedence & 17th International Conference on electrical impedence Tomography, Stockholm, 2016, p. 18.

[163] “AC Current Probes Datasheet | Tektronix.” [Online]. Available: http://www.tek.com/datasheet/current-probe/ct1-%E2%80%A2-ct2-%E2%80%A2-ct6-0. [Accessed: 27-Sep-2016].
[164] “33120A Function / Arbitrary Waveform Generator, 15 MHz [Obsolete] | Keysight (formerly Agilent’s Electronic Measurement).” [Online]. Available: http://www.keysight.com/en/pd-1000001289%3Aepsg%3Apro/function-arbitrary-waveform-generator-15-mhz?cc=IT&lc=ita. [Accessed: 27-Sep-2016].
[165] “Water conductivity - Lenntech.” [Online]. Available: http://www.lenntech.com/applications/ultrapure/conductivity/water-conductivity.htm. [Accessed: 02-Aug-2016].
[166] “LCR Meters & Impedance Measurement Products | Keysight (Agilent).” [Online]. Available: http://www.keysight.com/en/pc-1000000391%3Aepsg%3Apgr/lcr-meters-impedance-measurement-products?nid=-536902441.0.00&cc=IT&lc=ita&cmpid=93159. [Accessed: 01-Dec-2015].
[167] A. P. Morais, A. V. Pino, and M. N. Souza, “Assessment of tooth structure using an alternative electrical bioimpedance spectroscopy method,” *Braz. Dent. J.*, vol. 25, no. 2, pp. 146–152, 2014.
[168] C. Yong Ryu, S. Hoon Nam, and S. Kim, “Conductive rubber electrode for wearable health monitoring,” *Conf. Proc. Annu. Int. Conf. IEEE Eng. Med. Biol. Soc. IEEE Eng. Med. Biol. Soc. Annu. Conf.*, vol. 4, pp. 3479–3481, 2005.
[169] V. D. Santis, P. A. Beeckman, D. A. Lampasi, and M. Feliziani, “Assessment of Human Body Impedance for Safety Requirements Against Contact Currents for Frequencies up to 110 MHz,” *IEEE Trans. Biomed. Eng.*, vol. 58, no. 2, pp. 390–396, Feb. 2011.
[170] C. Maggiore, L. Gallottini, and J. P. Resi, “Mandibular first and second molar. The variability of roots and root canal system,” *Minerva Stomatol.*, vol. 47, no. 9, pp. 409–416, Sep. 1998.
[171] “The Number of Roots and Canals in the Maxillary Second Premolars in a Group of Jordanian Population.” [Online]. Available: http://www.hindawi.com/journals/ijd/2014/797692/. [Accessed: 29-Jul-2016].
[172] P. Bertemes Filho, “Tissue characterisation using an impedance spectroscopy probe,” University of Sheffield, 2002.
[173] M. C. Huysmans, C. Longbottom, N. B. Pitts, P. Los, and P. G. Bruce, “Impedance spectroscopy of teeth with and without approximal caries lesions--an in vitro study,” *J. Dent. Res.*, vol. 75, no. 11, pp. 1871–1878, Nov. 1996.
[174] M. E. Orazem and B. Tribollet, *Electrochemical Impedance Spectroscopy*. John Wiley & Sons, 2011.
[175] K. Yoon *et al.*, “Electrical impedance spectroscopy and diagnosis of tendinitis,” *Physiol. Meas.*, vol. 31, no. 2, p. 171, 2010.
[176] N. E. Beltran, G. Sanchez-Miranda, M. Godinez, U. Diaz, and E. Sacristan, “Gastric impedance spectroscopy in elective cardiovascular surgery patients,” *Physiol. Meas.*, vol. 27, no. 3, p. 265, 2006.
[177] D. A. Dean, T. Ramanathan, D. Machado, and R. Sundararajan, “Electrical impedance spectroscopy study of biological tissues,” *J. Electrost.*, vol. 66, no. 3–4, pp. 165–177, Mar. 2008.

[178] Kitchen, Ronald, “RF and Microwave Radiation Safety, 2nd Edition.” [Online]. Available: http://store.elsevier.com/RF-and-Microwave-Radiation-Safety/Ronald-Kitchen/isbn-9780750643559/. [Accessed: 01-Aug-2016].
[179] Hitchcock, R. T. and Patterson, R. M., “Wiley: Radio-Frequency and ELF Electromagnetic Energies: A Handbook for Health Professionals -.” [Online]. Available: http://eu.wiley.com/WileyCDA/WileyTitle/productCd-0471284548.html. [Accessed: 01-Aug-2016].
[180] *Non-ionizing Radiation: Static and extremely low-frequency (ELF) electric and magnetic fields*. World Health Organization, 2002.
[181] P. J. Rosch, *Bioelectromagnetic and Subtle Energy Medicine, Second Edition*. CRC Press, 2014.
[182] “ICNIRP.” [Online]. Available: http://www.icnirp.org/. [Accessed: 01-Aug-2016].
[183] “IEEE.” [Online]. Available: https://www.ieee.org/index.html. [Accessed: 01-Aug-2016].
[184] “Welcome to the IEC - International Electrotechnical Commission.” [Online]. Available: http://www.iec.ch/. [Accessed: 01-Aug-2016].
[185] “CE marking - Growth - European Commission,” *Growth*. [Online]. Available: https://ec.europa.eu/growth/single-market/ce-marking_en. [Accessed: 01-Aug-2016].
[186] “Applied Biophysics.” [Online]. Available: http://www.biophysics.com/ecis-theory.php. [Accessed: 01-Aug-2016].
[187] *Norma CEI 64-18 “Effetti della corrente elettrica attraverso il corpo umano.”* .
[188] “EUR-Lex - 01993L0042-20071011 - EN - EUR-Lex.” [Online]. Available: http://eur-lex.europa.eu/legal-content/EN/TXT/?uri=CELEX:01993L0042-20071011. [Accessed: 01-Aug-2016].
[189] “WHO | World Health Organization,” *WHO*. [Online]. Available: http://www.who.int/en/. [Accessed: 03-Aug-2016].
[190] “DMEM - Dulbecco’s Modified Eagle Medium.” [Online]. Available: https://www.thermofisher.com/it/en/home/life-science/cell-culture/mammalian-cell-culture/classical-media/dmem.html?gclid=CKiwktDaos4CFWwq0wodbewGJg&s_kwcid=AL!3652!3!104671989868!p!!g!!dmem&mkwid=sqnyxX8ye-dc_pcrid_104671989868_pkw_dmem_pmt_p_slid__&ef_id=V5r6pQAABOq3cwYI:20160802121453:s. [Accessed: 02-Aug-2016].
[191] E. Bonfoco, D. Krainc, M. Ankarcrona, P. Nicotera, and S. A. Lipton, “Apoptosis and necrosis: two distinct events induced, respectively, by mild and intense insults with N-methyl-D-aspartate or nitric oxide/superoxide in cortical cell cultures,” *Proc. Natl. Acad. Sci.*, vol. 92, no. 16, pp. 7162–7166, Aug. 1995.
[192] *Fondamenti di Ingegneria Clinica - Volume 1 | Francesco P. Branca | Springer*. .
[193] F. A. Duck, *Physical properties of tissue: a comprehensive reference book*. London; San Diego: Academic Press, 1990.
[194] R. L. Mcintosh and V. Anderson, “A comprehensive tissue properties database provided for the thermal assessment of a human at rest,” *Biophys. Rev. Lett.*, vol. 5, no. 3, pp. 129–151, Sep. 2010.
[195] L. R. Williams and R. W. Leggett, “Reference values for resting blood flow to organs of man,” *Clin. Phys. Physiol. Meas. Off. J. Hosp. Phys. Assoc. Dtsch. Ges. Für Med. Phys. Eur. Fed. Organ. Med. Phys.*, vol. 10, no. 3, pp. 187–217, Aug. 1989.

[196] C. M. Collins *et al.*, "Temperature and SAR Calculations for a Human Head Within Volume and Surface Coils at 64 and 300 MHz," *J. Magn. Reson. Imaging*, vol. 19, no. 5, pp. 650–656, 2004.
[197] S. I. Kim and T. S. Suh, *World Congress of Medical Physics and Biomedical Engineering 2006: August 27 - Septmber 1, 20006 COEX Seoul, Korea*. Springer Science & Business Media, 2007.
[198] M. F. J. Cepeda Rubio, A. Vera, and L. Leija, "High Temperature Hyperthermia in Breast Cancer Treatment," in *Hyperthermia*, N. Huilgol, Ed. InTech, 2013.
[199] G. Kelly, "Body temperature variability (Part 1): a review of the history of body temperature and its variability due to site selection, biological rhythms, fitness, and aging," *Altern. Med. Rev. J. Clin. Ther.*, vol. 11, no. 4, pp. 278–293, Dec. 2006.
[200] K. M. Takami and H. Hekmat, *Simulation and Calculation of Magnetic and Thermal Fields of Human using Numerical Method and Robust Soft wares*. unpublished, 2008.
[201] "ISO 13485:2003 - Medical devices -- Quality management systems -- Requirements for regulatory purposes," *ISO*. [Online]. Available: http://www.iso.org/iso/catalogue_detail?csnumber=36786. [Accessed: 03-Oct-2016].
[202] "ISO 9001:2008 - Quality management systems -- Requirements," *ISO*. [Online]. Available: http://www.iso.org/iso/catalogue_detail?csnumber=46486. [Accessed: 05-Aug-2016].